

University of Groningen

Pre-treatment 3D dose verification for intensity modulated radiotherapy (IMRT)

Visser, Ruurd

IMPORTANT NOTE: You are advised to consult the publisher's version (publisher's PDF) if you wish to cite from it. Please check the document version below.

Document Version

Publisher's PDF, also known as Version of record

Publication date:

2017

[Link to publication in University of Groningen/UMCG research database](#)

Citation for published version (APA):

Visser, R. (2017). Pre-treatment 3D dose verification for intensity modulated radiotherapy (IMRT). [Groningen]: Rijksuniversiteit Groningen.

Copyright

Other than for strictly personal use, it is not permitted to download or to forward/distribute the text or part of it without the consent of the author(s) and/or copyright holder(s), unless the work is under an open content license (like Creative Commons).

Take-down policy

If you believe that this document breaches copyright please contact us providing details, and we will remove access to the work immediately and investigate your claim.

Downloaded from the University of Groningen/UMCG research database (Pure): <http://www.rug.nl/research/portal>. For technical reasons the number of authors shown on this cover page is limited to 10 maximum.

Pre-treatment 3D dose verification for intensity modulated radiotherapy (IMRT)

Ruurd Visser

Visser, R.

Pre-treatment 3D dose verification for intensity modulated radiotherapy (IMRT)

PhD dissertation, University of Groningen, The Netherlands

ISBN: 978-94-6332-179-2

© Copyright 2017 Ruurd Visser, Groningen, The Netherlands

All right reserved. No part of this thesis may be produced, stored in a retrieval system, or transmitted in any form or by any means without prior permission of the author or, when appropriate, of the publishers of the published articles.

Cover design: Pascal Montsma, Magicolr advies en ontwerpbureau

Printed by: GVO drukkers en vormgevers B.V.


magicolr.com

Financial support for the publication and printing of this thesis was kindly provided by:

- Ion Beam Applications s.a. (IBA sa)
- Research group Healthy Ageing, Allied Health Care and Nursing of the Hanze University of Applied Sciences
- Medical Imaging and Radiation Therapy (MIRT) of the Hanze University of Applied Sciences
- Graduate School for Drug Exploration (GUIDE)
- University Medical Center Groningen (UMCG)
- RT-IDEA B.V.
- Elekta B.V.



DIGITAL VERSION



rijksuniversiteit
groningen

Pre-treatment 3D dose verification for intensity modulated radiotherapy (IMRT)

Proefschrift

ter verkrijging van de graad van doctor aan de
Rijksuniversiteit Groningen
op gezag van de
rector magnificus prof. dr. E. Sterken
en volgens besluit van het College voor Promoties.

De openbare verdediging zal plaatsvinden op

woensdag 17 mei 2017 om 16.15 uur

door

Ruurd Visser

geboren op 27 februari 1983
te Smalingerland

Promotores

Prof. dr. J.A. Langendijk

Prof. dr. C.P. van der Schans

Copromotores

Dr. ir. E.W. Korevaar

Dr. ir. A.A. van 't Veld

Beoordelingscommissie

Prof. dr. S. Brandenburg

Prof. dr. B.W. Raaymakers

Prof. dr. B. Poppe

Paranimfen

Froukje Visser-Smids

Wouter Schaake

Contents

Chapter 1	
General introduction and outline of the thesis	9
Chapter 2	21
Reconstruction of high resolution 3D dose from matrix measurements: error detection capability of the COMPASS correction kernel method <i>Phys. Med. Biol.</i> 56(2011) 5029-5043	
Chapter 3	43
Development of an iterative reconstruction method to overcome 2D detector low resolution limitations in MLC leaf position error detection for 3D dose verification in IMRT <i>Phys. Med. Biol.</i> 61(2016) 3843-3856	
Chapter 4	65
Reconstruction of high resolution MLC leaf positions using a low resolution detector for accurate 3D dose reconstruction in IMRT <i>Phys. Med. Biol.</i> 61(2016) N642-N649	
Chapter 5	79
Efficient and reliable 3D dose quality assurance for IMRT by combining independent dose calculations with measurements <i>Med. Phys.</i> 40(2013) 021710	
Chapter 6	95
Evaluation of DVH-based treatment plan verification in addition to gamma passing rates for head and neck IMRT <i>Radiother. Oncol.</i> 112(2014) 389-395	
Chapter 7	113
Summarizing discussion and future perspectives	
Appendices	
Nederlandse samenvatting	131
Dankwoord	139
Curriculum Vitae	145
Publications	149

Chapter 1

General introduction and outline of the thesis

General introduction

Currently, cancer is the leading cause of death worldwide [1]. With the increase in life expectancy, cancer is expected to be a predominant mortality factor for the future. Treatment of cancer may consist of various interventions, such as surgery, chemotherapy, brachytherapy and/or external beam radiotherapy, either alone but in most cases different modalities are combined. Approximately 50% of all cancer patients is currently treated with external beam radiotherapy using photons [2,3].

In external beam radiotherapy, a photon beam is produced by a linear accelerator (linac) by bombarding a material with a high atomic number with high energy electrons. This photon beam, typically with an energy spectrum with a nominal maximum in the range of 6 MeV to 25 MeV, is then directed to the treatment site, penetrating the tissue in which the tumour is situated. For any such a photon beam, a certain amount of dose is released in healthy and tumour tissue, damaging the DNA, and destroying the cell structure with cell death as a result. To minimize the damage to healthy tissue, a combination of photon beams is usually directed to the treatment site from several angles and shaped to match the tumour for each treatment angle using multi leaf collimators (MLC). An MLC consists of many collimator leaves which can be moved independently from each other. Application of an MLC allows, in addition to beam shaping, modulation of the intensity of the photon beam for each treatment angle by a composition of various shaped segments within each treatment beam. This advanced radiotherapy treatment technique is known as intensity modulated radiotherapy (IMRT). IMRT results in complex treatments containing steep dose gradients, intentionally on a per-beam basis also within target volumes, allowing better sparing of organs at risk (OAR) whilst maintaining sufficient tumour coverage and dose homogeneity [4–7].

Patients planned for external beam radiotherapy are generally subjected to extensive and complex preparatory procedures. It starts with an intake in which the radiation oncologist talks through the entire procedure and it ends with the follow up which can take up to the patients entire lifetime (figure 1).



Figure 1:
Flow chart of external radiotherapy treatment procedure.

In terms of patient safety, each process within the procedure needs to be carefully monitored. Therefore, many processes within the procedure have been standardised, such as dose prescription, commissioning of the treatment systems and assessment of quality of life and acute and late radiation-induced toxicities [8–12]. As complexity of the entire procedure is high, dose delivery errors can occur, even after extensive commissioning [13], emphasizing the need for treatment verification prior to the actual treatment by patient specific quality assurance (QA).

Patient specific QA

In patient specific QA the treatment plan is verified in terms of dose deposition, independent of the treatment planning system (TPS). This can be performed by dose calculations, direct dose measurements, or a combination of both. The accuracy and speed of 3 dimensional (3D) dose calculations have considerably improved over the last years as computational power increased. Simple pencil beam algorithms evolved into more sophisticated collapsed cone algorithms and Monte Carlo calculations were introduced as computation time decreased significantly [14–16]. But, although high precision dose calculation algorithms are available, dose measurements within the dose verification procedure are still considered necessary as only a measurement provides a full representation of the effect of treatment planning and treatment machine discrepancies on actual delivered dose.

Dose verification based on measurements can be performed with a broad variety of detectors [17,18]. In the past, when linacs were introduced for external beam radiotherapy, mainly point measurements were performed. Simple point measurements however are insufficient for dose verification of complex dose depositions with high dose gradients such as for IMRT. This was partly overcome by the introduction of 2D dose measurements with radiographic films [18,19]. Film measurements allow a 2D plane to be verified. Unfortunately, film measurements are limited to planes and the dose evaluation is a cumbersome procedure reducing efficiency of the QA procedure. For a full 3D dose verification, 3D detectors such as gel and solid plastic dosimetry have been developed [20–25]. These techniques allow for a full 3D dose verification but are labour intensive and cannot be performed in nor easily transferred to the actual patient geometry.

To verify a dose deposition in patient geometry based on measurements using fluence modelling, two different approaches have been developed. The first approach compares the measured detector response with the expected detector response in the validation geometry and corrects with, thus found perturbations, the calculated dose in patient

geometry using ray-tracing techniques [26]. The second approach uses the measured detector response to reconstruct the fluence with which the dose is recalculated in patient geometry by a dose engine [27–32]. In this approach, as an initial step an independent fluence model calculates the expected fluence based on a radiotherapy treatment plan (RT-plan). This calculated fluence is used to determine the expected detector response based on a detector model. By comparing this calculated detector response with the measured detector response, the calculated fluence can then be corrected according to the measurement. Finally, the corrected fluence is used to recalculate the dose in a CT representing the patient geometry which can be compared with the prescribed dose distribution enabling 3D *in vivo* dose verification.

The two most common detector types available and used for fluence modelling are the electronic portal imaging device (EPID) and 2D detector arrays composed of ionization chambers. The EPID detector consists of a scintillating screen that produces photons when hit by x-rays, followed by detection of these photons in an amorphous silicon plate. The emitted light can then be used to model fluence. The EPID detector was historically introduced as a position verification device, but extensive research has led to the development of sophisticated fluence modelling based on EPID dosimetry [33]. A major advantage of an EPID detector is the fact that it has a high resolution and is incorporated within the treatment machine behind the patient allowing measurement based fluence modelling during patient treatment. The intrinsic advantage of including patient geometry has a downside that differences in expected and measured detector response can originate from either the treatment machine, the patient geometry or both. Furthermore, as this technique is not yet broadly commercially available, only departments with extensive knowledge on EPID dosimetry can use this technique for dose verification purposes. In general, commercially available dose verification tools use detector arrays composed of diodes or ionization chambers. In comparison to EPID dosimetry, 2D detector arrays are commonly mounted on the linac or positioned on the treatment table without a patient in place which excludes the ability of fluence modelling based on actual patient treatment delivery [29,30,34]. Importantly, current 2D detector arrays have a limited spatial resolution. Nevertheless, research has shown that high resolution dose verification can be performed using low resolution measurements [35], and new detectors are still being developed allowing fluence modelling during patient treatment [36]. Even so, pre-treatment dose verification based on 2D measurements is a cumbersome methodology as it is performed prior to the actual treatment and demands, the already limited, linac time. With the increase in the number of patients that require 3D dose verification, efficient and reliable pre-treatment dose verification procedures are therefore needed.

An important aspect of pre-treatment dose verification is the evaluation of observed dose differences. From a clinical point of view, under dosage in tumour tissue should be prevented to maintain sufficient tumour control and over dosage should be prevented for both the tumour and healthy tissue to minimize health related complaints for the patient. Traditionally, dose differences are evaluated using percentile dose difference, and distance-to-agreement for a 2D plane [18]. Subsequently, these were combined successfully resulting in the gamma evaluation [37]. The gamma evaluation showed to be a strong dose evaluation methodology as it allowed a fast evaluation of dose differences in both 2D and 3D [38,39]. Nevertheless, the gamma evaluation is difficult to interpret in terms of clinical relevance [40], which is underlined by a weak correlation between dose differences and dose volume histograms (DVH's) [26,41–43]. Pre-treatment dose verification based on DVH's will result in a more clinical patient specific QA procedure. Clear DVH criteria are still lacking however.

Aim and outline of the thesis

The aim of this thesis was to evaluate and improve the accuracy and efficiency of high resolution pre-treatment 3D dose verification using low resolution detector measurements, and to improve the clinical interpretation of observed dose differences.

As previously described, several techniques are available for pre-treatment dose verification. The technique described in this thesis is based on the combination of dose calculations and high resolution fluence modelling from actual measurements at the linac using a low resolution detector. The detector used for measurements consists of an array of ionisation chambers. The resolution of the detector limits the accuracy of the fluence reconstruction. This limitation is overcome by the introduction of a correction kernel which corrects the high resolution modelled fluence in case of a difference between measured and calculated detector response. To what extent the use of this correction kernel is suitable for dose verification purposes is described in **chapter 2**. **Chapter 3** focuses on a new iterative reconstruction method to reconstruct individual MLC leaf positions for a better representation of the actual given treatment reducing the need for the correction kernel method, and **chapter 4** evaluates the iterative reconstruction method for a high resolution MLC system.

Due to inherently limited departmental resources and steady increases in the number of complex treatment plans, an efficient QA-procedure is needed. Furthermore, reliability is of the utmost importance to guarantee treatment outcome. Reliability is sustained by including actual fluence measurements of the linac within the QA-procedure. Unfortunately, this is a cumbersome approach reducing efficiency substantially. A new

methodology to combine the reliability of measurements with the efficiency of independent dose calculations is described in **chapter 5**.

Evaluation of pre-treatment dose verification is generally performed by a physicist using the gamma evaluation which lacks information on actual dose delivered to treatment volumes, *i.e.* planning targets and OAR. In case of relevant dose differences the radiation oncologist is consulted and an clinical meaningful interpretation from gamma evaluation to patient dose distribution has to be achieved. **Chapter 6** describes a new approach in which dose is verified according to dose delivery to treatment volumes and new criteria are introduced which better involve the radiation oncologist in clinically more representative pre-treatment 3D dose verification of advanced radiotherapy treatment plans.

References

- [1] Stewart BS, Wild CP. World Cancer Report 2014. WHO, WHO; 2014.
- [2] Slotman BJ, Cottier B, Bentzen SM, Heeren G, Lievens Y, van den Bogaert W. Overview of national guidelines for infrastructure and staffing of radiotherapy. ESTRO-QUARTS: work package 1. *Radiother Oncol* 2005;75:349–54.
- [3] Delaney G, Jacob S, Featherstone C, Barton M. The role of radiotherapy in cancer treatment: Estimating optimal utilization from a review of evidence-based clinical guidelines. *Cancer* 2005;104:1129–37.
- [4] Arbea L, Ramos LI, Martinez-Monge R, Moreno M, Aristu J. Intensity-modulated radiation therapy (IMRT) vs. 3D conformal radiotherapy (3DCRT) in locally advanced rectal cancer (LARC): dosimetric comparison and clinical implications. *Radiat Oncol* 2010;5:17.
- [5] Chandra A, Guerrero TM, Liu HH, Tucker SL, Liao Z, Wang X, Murshed H, Bonnen MD, Garg AK, Stevens CW, Chang JY, Jeter MD, Mohan R, Cox JD, Komaki R. Feasibility of using intensity-modulated radiotherapy to improve lung sparing in treatment planning for distal esophageal cancer. *Radiother Oncol* 2005;77:247–53.
- [6] Longobardi B, De Martin E, Fiorino C, Dell’oca I, Broggi S, Cattaneo GM, Calandrino R. Comparing 3DCRT and inversely optimized IMRT planning for head and neck cancer: equivalence between step-and-shoot and sliding window techniques. *Radiother Oncol* 2005;77:148–56.
- [7] Schubert LK, Gondi V, Sengbusch E, Westerly DC, Soisson ET, Paliwal BR, Mackie TR, Mehta MP, Patel RR, Tomé WA, Cannon GM. Dosimetric comparison of left-sided whole breast irradiation with 3DCRT, forward-planned IMRT, inverse-planned IMRT, helical tomotherapy, and tomotherapy. *Radiother Oncol* 2011;100:241–6.
- [8] Marks LB, Yorke ED, Jackson A, Ten Haken RK, Constine LS, Eisbruch A, Bentzen SM, Nam J, Deasy JO. Use of normal tissue complication probability models in the clinic. *Int J Radiat Oncol Biol Phys* 2010;76:S10-9.
- [9] Ezzell GA, Galvin JM, Low D, Palta JR, Rosen I, Sharpe MB, Xia P, Xiao Y, Xing L, Yu CX. Guidance document on delivery, treatment planning, and clinical implementation of IMRT: report of the IMRT Subcommittee of the AAPM Radiation Therapy Committee. *Med Phys* 2003;30:2089–115.
- [10] Aaronson NK, Ahmedzai S, Bergman B, Bullinger M, Cull A, Duez NJ, Filiberti A, Flechtner H, Fleishman SB, Haes JCJM d., Kaasa S, Klee M, Osoba D, Razavi D, Rofe PB, Schraub S, Sneeuw K, Sullivan M, et al. The European Organization for Research and Treatment of Cancer QLQ-C30: A Quality-of-Life Instrument for Use in International Clinical Trials in Oncology. *JNCI J Natl Cancer Inst* 1993;85:365–76.

- [11] Trotti A, Colevas AD, Setser A, Rusch V, Jaques D, Budach V, Langer C, Murphy B, Cumberlin R, Coleman CN, Rubin P. CTCAE v3.0: development of a comprehensive grading system for the adverse effects of cancer treatment. *Semin Radiat Oncol* 2003;13:176–81.
- [12] Stiggelbout AM, Kunneman M, Baas-Thijssen MCM, Neijenhuis PA, Loo AK, Jägers S, Vree R, Marijnen CAM, Pieterse AH. The EORTC QLQ-CR29 quality of life questionnaire for colorectal cancer: validation of the Dutch version. *Qual Life Res* 2015.
- [13] Nelms BE, Chan MF, Jarry G, Lemire M, Lowden J, Hampton C, Feygelman V. Evaluating IMRT and VMAT dose accuracy: practical examples of failure to detect systematic errors when applying a commonly used metric and action levels. *Med Phys* 2013;40:111722.
- [14] Ma C-M, Li JS, Pawlicki T, Jiang SB, Deng J, Lee MC, Koumrian T, Luxton M, Brain S. A Monte Carlo dose calculation tool for radiotherapy treatment planning. *Phys Med Biol* 2002;47:1671–89.
- [15] Kawrakow I, Rogers DWO, Walters BRB. Large efficiency improvements in BEAMnrc using directional bremsstrahlung splitting Uniform and Selective Bremsstrahlung Splitting 2004;2.
- [16] Fippel M, Laub W, Huber B, Nüsslin F. Experimental investigation of a fast Monte Carlo photon beam dose calculation algorithm. *Phys Med Biol* 1999;44:3039–54.
- [17] Mijnheer B, Beddar S, Izewska J, Reft C. In vivo dosimetry in external beam radiotherapy. *Med Phys* 2013;40:70903.
- [18] Low DA, Moran JM, Dempsey JF, Dong L, Oldham M. Dosimetry tools and techniques for IMRT. *Med Phys* 2011;38:1313–38.
- [19] Pai S, Das IJ, Dempsey JF, Lam KL, LoSasso TJ, Olch AJ, Palta JR, Reinstein LE, Ritt D, Wilcox EE. TG-69: Radiographic film for megavoltage beam dosimetry. *Med Phys* 2007;34:2228.
- [20] Vergote K, De Deene Y, Claus F, De Gersem W, Van Duyse B, Paelinck L, Achten E, De Neve W, De Wagter C. Application of monomer/polymer gel dosimetry to study the effects of tissue inhomogeneities on intensity-modulated radiation therapy (IMRT) dose distributions. *Radiother Oncol* 2003;67:119–28.
- [21] Vandecasteele J, De Deene Y. Evaluation of radiochromic gel dosimetry and polymer gel dosimetry in a clinical dose verification. *Phys Med Biol* 2013;58:6241–62.

- [22] De Deene Y, De Wagter C, Van Duyse B, Derycke S, Mersseman B, De Gersem W, Voet T, Achten E, De Neve W. Validation of MR-based polymer gel dosimetry as a preclinical three-dimensional verification tool in conformal radiotherapy. *Magn Reson Med* 2000;43:116–25.
- [23] Baldock C, De Deene Y, Doran S, Ibbott G, Jirasek A, Lepage M, McAuley KB, Oldham M, Schreiner LJ. Polymer gel dosimetry. *Phys Med Biol* 2010;55:R1–63.
- [24] Oldham M, Sakhalkar H, Guo P, Adamovics J. An investigation of the accuracy of an IMRT dose distribution using two- and three-dimensional dosimetry techniques. *Med Phys* 2008;35:2072–80.
- [25] Adamovics J, Maryanski MJ. Characterisation of PRESAGE: A new 3-D radiochromic solid polymer dosimeter for ionising radiation. *Radiat Prot Dosimetry* 2006;120:107–12.
- [26] Carrasco P, Jornet N, Latorre A, Eudaldo T, Ruiz A, Ribas M. 3D DVH-based metric analysis versus per-beam planar analysis in IMRT pretreatment verification. *Med Phys* 2012;39:5040.
- [27] van Zijtveld M, Dirkx ML, de Boer HC, Heijmen BJ. 3D dose reconstruction for clinical evaluation of IMRT pretreatment verification with an EPID. *Radiother Oncol* 2007;82:201–7.
- [28] Wendling M, McDermott LN, Mans A, Sonke J-J, van Herk M, Mijnheer BJ. A simple backprojection algorithm for 3D in vivo EPID dosimetry of IMRT treatments. *Med Phys* 2009;36:3310–21.
- [29] Korevaar EW, Wauben DJ, van der Hulst PC, Langendijk JA, Van't Veld AA. Clinical introduction of a linac head-mounted 2D detector array based quality assurance system in head and neck IMRT. *Radiother Oncol* 2011;100:446–52.
- [30] Boggula R, Jahnke L, Wertz H, Lohr F, Wenz F. Patient-specific 3D Pretreatment and Potential 3D Online Dose Verification of Monte Carlo-calculated IMRT Prostate Treatment Plans. *Int J Radiat Oncol Biol Phys* 2010.
- [31] van Elmpt W, Nijsten S, Mijnheer B, Dekker A, Lambin P. The next step in patient-specific QA: 3D dose verification of conformal and intensity-modulated RT based on EPID dosimetry and Monte Carlo dose calculations. *Radiother Oncol* 2008;86:86–92.
- [32] van Elmpt W, Nijsten S, Petit S, Mijnheer B, Lambin P, Dekker A. 3D in vivo dosimetry using megavoltage cone-beam CT and EPID dosimetry. *Int J Radiat Oncol Biol Phys* 2009;73:1580–7.

- [33] van Elmpt W, McDermott L, Nijsten S, Wendling M, Lambin P, Mijnheer B. A literature review of electronic portal imaging for radiotherapy dosimetry. *Radiother Oncol* 2008;88:289–309.
- [34] Nakaguchi Y, Araki F, Maruyama M, Saiga S. Dose verification of IMRT by use of a COMPASS transmission detector. *Radiol Phys Technol* 2012;5:63–70.
- [35] Poppe B, Blehschmidt A, Djouguela A, Kollhoff R, Rubach A, Willborn KC, Harder D. Two-dimensional ionization chamber arrays for IMRT plan verification. *Med Phys* 2006;33:1005–15.
- [36] Venkataraman S, Malkoske KE, Jensen M, Nakonechny KD, Asuni G, McCurdy BM. The influence of a novel transmission detector on 6 MV x-ray beam characteristics. *Phys Med Biol* 2009;54:3173–83.
- [37] Low DA, Harms WB, Mutic S, Purdy JA. A technique for the quantitative evaluation of dose distributions. *Med Phys* 1998;25:656–61.
- [38] Depuydt T, Van Esch A, Huyskens DP. A quantitative evaluation of IMRT dose distributions: refinement and clinical assessment of the gamma evaluation. *Radiother Oncol* 2002;62:309–19.
- [39] Wendling M, Zijp LJ, McDermott LN, Smit EJ, Sonke J-J, Mijnheer BJ, van Herk M. A fast algorithm for gamma evaluation in 3D. *Med Phys* 2007;34:1647.
- [40] Chan MF, Li J, Schupak K, Burman C. Using a novel dose QA tool to quantify the impact of systematic errors otherwise undetected by conventional QA methods: clinical head and neck case studies. *Technol Cancer Res Treat* 2014;13:57–67.
- [41] Zhen H, Nelms BE, Tome WA. Moving from gamma passing rates to patient DVH-based QA metrics in pretreatment dose QA. *Med Phys* 2011;38:5477–89.
- [42] Nelms BE, Zhen H, Tome WA. Per-beam, planar IMRT QA passing rates do not predict clinically relevant patient dose errors. *Med Phys* 2011;38:1037–44.
- [43] Stasi M, Bresciani S, Miranti A, Maggio A, Sapino V, Gabriele P. Pretreatment patient-specific IMRT quality assurance : A correlation study. *Med Phys* 2012;39:7626–34.

Chapter 2

**Reconstruction of high resolution 3D dose
from matrix measurements: error detection
capability of the COMPASS correction kernel
method**

**J. Godart
E.W. Korevaar
R. Visser
D.J.L. Wauben
A.A. van 't Veld**

Phys. Med. Biol. 56(2011) 5029-5043

Abstract

The COMPASS system (IBA Dosimetry) is a quality assurance (QA) tool which reconstructs 3D doses inside a phantom or a patient CT. The dose is predicted according to the RT plan with a correction derived from 2D measurements of a matrix detector. This correction method is necessary since a direct reconstruction of the fluence with a high resolution is not possible because of the limited resolution of the matrix used, but it comes with a blurring of the dose which creates inaccuracies in the dose reconstruction. This paper describes the method, and verifies its capability to detect errors in the positioning of a MLC with 10 mm leaf width in a phantom geometry. Dose reconstruction was performed for MLC position errors of various sizes at various locations for both rectangular and IMRT fields and compared to a reference dose. It was found that the accuracy with which an error in MLC position is detected depends on the location of the error relative to the detectors in the matrix. The reconstructed dose in an individual rectangular field for leaf positioning errors up to 5 mm, was correct within 5% in 50% of the locations. At the remaining locations, the reconstruction of leaf position errors larger than 3 mm can show inaccuracies, even though these errors were detectable in the dose reconstruction. Errors larger than 9 mm created inaccuracies up to 17% in a small area close to the penumbra. The QA capability of the system was tested through gamma evaluation. Our results indicate that the mean gamma provided by the system is slightly increased and that the number of points above gamma 1 ensures error detection for QA purposes. Overall, the correction kernel method used by the COMPASS system is adequate to perform QA of IMRT treatment plans with a regular MLC, despite local inaccuracies in the dose reconstruction.

Introduction

Advanced radiotherapy techniques, like intensity modulated radiotherapy (IMRT) or arc therapy, aim at concentration of the dose inside the tumour, while sparing organs at risk. To achieve this, the treatment plans often have high gradient dose distributions, which emphasize the need of control of the beam delivery and of the patient positioning [1,2]. Efforts have been made to cover both aspects, with several detectors and methods. The patient positioning can be verified on-line via cone-beam CT and EPID detectors, and fixation techniques have been improved. Control of the beam delivery is performed by several methods, which can be used in parallel. The output of the linear accelerator can be determined via point measurements, and the shape and magnitude of the delivered dose distribution can be verified by multi-dimensional detectors.

The verification of both absolute and relative dose distributions to be delivered is traditionally performed in a phantom prior to treatment. Measurements are analyzed by comparing the expected with the measured dose, and a set of criteria is used to determine whether the plan passes or fails the verification. The criteria that can be applied depend on the technology used. A high resolution dose measurement is obtained in one or more planes with film based quality assurance (QA) procedures [3]. In contrast to films, 2D detector arrays of ionization chambers, diodes or scintillator detectors provide low spatial resolution measurements in one plane, with an output that is more reliable and instantly available during the QA procedure [4]. Alternatively, EPID dosimetry is possible, but has a limited field of view and is, by lack of commercial products, not yet easily implemented in a department [5].

Since these traditional QA procedures are done in a phantom and the criteria that can be used depend on limits of the applied technology, it is often difficult to quantify and interpret the results in terms of clinical impact for the patient. To assess this issue, Renner *et al* proposed a method to reconstruct the beam fluence and to compute 3D doses inside the patient CT [6]. The fluence is measured with films, and then a dose reconstruction is performed. With reconstructed 3D doses inside a patient CT, a direct comparison of the deposited dose in regions with tumour and organs-at-risk can be done, to achieve a more representative and complete QA at a patient level. The proposed film verification is strictly a dosimetric delivery check, as the measurements are performed without the patient and the reconstruction is done with the patient CT used for the planning. Such a method of fluence reconstruction can be applied to other 2D detector systems including on-line verification systems, and several authors have notably proposed EPID dosimetry solutions [7,8].

The COMPASS system (IBA Dosimetry) is a commercially available solution which uses a 2D ionization chamber matrix and is able to reconstruct 3D doses in phantom or patient CT. The system can be used independently from the detector: a dose calculation can be performed without measurement to provide an independent dose calculation. It contains several tools to analyse the data in patient anatomy such as dose volume histograms (DVHs). The motivation for our study is that these advanced possibilities require accurate dose reconstruction including error detection as a prerequisite. This paper focuses on QA of the treatment plan and the dose delivery as combined in a measurement-based procedure. The included dose reconstruction method is expected to suffer from the low spatial resolution of the ionization chamber matrix measurements (typically above 5 mm), in comparison to film QA or EPID dosimetry. This limited resolution can impair the reconstruction capability of the system, notably in case of small IMRT segments where a spatial frequency of at least 0.4 mm^{-1} would be required to represent the true dose distribution [9,10]. To mitigate this problem, the COMPASS system uses a model to predict the linac fluence, and then corrects the prediction according to the measurements obtained at the linac. This procedure, based on a correction kernel, allows an utilisation of high resolution fluence, but comes with potential inaccuracies in the dose reconstruction that need further analysis.

The purpose of this paper is to evaluate the capability of the COMPASS correction kernel method to reconstruct 3D doses that can be used to detect delivery errors. First the method of reconstruction by use of a correction kernel is described. Next, the accuracy in detecting errors in MLC position at the edge of a single field is quantified in terms of remaining position errors, reconstructed dose and gamma evaluation. Finally, the performance of the system in IMRT QA is evaluated with a clinical IMRT field.

Material and Method

Description of the COMPASS system

General workflow

In the measurement-based procedure, the aim of the COMPASS system is to reconstruct a high resolution 3D dose from low resolution detector measurements (figure 1). The system uses a model of the linear accelerator to generate, with a 2D high-resolution grid (typically $2 \times 2 \text{ mm}^2$ per pixel), a prediction of the fluence ($\psi_{\text{predicted}}$)

according to the radiotherapy treatment plan (DICOM RT Plan). The computation of a detector response prediction ($R_{\text{predicted}}$) is performed through a detector model, and this prediction is compared to the measured response obtained at the linac. The resulting difference is used to modify the predicted fluence, yielding the reconstructed fluence ($\Psi_{\text{reconstructed}}$). From this reconstructed fluence, the 3D dose is reconstructed, via the dose engine based on a collapsed cone model [11], inside a phantom or a patient CT (typically $2 \times 2 \times 2 \text{ mm}^3$).

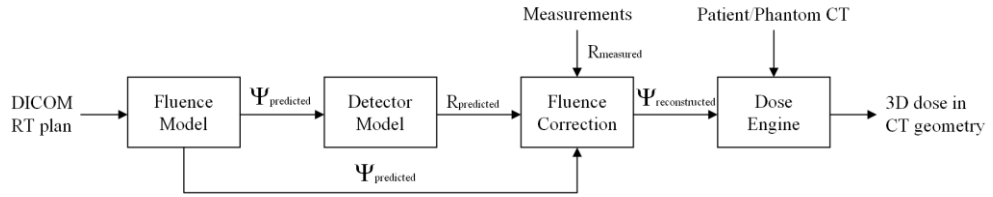


Figure 1:

The predicted detector response, computed from the predicted fluence, is compared to the measured response to correct the fluence and reconstruct the dose. The predicted and reconstructed fluences have a high spatial resolution, while the low resolution parts of the system concern the detector responses (predicted and measured). Symbols are explained in the text.

Comparison of the predicted and measured detector response

The fluence coming from the linac is measured with a 2D ionization chamber matrix. The analysis of the measurements follows a procedure similar to the one described by Poppe *et al* [4]. The measured detector response is compared to a predicted detector response, which is computed from the predicted fluence $\Psi_{\text{predicted}}$ and the detector response function f (formula 1):

$$R_{\text{predicted}} = \sum_{i=1}^{N_{\text{IC}}} f_i(x, y) \cdot \Psi_{\text{predicted}} \quad (1)$$

f_i : 2D detector response function of ionization chamber i in the MatriXX coordinate system

In this paper, the MatriXX detector [12] was used in several configurations. This detector array is a 2D matrix of 1020 ionization chambers, with a centre-to-centre distance of 7.62 mm; the chambers are cylindrical cavities of 5 mm height and 4 mm diameter. The dosimetric properties of the MatriXX detector have been described by Herzen *et al* [13]. Notably, the instrumental response function of the detector to a 1 mm wide beam can be approximated by a Gaussian with 5.8 mm full width at half maximum (extrapolated from Herzen *et al* [13], figure 4).

Fluence correction method

The fluence correction is applied in case of discrepancies between the predicted and the measured detector responses. The first step of this process is to scale the predicted fluence to the measured output of the linac (COMPASS user guide 2.0). The predicted fluence is scaled according to the difference between the measured matrix response and the predicted matrix response (sum over the whole matrix of the ionization chamber responses). The second step is called “residual response correction”. This procedure corrects the fluence according to the response difference of the individual ionization chambers (formula 2) with a fluence correction kernel (formula 3).

$$R_i = A_{scaling} R_{i\ predicted} - R_{i\ measured} \quad (2)$$

$$\Psi_{reconstructed} = A_{scaling} \Psi_{predicted} + \sum_{i=1}^{N_{IC}} R_i \bullet k_{\Psi_i}(x, y) \quad (3)$$

i : ionization chamber index

$A_{scaling}$: scaling factor

N_{IC} : number of ionization chambers

R_i : residual response in ionization chamber i

k_{Ψ_i} : fluence correction kernel of ionization chamber i

The fluence correction kernel follows from the detector response function as the theoretical fluence which would produce a response in a single ionization chamber (R_i) (figure 2).

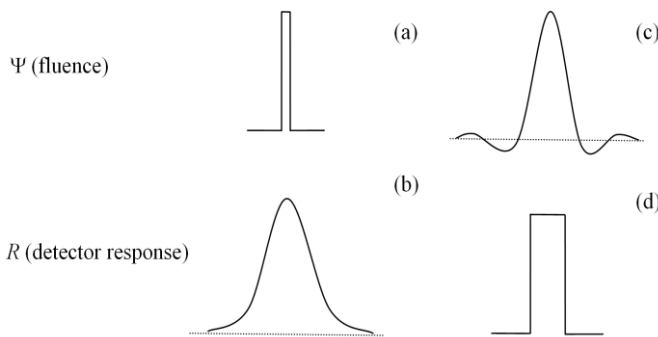


Figure 2:

An elementary fluence in one element of the fluence grid (a) gives a response in the detector according to the detector response function f (b). The fluence correction kernel k is the theoretical fluence (c) that produces a signal in exactly one single

ionization chamber (d). In practice, the correction kernel (c) is proportional to the difference in signal between the predicted and measured response. Note the negative parts in the fluence correction kernel that are required to cancel out responses in neighbouring ionization chambers.

Experimental determination of the fluence correction kernel

The fluence correction kernel was obtained experimentally by providing the COMPASS system artificial measurements in a single ionization chamber. The rest of the ionization chambers were set to a background value to prevent truncation of negative numbers. The fluence and the dose were reconstructed by the COMPASS system with a plan showing a closed MLC, to invoke the correction kernel on the unexpected signal. The dose coming from the background was then subtracted. The fluence was exported from a research version of the system (RaySearch laboratories).

An important parameter while considering the shape of the correction kernel is the effective associated detector resolution, which is determined by the physical distance (7.62 mm) between detectors in the MatriXX and the linac source to detector distance (SDD). A larger SDD results in a higher effective resolution but a smaller field of view. The vendor recommends an SDD such that one row is aligned with one MLC leaf pair. To investigate effects of a possible increase of the projected resolution, the detector was used in two configurations, described in the experimental configuration.

Effect of the correction kernel

The capability to detect leaf positioning errors is essential in IMRT QA, since a small position discrepancy can induce large output differences [14,15]. The correction kernel plays for this purpose a fundamental role, as the detected errors will be reconstructed by the correction kernel. The effect of the kernel was investigated by intentionally introducing errors in the position of the edge of a rectangular field. Since the correction kernels are applied in a fixed position bound to the detector device, its effect depends on the position of the MLC leaves with respect to the ionization chambers of the matrix. The overall effect was assessed by applying an error of a given size at various locations in the field: for every error size investigated (from 1 to 20 mm), at least 10 locations were used with steps of 1 mm.

Figure 3 shows typical profiles of an intentionally introduced 5 mm error. The *planned dose* and the *delivered dose* were obtained from the COMPASS system, without correction kernel. An error was deliberately introduced in the delivered dose. The *reconstructed dose* was the dose obtained from the system in case of disagreement between the plan and the delivery: the prediction (similar to the planned dose) is corrected by the correction kernel according to the real delivery (similar to the delivered dose). A comparison between the

delivered dose and the reconstructed dose was performed. The penumbra of the reconstructed dose is analysed with a home-made Matlab program, to determine the error position of the 50% dose, the maximum dose error, and to perform a gamma evaluation [16]. The gamma index was obtained with 1 mm interpolation, and two parameters were chosen as clinically used in our department: the mean gamma value and the number of points above gamma=1.

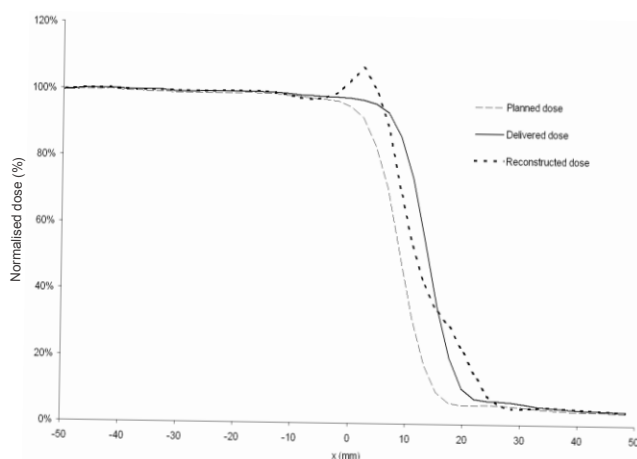


Figure 3: Planned, delivered and reconstructed dose profiles in case of an intentionally introduced 5 mm error in the field edge position (relative to the planned position). The reconstructed dose is a typical dose that can be obtained with the COMPASS system in case of an error in leaf positioning. The SDD is 762 mm.

Clinical IMRT field

In a clinical IMRT plan, multiple adjacent and overlapping field segments are created for one beam, and several beam directions are used. If a minor calibration error in one leaf pair occurs, every segment will show the error, but the overall effect of this error will be integrated over the different fields and segments. To validate the capability of the COMPASS system to perform accurate QA of such plans, a typical head-and-neck patient plan was used. Results will be shown for one of the 7 beams, which includes 12 segments. Position errors were introduced for 5 leaves, sufficiently separated to be considered as independent effects. Those 5 leaves were retracted from 1 to 10 mm. Analysis of this plan was performed according to our standard, by using an adapted version of Doselab (<http://doselab.sourceforge.net>). A gamma analysis with 3%/3 mm criterion was performed. This plan was also measured with EBT2 films, for an intentionally introduced error of 5 mm, the plans with and without the introduced error were irradiated and measured. The measurements were then subtracted.

Experimental configuration

Measurements were done with an Elekta linac equipped with an MLC with 10 mm leaf width. A 6 MV beam was delivered with gantry angle 0°. The MatriXX Evolution detector was used with 20 mm solid water build up, in two configurations:

- *SDD=762 mm*: short holder configuration. In that situation the rows and the MLC leaf pairs are aligned.
- *SDD=1000 mm*: long holder configuration. In that situation the detector is at the isocenter: the distance between detector elements is 7.62 mm, and the detector rows and the leaf pairs are not aligned.

The dose was reconstructed by the COMPASS system in a 300x300x500 mm³ solid water phantom. Analysis was performed at 12 mm depth. The dose grid had a 2x2x2 mm³ resolution, interpolated to 1x1x1 mm³ for analysis.

The irradiated films, used for the IMRT field, were radiochromic films (Gafchromic EBT2, ISP Corp.), positioned in coronal orientation in the middle of a 300x300x500 mm³ solid water phantom. The day after irradiation the films were scanned on a commercial flatbed scanner (V700, Epson), followed by conversion of optical density to dose. The conversion method was corrected for non-uniformity artefacts intrinsic in flatbed film scanners as described in recent publications [17,18]. The film inhomogeneities were corrected by a double exposure procedure [19].

Results

Description of the fluence correction kernel

The fluence correction kernel profile, used by the COMPASS system, is given in figure 4. The profile runs over the central horizontal axis of the 2D correction kernel that is indicated in the insert. The peak value was proportional to the difference between the predicted detector response and the measured one. The reconstructed dose profile of the residual response of one ionization chamber is also provided for comparison. The deposited dose at 12 mm depth corresponds to a slight blurring by convolution of the photon fluence.

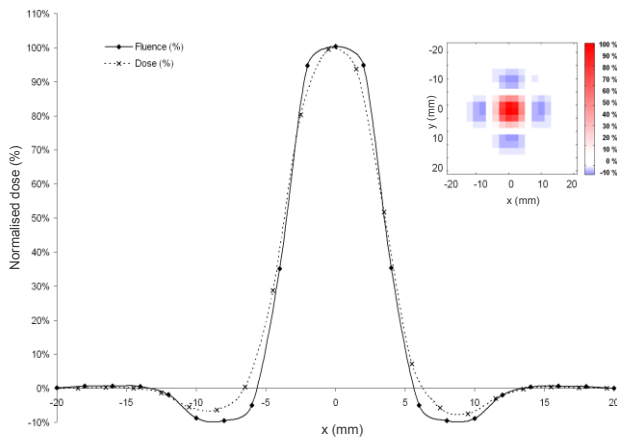


Figure 4: Experimental profile of the fluence correction kernel (photons), and its corresponding reconstructed dose profile at 12 mm depth in a water phantom (2x2 mm² grids). Both results were normalised to their maximal value (100%). Top-right: 2D shape of the correction kernel. The SDD is 1000 mm.

The shape of this fluence profile had a full width at half maximum of 7.0 mm. The 2D fluence reconstructed by the correction kernel of one ionization chamber showed 4 negative parts, distributed on both sides of the peak along the vertical and horizontal directions. Those negative parts describe the positions of the 4 adjacent ionization chambers, and their amplitude is -10% of the maximum value.

Effect of the correction kernel

Dose reconstruction

The accuracy of the reconstructed dose depended on where the error was localised on the 2D array. If a leaf tip was located at the projected centre of one ionization chamber, and if this leaf was erroneously retracted, it resulted in a too high dose that was reconstructed at the position of the ionization chamber, created by the superposition of the planned dose and the correction kernel of the ionization chamber. In that situation, the position of the 50% dose was inaccurately reconstructed, as is illustrated in fig. 3. If the leaf was pushed in the field, opposite errors in the reconstruction could be observed. However in case the leaf tip was in between two ionization chambers, no error in the reconstruction was made.

The error in the position of the 50% dose in comparison to the planned position and the error in the maximum dose were recorded in different positions of the field edge, for error sizes from 1 to 20 mm. The position of the field edge was moved every mm in order to obtain every possible configuration of the penumbra position with respect to the ionization chamber inside the matrix. Figure 5 shows the example of 5 mm errors, for a

SDD of 762 mm. Because of the effective detector distance of 10 mm the pattern shows a repetition at 10 mm.

- for 50% of the locations (see figure 5, locations 1, 2, 3, 9 and 10), the COMPASS dose reconstruction had a limited artefact (<5% and <2 mm in the dose reconstruction),
- for the other 50% locations (positions 4 to 8), the artefact created local dose inaccuracies from 5% to 11%, while the error in position of the 50% dose stayed within 2 mm.

Whatever the error size, the inaccuracy in the field edge position was always smaller than 2.5 mm. The artefact in the maximum dose reconstruction increased according to the size of the leaf position error. Up to 3 mm error, the artefact in the reconstructed dose was smaller than 5%. The maximum inaccuracy due to COMPASS artefact was found for 9 mm error, where the maximum dose inaccuracy was 17%. For errors larger than 9 mm (10 to 20 mm), the reconstructed dose showed the same inaccuracy values as for 9 mm error.

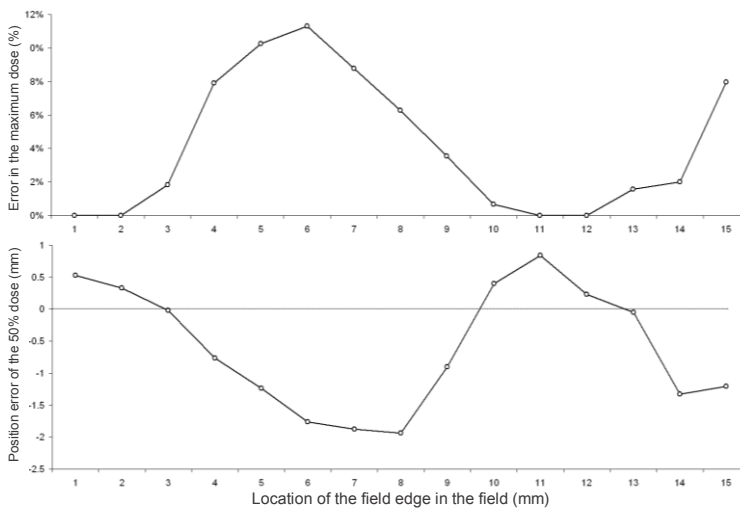


Figure 5: Dose reconstruction for a 5 mm field edge position error as a function of the location of the field edge. The dose blurring at the edge of the field is responsible for errors in the maximum dose up to 11.3% (top), and errors in the position of the 50% dose (bottom). Every point represents one location of the field edge, with 1 mm shift between two adjacent locations. The SDD is 762 mm.

Every point represents one location of the field edge, with 1 mm shift between two adjacent locations. The SDD is 762 mm.

Effect on the gamma evaluation

Gamma evaluation of the previous experiments was performed in a plan at 12 mm depth, to verify the QA capability of the system. Figures 6 and 7 summarise the results. The REFERENCE curves represent the difference between the delivered dose and the

planned dose, while the COMPASS curves correspond to the difference between the reconstructed dose and the planned dose. Every point represents the average over 10 successive locations of the field edge.

The COMPASS reconstruction algorithm overestimated the mean gamma value, obtained for several error sizes, from 2% to 8% (figure 6). Despite the variability of the result values obtained for the 10 field edge locations, the mean gamma value was proportional to the introduced error size, and a difference in error size could be shown by the mean gamma. The standard deviations between the 10 locations for one specific error size, were in the order of the COMPASS curve proportionality coefficient (0.032 mean gamma error per mm edge error for gamma 3%/3 mm, and 0.019 for gamma 5%/5 mm). These standard deviations can be explained by the gamma algorithm which uses a limited 1 mm interpolation in a very high dose gradient region.

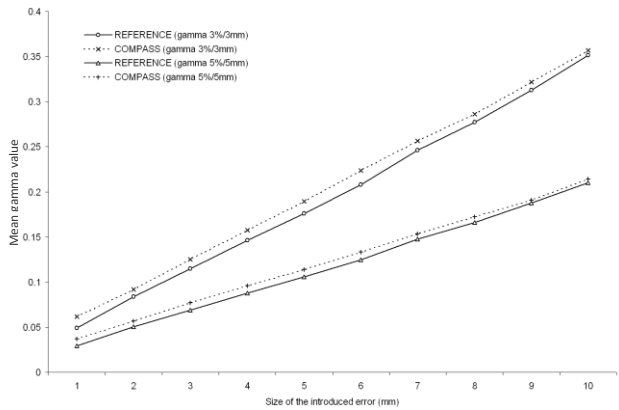


Figure 6: Mean gamma evaluation of edge positioning errors reconstructed by the COMPASS system, for several sizes of the introduced error. Every point represents the average over 10 successive locations of the field edge. The SDD is 762 mm.

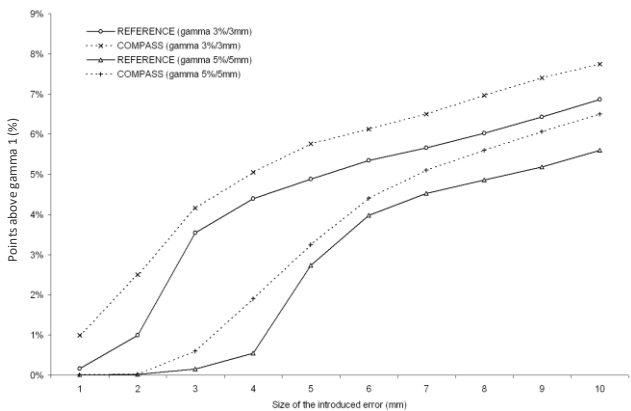


Figure 7: Gamma evaluation of edge positioning errors reconstructed by the COMPASS system, for several sizes of the introduced error. The curves show the relative number of points above gamma=1. Every point represents the average over 10 successive locations of the field edge. The SDD is 762 mm.

Concerning the number of points above $\gamma=1$, the number of points that fail the evaluation was higher with the COMPASS reconstruction algorithm (figure 7) than the REFERENCE values. The standard deviations of these values were smaller than 1%. One can notice also that, as expected for a γ 5%/5 mm evaluation, going from a 4 mm error to a 5 mm error increases significantly the number of points above $\gamma=1$ (+ 2.2%) in the REFERENCE curve, which is not the case with the COMPASS reconstruction method.

Overall, the effects of the inaccuracies in the dose reconstruction did not seem to compromise the COMPASS capability to detect an error in the delivery, as the mean γ of the evaluated plan was always slightly increased by the correction kernel method. The increase in the number of points above $\gamma=1$ still ensures a good error detection of MLC leaves with the COMPASS system.

Clinical IMRT field

To validate our results, a clinical case of one beam from a head-and-neck patient was used, with introduced errors from 1 to 10 mm. The results represent the superposition effect of several segments, for which the introduced errors occurred each time in the same leafs. A visualisation of the introduced errors is given in figure 8 in terms of dose differences.

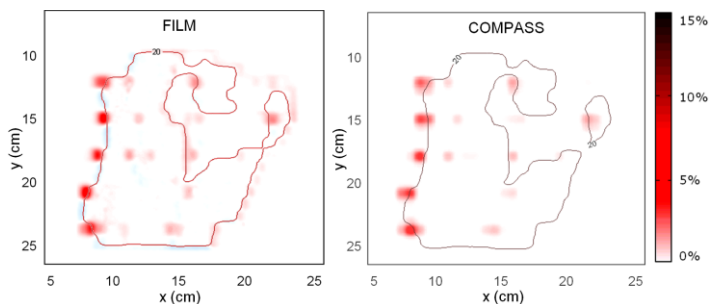


Figure 8:
Dose difference (% relative to the prescribed dose) of a beam (12 segments) in the H&N plan, for 5 leafs with 5 mm introduced errors. COMPASS dose difference agreed with the film but

shows more blurring. A film to film registration error of the order of 0.5mm introduced dose differences in the high gradient regions (field edges). The SDD is 1000 mm.

Figure 9 describes γ evaluation results with a 3%/3 mm criterion, with a recommended position of the matrix where the rows were aligned with the leaf pairs. The correction kernel had a small impact on the γ values. The mean γ value and the number of points above $\gamma=1$ of the correction kernel method were sufficiently accurate to warrant detection of errors in MLC leaf positions.

A similar evaluation was performed with the matrix at the isocentre (figure 10). In this situation, the correction kernel was smaller, but a systematic blurring of the errors is done for the leaf pairs which are positioned between two detector rows of the matrix (see figure 8, the leaf pair in the top of the figure). The error made by the COMPASS reconstruction kernel was increased: the mean gamma value was overestimated, and the number of points above gamma=1 was decreased. These results are the consequences of the extra blurring of the dose in the vertical direction, which increases the error in distance and the mean gamma, and decreases the high gamma values of the plan, described by the number of points above gamma=1.

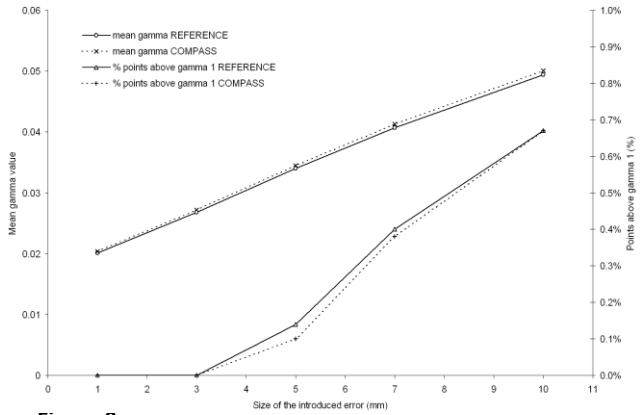


Figure 9: Mean gamma and number of points above gamma 1 (3%/3 mm) of several errors in 5 leaf pairs of the H&N case. The SDD is 762 mm.

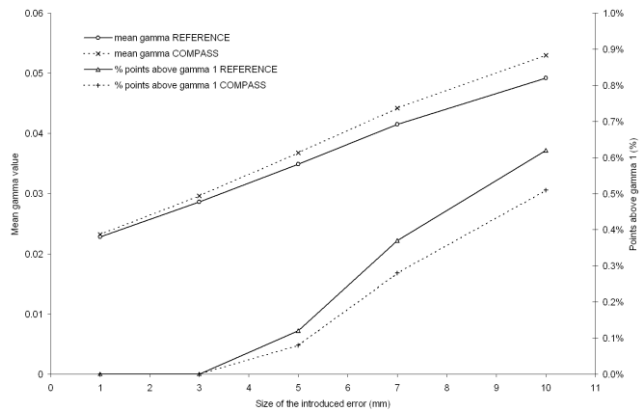


Figure 10: Mean gamma and number of points above (3%/3 mm) of several errors in 5 leaf pairs of the H&N case. The SDD is 1000 mm.

Discussion

2D detectors arrays are very effective tools in radiotherapy. They can be used to perform accurate QA of IMRT fields despite their low resolution [4,9], and they allow a gain in time in comparison to other methods such as film dosimetry. The main disadvantage, their low spatial resolution, is a technological issue with on-going improvements, and can be compensated by several methods, such as shifting the whole detector [9], or by using a holder at a longer distance. A comparison of the measured detector response and the predicted response is possible for every individual ionization chamber [4], with criteria set to determine whether a plan is correctly irradiated. This procedure gives a good indication of the plan quality, and can be performed with several detectors by knowing their response function. Concerning the MatriXX detector, this predicted/measured response analysis can be done directly via the COMPASS system, which provides such analysis. Nevertheless, this procedure is limited to a detector response comparison, and does not quantify the effect of possible delivery errors in terms of deposited dose inside the patient. The COMPASS system proposes a complementary approach which aims to reconstruct a 3D dose in a patient geometry by using the measurement information, a beam model and the treatment plan. This method allows a better understanding of the QA results, and can lead to a more robust and also more intuitive QA at a patient level, as described by several authors who used other systems of detection [6,7]. Such a procedure using a 2D detector array has clear advantages, but also presents drawbacks, at least at the current level of detector technology.

The major drawback of fluence reconstruction by using film measurements, is the necessity to do a time-consuming measurement per beam. Also, the measurement is relative, and such a method cannot provide information during the course of an irradiation. In comparison, a 2D detector array is able to monitor the irradiation during the delivery, and the analysis of the results is more straightforward. Such a procedure is more flexible and easier to integrate in a clinical routine. This procedure is comparable to EPID dosimetry, but its implementation is easier. Nevertheless, the limited resolution of current 2D arrays decreases the quality of the reconstruction. The method proposed inside the COMPASS system mitigates the low resolution effects but the implemented correction kernel comes with an artefact that leads to several inaccuracies. The first inaccuracy concerns the location dependency of the reconstruction. For IMRT fields with several segments, this effect is integrated and its impact is small for the quantification of an error, as seen in the clinical case of this paper. The second inaccuracy is due to the size of the correction kernel. It can create inaccuracies near field edges of individual IMRT segments.

This artefact can be misleading for the QA output, as the maximum dose in the hot area can be overestimated. It can also be expected that analysis with DVHs will suffer from this effect. A further study needs to be performed, which is beyond the scope of this paper.

In terms of QA capability, our results indicate that the correction kernel method allows an accurate determination of the mean gamma of evaluated plans. This aspect is fundamental to ensure good error detection with the system: the differences found on the number of points above gamma 1 suggest that COMPASS evaluation still ensures detection of MLC positioning errors via a gamma evaluation. At a large SDD, despite a smaller correction kernel, the misalignment of the leaf pairs and the matrix row reduces the gamma evaluation accuracy of the system. A configuration for which one row is aligned with one leaf pair has been found more reliable than a configuration that optimises the projected resolution.

An advantage of the COMPASS method is the possibility to use it with other detectors and irradiation techniques. Two detectors are at the moment available to perform the measurements and apply kernel corrections; the MatriXX detector [12] and the transmission detector, dedicated to on-line measurements [20]. The correction kernel method would also be usable with future detectors with potentially higher spatial resolution, which should decrease the size of the correction kernel. Also, 2D detector arrays seem ideal to monitor complex dynamic treatments plan such as arc therapy [21], due to the time resolved character of the measurements.

Overall, the effect of the correction kernel does not jeopardize the QA capability of the system, but one has to keep in mind that an artefact can occur at the edge of a treatment field. Errors in the beam delivery are detected by the system, and its location can be visualized in 3D. This information is expected to be usable by the physicist and the physician to determine whether the plan is acceptable or not, knowing that the localisation of the error is accurate within a few mm. Note that this paper focused only on inaccuracies introduced by the implemented correction kernel method in case of MLC leaf position errors by comparison of reconstructed dose with and without correction. This way, inaccuracies in the reconstructed dose without correction, e.g. caused by the fluence model, detector model and dose engine, were excluded from the investigation. Furthermore, detection of linac output errors were excluded, as this is directly linked to the detector detection capability that has already been described by Herzen *et al* [13].

Conclusion

The COMPASS dose reconstruction method uses a high resolution fluence map to compute 3D doses. If the delivered and the planned irradiation are similar, this offers a high resolution dose prediction. In case of errors during the beam delivery, the predicted fluence is corrected, and this correction can cause a blurring artefact of the dose. Nevertheless, the system is still able to accurately reconstruct the position of field edges with a maximum error of 2.5 mm. Also, inaccuracies in the reconstructed dose error can occur, up to 17% for large delivery errors, in small areas near the field edge, due to displacement of the dose during the reconstruction. In terms of plan evaluations, the mean gamma value is slightly overestimated by the COMPASS system. Furthermore, the number of points above gamma 1 is sufficiently accurate to ensure error detection. The correction kernel method used by the COMPASS system is thus suitable to perform QA of IMRT treatment plans. The correction kernel method is not bound to the particular detector or technique used in this study and may be applied to other detectors or situations.

Acknowledgements

The authors want to thank IBA dosimetry and Raysearch Laboratories for providing a research version of the COMPASS system.

References

- [1] Group IMRTCW, CWG I, Boyer AL, Butler EB, DiPetrillo TA, Engler MJ, Fraass B, Grant W, Ling CC, Low DA, Mackie TR, Mohan R, Purdy JA, Roach M, Rosenman JG, Verhey LJ, Wong JW, Cumberlin RL, et al. Intensity-modulated radiotherapy: current status and issues of interest. *Int J Radiat Oncol Biol Phys* 2001;51:880–914.
- [2] Ezzell GA, Galvin JM, Low D, Palta JR, Rosen I, Sharpe MB, Xia P, Xiao Y, Xing L, Yu CX. Guidance document on delivery, treatment planning, and clinical implementation of IMRT: report of the IMRT Subcommittee of the AAPM Radiation Therapy Committee. *Med Phys* 2003;30:2089–115.
- [3] Low DA, Dempsey JF, Markman J, Mutic S, Klein EE, Sohn JW, Purdy JA. Toward automated quality assurance for intensity- modulated radiation therapy. *Int J Radiat Oncol Biol Phys* 2002;53:443–52.
- [4] Poppe B, Blehschmidt A, Djouguela A, Kollhoff R, Rubach A, Willborn KC, Harder D. Two-dimensional ionization chamber arrays for IMRT plan verification. *Med Phys* 2006;33:1005–15.
- [5] Boellaard R, Essers M, van Herk M, Mijnheer BJ. New method to obtain the midplane dose using portal in vivo dosimetry. *Int J Radiat Oncol Biol Phys* 1998;41:465–74.
- [6] Renner WD, Sarfaraz M, Earl MA, Yu CX. A dose delivery verification method for conventional and intensity-modulated radiation therapy using measured field fluence distributions. *Med Phys* 2003;30:2996–3005.
- [7] Van Zijtveld M, Dirkx M, Breuers M, Kuipers R, Heijmen B. Evaluation of the “dose of the day” for IMRT prostate cancer patients derived from portal dose measurements and cone-beam CT. *Radiother Oncol* 2010;96:172–7.
- [8] van Elmpt W, Nijsten S, Mijnheer B, Dekker A, Lambin P. The next step in patient-specific QA: 3D dose verification of conformal and intensity-modulated RT based on EPID dosimetry and Monte Carlo dose calculations. *Radiother Oncol* 2008;86:86–92.
- [9] Poppe B, Djouguela A, Blehschmidt A, Willborn K, Rühmann A, Harder D. Spatial resolution of 2D ionization chamber arrays for IMRT dose verification: single-detector size and sampling step width. *Phys Med Biol* 2007;52:2921–35.
- [10] Dempsey JF, Romeijn HE, Li JG, Low DA, Palta JR. A Fourier analysis of the dose grid resolution required for accurate IMRT fluence map optimization. *Med Phys* 2005;32:380.
- [11] Ahnesjo A. Collapsed cone convolution of radiant energy for photon dose calculation in heterogeneous media. *Med Phys* 1989;16:577–92.

- [12] Amerio S, Boriano A, Bourhaleb F, Cirio R, Donetti M, Fidanzio A, Garelli E, Giordanengo S, Madon E, Marchetto F, Nastasi U, Peroni C, Piermattei A, Sanz Freire CJ, Sardo A, Trevisiol E. Dosimetric characterization of a large area pixel-segmented ionization chamber. *Med Phys* 2004;31:414–20.
- [13] Herzen J, Todorovic M, Cremers F, Platz V, Albers D, Bartels A, Schmidt R. Dosimetric evaluation of a 2D pixel ionization chamber for implementation in clinical routine. *Phys Med Biol* 2007;52:1197–208.
- [14] Sastre-Padro M, Welleweerd J, Malinen E, Eilertsen K, Olsen DR, van der Heide UA. Consequences of leaf calibration errors on IMRT delivery. *Phys Med Biol* 2007;52:1147–56.
- [15] Losasso T, Chui CS, Ling CC. Physical and dosimetric aspects of a multileaf collimation system used in the dynamic mode for implementing intensity modulated radiotherapy. *Med Phys* 1998;25:1919–27.
- [16] Low DA, Harms WB, Mutic S, Purdy JA. A technique for the quantitative evaluation of dose distributions. *Med Phys* 1998;25:656–61.
- [17] Menegotti L, Delana A, Martignano A. Radiochromic film dosimetry with flatbed scanners: A fast and accurate method for dose calibration and uniformity correction with single film exposure. *Med Phys* 2008;35:3078.
- [18] van Battum LJ, Hoffmans D, Piersma H, Heukelom S. Accurate dosimetry with GafChromic™ EBT film of a 6 MV photon beam in water: What level is achievable? *Med Phys* 2008;35:704.
- [19] Zhu Y, Kirov A, Mishra V, Meigooni A, Williamson J. Quantitative evaluation of radiochromic film response for two-dimensional dosimetry. *Med Phys* 1997;24:223–31.
- [20] Venkataraman S, Malkoske KE, Jensen M, Nakonechny KD, Asuni G, McCurdy BM. The influence of a novel transmission detector on 6 MV x-ray beam characteristics. *Phys Med Biol* 2009;54:3173–83.
- [21] Boggula R, Lorenz F, Mueller L, Birkner M, Wertz H, Stieler F, Steil V, Lohr F, Wenz F. Experimental validation of a commercial 3D dose verification system for intensity-modulated arc therapies. *Phys Med Biol* 2010;55:5619–33.

Chapter 3

Development of an iterative reconstruction method to overcome 2D detector low resolution limitations in MLC leaf position error detection for 3D dose verification in IMRT

R Visser
J Godart,
D J L Wauben
J A Langendijk
A A van 't Veld
E W Korevaar

Phys. Med. Biol. 61(2016) 3843-3856

Abstract

The objective of this study was to introduce a new iterative method to reconstruct multi leaf collimator (MLC) positions based on low resolution ionization detector array measurements and to evaluate its error detection performance. The iterative reconstruction method consists of a fluence model, a detector model and an optimizer. Expected detector response was calculated using a radiotherapy treatment plan in combination with the fluence model and detector model. MLC leaf positions were reconstructed by minimizing differences between expected and measured detector response. The iterative reconstruction method was evaluated for an Elekta SLi with 10.0 mm MLC leaves in combination with the COMPASS system and the MatriXX Evolution (IBA Dosimetry) detector with a spacing of 7.62 mm. The detector was positioned in such a way that each leaf pair of the MLC was aligned with one row of ionization chambers. Known leaf displacements were introduced in various field geometries ranging from -10.0 mm to 10.0 mm. Error detection performance was tested for MLC leaf position dependency relative to the detector position, gantry angle dependency, monitor unit dependency, and for ten clinical IMRT treatment beams. For one clinical head and neck IMRT treatment beam, influence of the iterative reconstruction method on existing 3D dose reconstruction artifacts was evaluated. The described iterative reconstruction method was capable of individual MLC leaf position reconstruction with millimeter accuracy, independent of the relative detector position within the range of clinically applied monitor units for IMRT. Dose reconstruction artifacts in a clinical IMRT treatment beam were considerably reduced as compared to the current dose verification procedure. The iterative reconstruction method allows high accuracy 3D dose verification by including actual MLC leaf positions reconstructed from low resolution 2D measurements.

Introduction

Advanced radiotherapy treatment modalities such as Intensity Modulated Radiotherapy (IMRT) and Volumetric Modulated Arc Therapy (VMAT) allow to generate steep 3D dose gradients by complex treatment plans that consist of many segments. The delivery of these steep dose gradients need to be carefully monitored to guarantee patient safety [1]. Various 3D dose verification methods have been described in literature based on independent dose calculations [2,3] or dose reconstruction by incorporating 2D measurements which enables the inclusion of actual linac output during dose verification [4–7].

A drawback of 2D detector array measurements is the spatial resolution which is limited by the size of a single elementary detector and the center-to-center distance between detectors. In particular detector arrays composed of ionization chambers have a limited resolution due to the relatively large detector spacing. Poppe *et.al.* showed that according to the Nyquist sampling theorem, IMRT dose reconstruction requires a detector with a spatial frequency of 0.4 mm^{-1} which is higher than commonly available [8]. Prior knowledge can help to overcome this limitation, e.g. by use of a lower resolution measurement as a correction to a high resolution calculation. An example is the COMPASS system (IBA Dosimetry) which reconstructs 3D dose in a patient CT based on 2D measurements obtained with a low resolution ionization chamber array (MatriXX, IBA Dosimetry). Differences between expected fluence and measured fluence due to incorrect multi leaf collimator (MLC) positioning are accounted for by a correction kernel method [9].

In a previous study, we showed the limitations of the MatriXX detector in combination with the COMPASS system to accurately reconstruct delivered dose in case of MLC leaf positioning errors [10]. The local dose reconstruction inaccuracies of the correction kernel method are expected to become more limiting artifacts as dose verification to patient specific structures becomes increasingly important [11,12]. In this study, a new iterative method to reconstruct actual leaf positions from low resolution 2D measurements was introduced. The method uses as prior knowledge the fact that energy fluence generated from a treatment head is dependent on a limited set of parameters. Thus, although the information density from 2D measurements is low, our hypothesis is that it is sufficient to determine multiple parameters affecting the energy fluence such as penumbra shape, jaw and MLC settings. The objective of this study was to introduce the iterative reconstruction method and to evaluate its error detection performance in reconstructing actual leaf positions which is necessary for correct 3D dose verification.

Material and method

Iterative reconstruction method

The iterative reconstruction method used for MLC leaf position reconstruction was implemented using Matlab (version R2014a). It consists of a fluence model, a detector model and an optimizer that minimizes differences between measured and modeled detector response by adjusting fluence model optimization parameters independent of the treatment planning system (figure 1). In terms of dose verification, MLC leaf positions were reconstructed and adjusted in the original RT-plan. The adjusted RT-plan and measured detector response was then used in combination with the COMPASS system (v2.0) and the planning CT for 3D dose reconstruction.

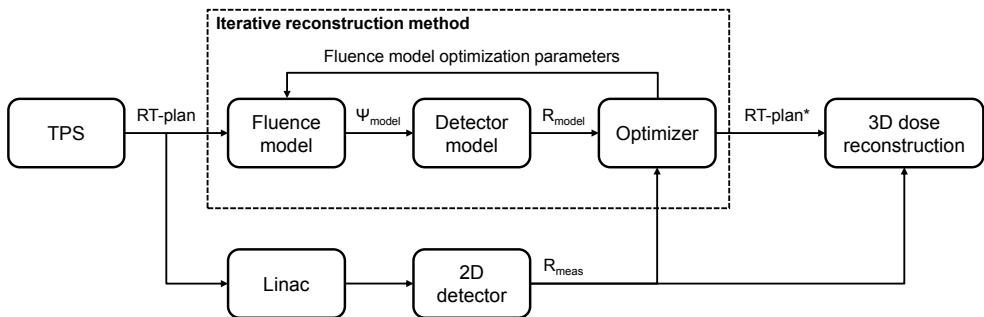


Figure 1:

Reconstruction of MLC positions by an iterative reconstruction method and 2D detector measurements. The initial fluence (Ψ_{model}) is based on the original treatment plan (RT-plan) from the treatment planning system (TPS). Subsequently, from the fluence model and the detector model, the detector response (R_{model}) is determined. Differences in calculated detector response and measured detector response (R_{meas}) were minimized by adjusting fluence model optimization parameters. For MLC position reconstruction, only a selection of source parameters and MLC leaf positions were optimized. Reconstructed MLC leaf positions were implemented in the original treatment plan (RT-plan) for a better representation of the actual given treatment plan which was eventually used in combination with the measured detector response for 3D dose reconstruction.*

Fluence model

The fluence generated by the linac head was modeled with an RT-plan and the fluence model with fluence model parameters that comprised of source parameters, jaw settings and MLC settings (table 1).

Table 1:

Fluence model optimization parameters. Each parameter could be optimized independently per IMRT segment (single optimization) or per IMRT treatment beam (group optimization). For MLC leaf position reconstruction, a selection of source parameters and MLC leaf positions were optimized.

Fluence model optimization parameters		Description
Source parameters	Penumbra	Penumbra shape for the primary and secondary fluence source in x and y direction. The slope was modeled using the error function and could be optimized in the +/-x and +/-y direction independently allowing asymmetrical beam modeling.
	Flattening filter	Non-flatness of the beam. The effect of the flattening filter is described by a rotational symmetry.
	Output	Output corrections for the primary and secondary fluence source.
	Weight	Relative weight of the primary fluence source relative to the secondary fluence source.
	Position	Primary and secondary fluence source position in x, y, and z direction simulating detector array shifts.
	Angle	Angle correction for the calculated fluence simulating detector array in-plane rotation.
Jaw settings	Position	Position offset of the x-jaw and y-jaw.
	Transmission	Transmission of the jaws.
Multi leaf collimator (MLC) settings	Leaf tip transmission	Systematic offset of all MLC leaves in the x-direction.
	Tongue and groove	Overlap of adjacent MLC leaves in the y-direction.
	Leaf position error	Shift MLC leaf in x-direction with respect to original RT-plan settings. The shift was optimized independently for all MLC leaves.

Detector model

The detector model describes the geometry of the MatriXX detector (IBA, Dosimetry) consisting of 1,020 ionization chambers (4.5 (\emptyset) mm x 5.0 (h) mm, 80.0 mm³). The detector response function of an individual ionization chamber of the MatriXX detector was simulated by Monte-Carlo simulations using ESGnrc code. A 6MV pencil beam of 1.0 mm wide was used for this simulation with an energy cutoff of 0.521 MeV and 0.010 MeV for electrons and photons respectively (figure 2).

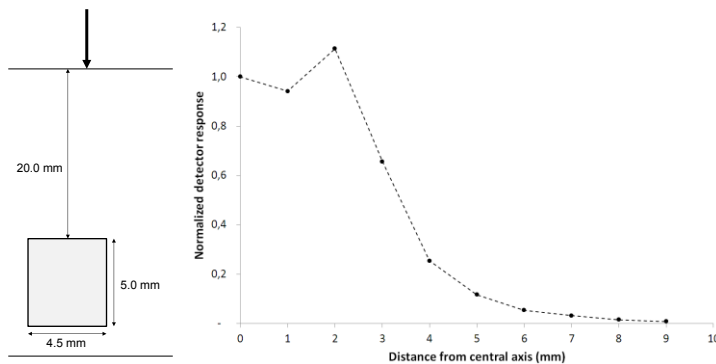


Figure 2:

Left: Monte Carlo setup of a 6MV pencil beam (arrow) simulation for an air filled ionization chamber (4.5 (∅) mm x 5.0 (h) mm, 80.0 mm³) with 20.0 mm build-up composed of water.

Right: Monte Carlo based detector response

function for a pencil beam displacement in the lateral direction normalized to the central axis of an individual ionization chamber. A clear peak in detector response is seen for a pencil beam position at the edge of the detector due to secondary electrons caused by detector material surrounding the air cavity.

Optimizer

Fluence model parameters were adjusted using the optimizer function *fminsearch* of Matlab. The optimizer minimized the difference between simulated detector response (R_{model}) and measured detector response (R_{meas}), formula 1.

$$\text{Minimize } \sum_{i=1}^n (R_{\text{model},i}(\psi_{\text{model}}(x)) - R_{\text{meas},i})^2 \quad (1)$$

with n the number of ionization chambers of the entire detector, ψ_{model} the energy fluence determined according to the fluence model, and x the fluence model optimization parameters. Optimization could be performed for each segment independently (e.g. output corrections) or per treatment beam (e.g. leaf position reconstruction).

Commissioning

Commissioning of the fluence model was performed using several treatment fields. A 20x26 cm² rectangular field was used to model the source parameters, jaw settings and leaf tip transmission. Furthermore, two complementary fields with several inserted MLC leaves were used for further modeling the source parameters and the tongue and groove effect of the MLC leaves.

2D detector measurements

Measurements were performed using the MatriXX Evolution detector (IBA dosimetry). The detection time per frame was 300 msec. The detector was fixed to the gantry head using a holder from IBA dosimetry. The measurements were performed using an Elekta SLI linac with an MLC leaf width projected at the isocenter of 10.0 mm and a nominal beam energy of 6MV. The detector consists of 1020 ionization chambers with a spacing of 7.62 mm and the source to detector distance was 762 mm, such that each leaf pair of the MLC was aligned with one row of ionization chambers on the detector. Details of the detector were previously published [13].

Film measurements

Film measurements were used to demonstrate the impact of reconstructed MLC leaf positions on the dose deposition for one clinical head and neck IMRT treatment field. Radiochromic films (Gafchromic EBT2, ISP Corp.) were positioned in coronal orientation in the middle of a 30x30x10 cm³ solid water phantom. The day after irradiation the films were scanned on a commercial flatbed scanner (V700, Epson), followed by conversion of optical density to dose. The conversion method was corrected for non-uniformity artifacts intrinsic in flatbed film scanners [14,15]. Film inhomogeneities were corrected using a double exposure procedure [16].

MLC leaf position reconstruction

MLC leaf position error detection performance of the iterative reconstruction method was evaluated for various error locations relative to the ionization chamber, a range of introduced error sizes, varying noise levels (i.e. monitor unit (MU) dependency), and for ten clinical IMRT treatment beams (each beam was obtained from a treatment plan of a different patient). First, the output was optimized per segment (single optimization). Second, the source position was optimized per treatment field (group optimization), and finally, individual MLC leaf positions were reconstructed per treatment field (group optimization). Furthermore, one clinical head and neck IMRT treatment beam was used to demonstrate the difference between the iterative reconstruction method and the correction kernel method [10] in comparison to film measurements. Iterative MLC leaf reconstruction was performed on a basic desktop PC (Intel Core 3.2 GHz), and all RT-plans were created using Pinnacle (v9.0).

Error location dependency

To test whether the accuracy of reconstructed leaf positions depended on the location of the MLC leaf tip relative to the ionization chambers, a rectangular field (10x26 cm²) covering half of the detector up to the middle with an MLC leaf position error of 5.0 mm was used (same treatment field as included in figure 4a in the results section). The 26 MLC leaves with off-axis leaf tip positions were moved 15.0 mm in steps of one millimeter, thus two ionization chambers were passed by each leaf.

Error size dependency

Error size dependency was tested using two treatment fields. The first field was identical to the treatment field used to evaluate the error location dependency; a rectangular field covering half of the detector up to the middle. MLC leaf position errors ranged from -1.0 mm to 5.0 mm. The second field was an irregular field (approximately 20x26cm²) with introduced MLC leaf position errors by inserting or retracting MLC leaves from -10.0 mm to 10.0 mm (same treatment field as included in figure 4b in the results section). Leaf displacements occurred every three leaves. Two subsequent leaves were kept at their nominal positions and every third leaf was displaced. This field was also used to test whether MLC leaves at their nominal position next to an MLC leaf with an introduced positional error were affected by the iterative reconstruction method.

Gantry angle dependency

Korevaar *et. al.* showed that dose verification performed with the MatriXX detector was affected by gravity due to changing gantry angles used for IMRT [9]. Whether gravity had an effect on MLC leaf position reconstruction was tested with the same irregular field used for error size dependency for a gantry angle of 0° and 90°.

Monitor unit dependency

Influence of the noise level for 2D measurements on the accuracy of MLC leaf position reconstruction was tested by varying MU's for irradiation. MU ranged from 2.5 MU (1 frame) to 200 MU (80 frames). The same irregular field as for the error size dependency was used.

Clinical IMRT treatment beams

Error detection performance of the iterative reconstruction method for clinical IMRT treatment beams was tested for ten patients (two prostate, and eight head and neck treatment plans). For each patient, one treatment beam was evaluated with an MLC leaf position error of 2.0 mm, 4.0 mm and 6.0 mm for randomly selected leaves. The treatment beams consisted of various segments ranging between 4 to 15 segments.

To demonstrate the effect of the iterative reconstruction method on the dose deposition in comparison to dose reconstruction artifacts caused by the correction kernel method, one treatment beam of a clinical head and neck IMRT treatment plan was used. The treatment beam was composed of 12 segments with introduced errors of 5.0 mm for five MLC leaves. The treatment beam was measured first with a high resolution film inside a solid-water phantom, and second using the MatriXX detector. Dose reconstruction based on MatriXX measurements was done using the COMPASS system (v2.0) on a 2x2x2 mm³ dose grid, with and without the iterative reconstruction method. When no iterative reconstruction was performed, differences in measured and calculated detector response were corrected only by the correction kernel. Measurements were performed at a gantry angle of 0°.

Results

Error location dependency

Error detection results for the rectangular field with an introduced error of 5.0 mm indicated that the reconstruction of the MLC leaf position was independent of the leaf position with respect to the ionization chamber positions. The introduced error was reconstructed with an accuracy of ± 0.5 mm for 15 consecutive MLC leaf positions on the detector (figure 3).

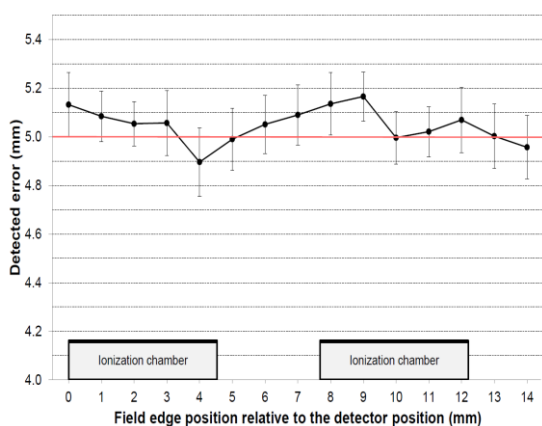


Figure 3:

Reconstruction of MLC leaf positions with 5.0 mm errors for the rectangular field at 15 consecutive MLC leaf positions. In red: actual leaf position. Each data point corresponds to the pooled mean reconstructed leaf position for all individual leaves (26 in total for each position). The error bars indicate one standard deviation of the pooled reconstructed leaf positions. Each MLC leaf passed at least two ionization chambers. The accuracy of reconstructed leaf positions was not affected by the projected leaf position on the detector.

Error size dependency

The iterative reconstruction method was capable of detecting MLC leaf position errors with millimeter accuracy (figure 4). For the rectangular field, error sizes ranging from -1.0 mm to 5.0 mm were correctly reconstructed for all leaves ($n=26$) with an accuracy within 1.0 mm. For the irregular field, reconstruction of individual MLC leaf positional errors ranging from -10.0 mm to 10.0 mm was performed with sub-millimeter accuracy for 98% of the leaves. Only one MLC leaf with an introduced error of -10.0 mm resulted in a residual error of -1.1 mm. The remaining errors were all reconstructed within -1.0 mm or 1.0 mm accuracy. For the irregular field, the iterative reconstruction method led to minor positional errors for individual MLC leaves which were positioned on their nominal position (*i.e.* an introduced error of 0.0 mm).

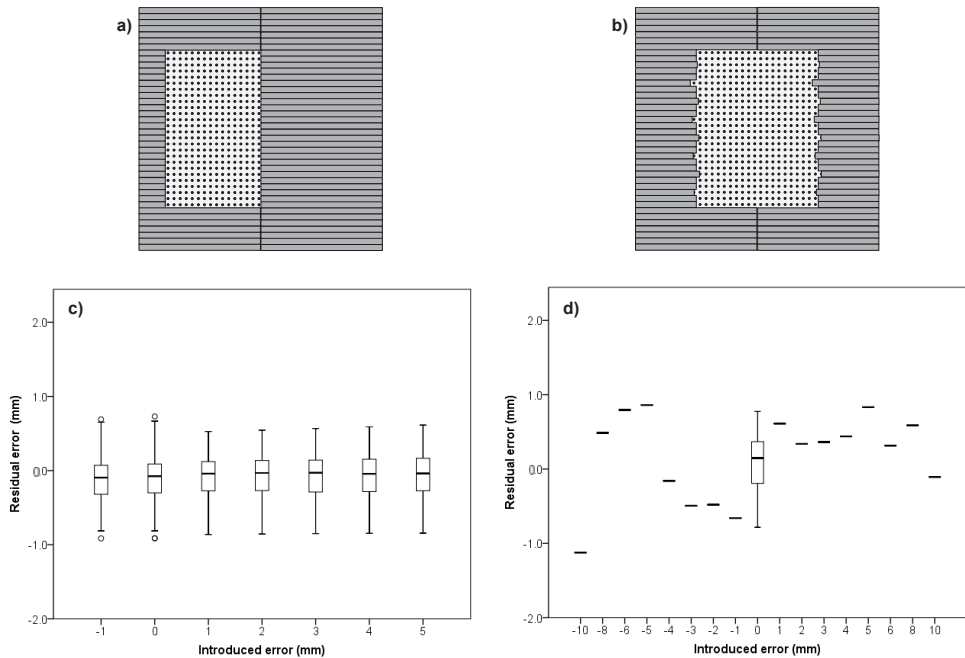


Figure 4:

Illustration of the rectangular (a) and irregular (b) treatment fields showing MLC and ionization chambers positions. The boxplots show the residual error of reconstructed MLC leaf positions compared to the actual leaf positions for the rectangular field (c with $n=26$ for each introduced error) and irregular field (d with $n=36$ for an introduced error of 0 mm, and $n=1$ for each other introduced error).

Gantry angle dependency

The iterative reconstruction method showed to be sensitive for the gantry angle used for irradiation. Due to the weight of the MatrixX detector and its holder, the system was affected by gravity resulting in reconstructed MLC leaf positions with a systematic offset of 0.52 ± 0.21 mm for the irregular field with a gantry angle of 90° .

Monitor unit dependency

The number of MU's had little effect on the accuracy of reconstruction of MLC leaf positions as the majority of MLC leaf positions changed less than 0.1 mm for measurements in the range of 2.5 MU to 200 MU (figure 5). Furthermore, variation of MLC leaf position change reduced with increasing monitor units.

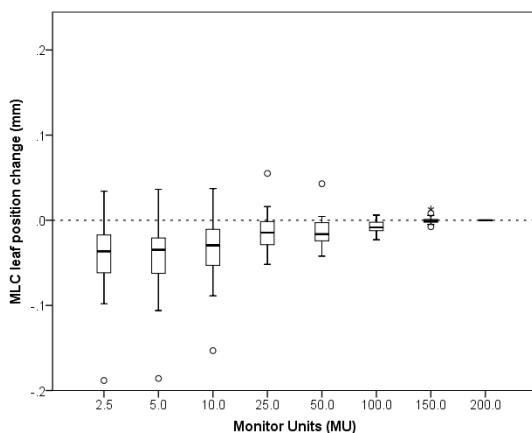


Figure 5:

Boxplot of the MLC leaf position change for varying monitor units ranging from 2.5 MU to 200 MU for the irregular treatment field. One detection frame of 300 msec corresponded to 2.5 MU. The MLC leaf position change was the difference with the residual error at 200 MU (80 frames) for all leafs (n=52). Outliers for 2.5, 5.0, 10.0, and 50.0 MU originated from one MLC leaf.

Clinical IMRT treatment beams

Introduced MLC leaf position errors of 2.0 mm, 4.0 mm and 6.0 mm for ten clinical IMRT treatment beams were reconstructed with millimeter accuracy (figure 6). The iterative reconstruction method resulted in a mean residual error of -0.04 ± 0.53 mm, 0.01 ± 0.62 mm, 0.27 ± 0.47 mm, and 0.40 ± 0.61 mm for MLC positional errors of 0.0 mm, 2.0 mm, 4.0 mm, and 6.0 mm respectively. For MLC leaves positioned at their nominal position, a residual error exceeding -1.0 mm or 1.0 mm was observed for 4.1% (n=15) of all MLC leafs (n=362). Furthermore, an underestimation of the introduced MLC leaf position error for three MLC leafs with an introduced error of 4.0 mm (one out of ten) and 6.0 mm (two out of ten) resulted in a residual error larger than 1.0 mm.

For a clinical head and neck IMRT treatment beam, the iterative reconstruction method reduced dose reconstruction artifacts (blurring caused by the correction kernel method) of the COMPASS system (figure 7). Note, MLC leaf position errors occurred in all 12 segments resulting in dose reconstruction errors at various positions. The correction kernel was applied to differences between measured and expected response caused by incorrect MLC leaf positioning. The iterative reconstruction method was able to correctly detect the 5.0 mm error

with a millimeter accuracy resulting in a residual error of 0.22 ± 0.35 mm. Using the corrected RT-plan with reconstructed MLC leaf positions, the dose reconstructed by the COMPASS system showed less blurring of the dose (figure 7d) than the correction kernel method (figure 7c), and was in better agreement with the film measurement (figure 7e). MLC leaf position reconstruction was performed within 17 minutes.

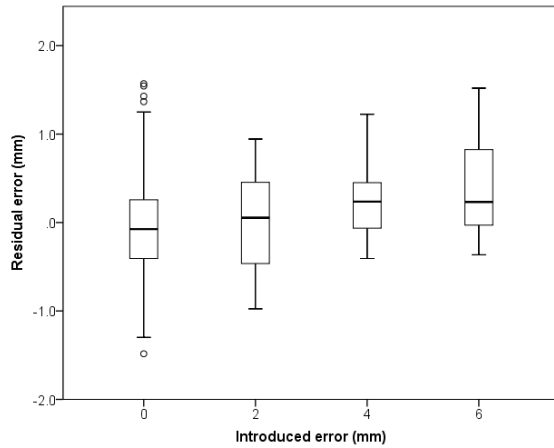


Figure 6:

Residual error of reconstructed MLC leaf positions for introduced errors of 0.0 mm (n=362), 2.0 mm (n=10), 4.0 mm (n=10), and 6.0 mm (n=10) for ten clinical IMRT treatment beams.

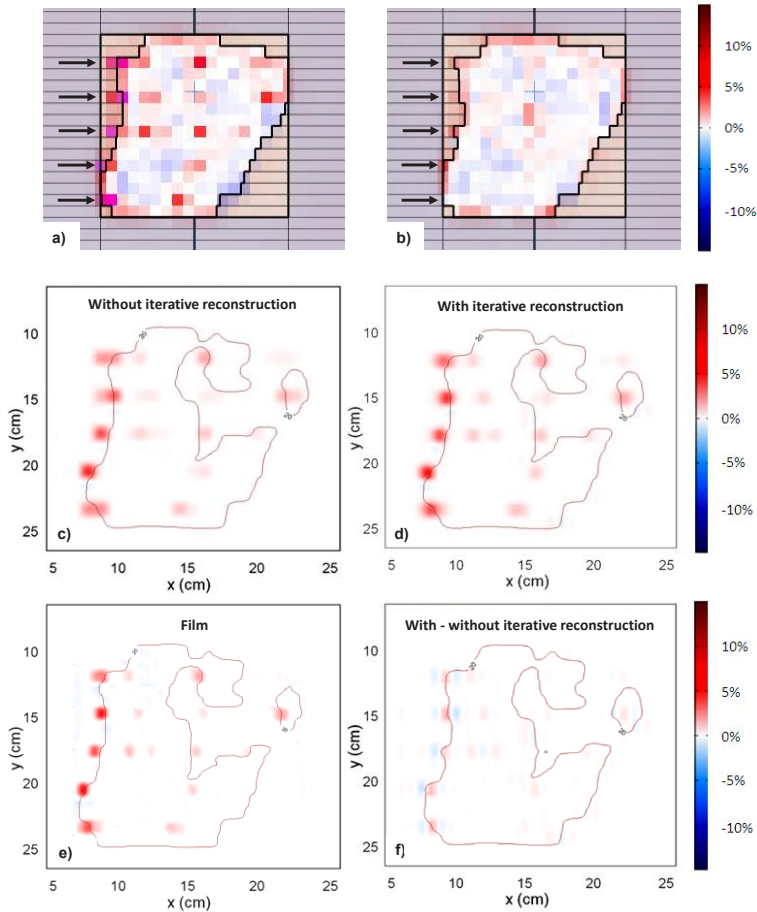


Figure 7:

Effect of 5.0 mm introduced position errors for five MLC leaves in all 12 IMRT segments of a clinical head and neck treatment beam. The top two images illustrate the difference between the expected and detected detector response for the COMPASS system without (a) and with (b) the iterative reconstruction method. The arrows indicate the MLC leaves for which errors were introduced. The middle and bottom images illustrate the dose differences (% relative to the prescribed dose for reconstructed dose with MLC leaf position errors minus reconstructed dose without MLC leaf position errors) as detected by the COMPASS system in combination with the correction kernel method (c), the COMPASS system in combination with the iterative reconstruction method (d), and film dosimetry (e; film dose with MLC leaf position errors minus film dose without MLC leaf position errors). The difference between the dose reconstructed by the COMPASS system with (c) and without (d) the iterative reconstruction method is given in (f). The 20 cGy isodose line is represented. The colorbar represents the dose differences caused by introduced MLC position errors.

Discussion

MLC leaf positions can be reconstructed successfully using an iterative reconstruction method in combination with low resolution 2D ionization chamber array measurements. Even with a spatial resolution of 1.0 cm (isocenter distance projected spacing between two ionization chambers of the MatriXX detector with a source to detector distance of 76.2 cm), MLC leaf positions were reconstructed with millimeter accuracy independent of the position of the MLC relative to the ionization chambers and for low MU's. This is in line with MLC leaf position reconstruction research discussed in literature [17,18]. Furthermore, results of this study showed that the iterative reconstruction method also introduces minor positional errors for MLC leafs with no introduced errors. The majority of these minor positional errors were all within -1.0 mm or 1.0 mm which complies with MLC leaf position tolerance levels discussed in the AAPM TG-142 report [19]. For the clinical IMRT treatment beam with introduced MLC leaf positional errors of 4.0 mm and 6.0 mm three out of twenty MLC leafs exceeded MLC leaf positional tolerance levels. For MLC leafs with positional errors after reconstruction, differences between calculated and measured detector response is detected by the COMPASS system and corrected for using the correction kernel method. Reconstructed leaf positions were in better agreement with leaf positions of the measurement for the iterative reconstruction method as compared to the correction kernel method, thus reducing dose reconstruction artifacts introduced by the correction kernel. When introducing such an MLC leaf position reconstruction system in clinical QA, MLC leaf position reconstruction accuracy should at least comply with the AAPM-TG 142 report [19]. The iterative reconstruction method would benefit from a faster calculation procedure as the reported reconstruction time of one clinical treatment beam composed of 12 segments takes about 17 minutes which is a drawback for routine clinical QA.

The described iterative reconstruction method allows robust MLC leaf position detection. Inclusion of actual linac output also enables the detection of a rotational and/or positional shift of the detector in the treatment field. Nevertheless, the fluence model is relatively simple and limited as multiple optimization parameters affect several beam properties. A skewed beam for instance can cause incorrect modeling of the penumbra slope. This underlines the need for accurate commissioning as described in literature [20]. For this study, the two treatment fields used for commissioning fluence parameters and MLC properties were found to be sufficient. Even so, one has to be aware that errors can occur even when commissioning has been performed accurately. This can be overcome by including a pre-irradiation to verify the beam model with the detector response prior to actual MLC leaf position reconstruction. Errors in the detector model can cause errors in

reconstructed MLC leaf positions as well. We found that after optimization, differences between measured and modeled detector response remained resulting in minor positional errors for MLC leaves with no introduced error. This could be caused by inaccuracies in the fluence and detector response models but also be attributed to limitations in the optimization related to incomplete convergence or the existence of local minima. Even so, the simplicity of the applied fluence and detector models illustrate the power of the iterative reconstruction method which lead to millimeter accuracy of MLC leaf position reconstruction enabling high accuracy 3D dose verification.

In theory, the described iterative reconstruction method can be used in combination with several detector types as the detector response function is exchangeable. An array of detector elements present nonetheless advantages in terms of dosimetry as the detector response functions of adjacent detector elements are overlapping which enables a measurement of the field edge displacement even between two detector elements. In this study, the measurement setup allowed only one pair of MLC leaves to block one row of ionization chambers. Therefore, the detector response function of a single ionization chamber was mainly affected by one MLC leaf. There are however situations, for instance using high resolution MLC systems, in which one leaf pair is not aligned with one row of ionization chambers. This can result in various MLC settings with a similar detector response. Further analyses are necessary to test the system for high resolution MLC systems.

Due to the weight of the detector and the holder, gravity effects appear and MLC leaf position reconstruction is affected by the gantry angle. This could be incorporated as a minor shift. Furthermore, because the detector has to be mounted on the linac and can only be used for pretreatment dose verification, no information can be obtained during the actual treatment. This could be solved by the use of a transmission detector [21,22], including MLC log file information [23,24] or by a different method of MLC position reconstruction [25].

For this study, the iterative reconstruction method was evaluated for IMRT which is based on a step and shoot approach. In theory, the described methodology is also applicable for VMAT or other techniques which introduce dynamic leaf displacement during treatment. This would require a modification of the fluence model to integrate fluence within a time interval; *e.g.* the time per control point. Different approaches of dynamic leaf displacement on dose reconstruction using EPID systems or Monte Carlo simulations have already been discussed in literature [26–28].

Conclusion

The introduced iterative reconstruction method is shown to allow reconstructing of individual MLC leaf positions with a millimeter accuracy using a low resolution ionization chamber detector array. By implementing reconstructed MLC leaf positions in the original RT-plan, the adjusted RT-plan gives a better representation of the actual given treatment enabling high accuracy 3D dose verification. The algorithm is independent of the position of the ionization chamber in the field, variations in MU's, and can reduce artifacts in dose reconstruction caused by incorrect MLC leaf positions such as reported previously in 3D dose reconstruction implementations. The introduced iterative reconstruction method is a universal method that is also suitable for other detector types.

References

- [1] Ezzell GA, Galvin JM, Low D, Palta JR, Rosen I, Sharpe MB, Xia P, Xiao Y, Xing L, Yu CX. Guidance document on delivery, treatment planning, and clinical implementation of IMRT: report of the IMRT Subcommittee of the AAPM Radiation Therapy Committee. *Med Phys* 2003;30:2089–115.
- [2] Anjum MN, Parker W, Ruo R, Aldahlawi I, Afzal M. IMRT quality assurance using a second treatment planning system. *Med Dosim* 2010;35:274–9.
- [3] Arumugam S, Xing A, Goozee G, Holloway L. Independent calculation-based verification of IMRT plans using a 3D dose-calculation engine. *Med Dosim* 2013;38:376–84.
- [4] Poppe B, Blehschmidt A, Djouguela A, Kollhoff R, Rubach A, Willborn KC, Harder D. Two-dimensional ionization chamber arrays for IMRT plan verification. *Med Phys* 2006;33:1005–15.
- [5] van Elmpt W, Nijsten S, Mijnheer B, Dekker A, Lambin P. The next step in patient-specific QA: 3D dose verification of conformal and intensity-modulated RT based on EPID dosimetry and Monte Carlo dose calculations. *Radiother Oncol* 2008;86:86–92.
- [6] Boggula R, Jahnke L, Wertz H, Lohr F, Wenz F. Patient-specific 3D pretreatment and potential 3D online dose verification of Monte Carlo-calculated IMRT prostate treatment plans. *Int J Radiat Oncol Biol Phys* 2011;81:1168–75.
- [7] Stathakis S, Myers P, Esquivel C, Mavroidis P, Papanikolaou N. Characterization of a novel 2D array dosimeter for patient-specific quality assurance with volumetric arc therapy. *Med Phys* 2013;40:71731.
- [8] Poppe B, Djouguela A, Blehschmidt A, Willborn K, Rühmann A, Harder D. Spatial resolution of 2D ionization chamber arrays for IMRT dose verification: single-detector size and sampling step width. *Phys Med Biol* 2007;52:2921–35.
- [9] Korevaar EW, Wauben DJ, van der Hulst PC, Langendijk JA, Van't Veld AA. Clinical introduction of a linac head-mounted 2D detector array based quality assurance system in head and neck IMRT. *Radiother Oncol* 2011;100:446–52.
- [10] Godart J, Korevaar EW, Visser R, Wauben DJL, Van't Veld AA. Reconstruction of high-resolution 3D dose from matrix measurements: error detection capability of the COMPASS correction kernel method. *Phys Med Biol* 2011;56:5029–43.
- [11] Chan MF, Li J, Schupak K, Burman C. Using a novel dose QA tool to quantify the impact of systematic errors otherwise undetected by conventional QA methods: clinical head and neck case studies. *Technol Cancer Res Treat* 2014;13:57–67.

- [12] Visser R, Wauben DJL, de Groot M, Steenbakkers RJHM, Bijl HP, Godart J, Van't Veld A a, Langendijk J a, Korevaar EW. Evaluation of DVH-based treatment plan verification in addition to gamma passing rates for head and neck IMRT. *Radiother Oncol* 2014;112:389–95.
- [13] Amerio S, Boriano A, Bourhaleb F, Cirio R, Donetti M, Fidanzio A, Garelli E, Giordanengo S, Madon E, Marchetto F, Nastasi U, Peroni C, Piermattei A, Sanz Freire CJ, Sardo A, Trevisiol E. Dosimetric characterization of a large area pixel-segmented ionization chamber. *Med Phys* 2004;31:414–20.
- [14] Menegotti L, Delana A, Martignano A. Radiochromic film dosimetry with flatbed scanners: A fast and accurate method for dose calibration and uniformity correction with single film exposure. *Med Phys* 2008;35:3078.
- [15] van Battum LJ, Hoffmans D, Piersma H, Heukelom S. Accurate dosimetry with GafChromic™ EBT film of a 6 MV photon beam in water: What level is achievable? *Med Phys* 2008;35:704.
- [16] Zhu Y, Kirov A, Mishra V, Meigooni A, Williamson J. Quantitative evaluation of radiochromic film response for two-dimensional dosimetry. *Med Phys* 1997;24:223–31.
- [17] Parent L, Seco J, Evans PM, Dance DR, Fielding A. Evaluation of two methods of predicting MLC leaf positions using EPID measurements. *Med Phys* 2006;33:3174–82.
- [18] Bayouth JE, Wendt D, Morrill SM. MLC quality assurance techniques for IMRT applications. *Med Phys* 2003;30:743–50.
- [19] Klein EE, Hanley J, Bayouth J, Yin F-F, Simon W, Dresser S, Serago C, Aguirre F, Ma L, Arjomandy B, Liu C, Sandin C, Holmes T. Task Group 142 report: Quality assurance of medical accelerators. *Med Phys* 2009;36:4197.
- [20] Ezzell GA, Burmeister JW, Dogan N, LoSasso TJ, Mechalakos JG, Mihailidis D, Molineu A, Palta JR, Ramsey CR, Salter BJ, Shi J, Xia P, Yue NJ, Xiao Y. IMRT commissioning: Multiple institution planning and dosimetry comparisons, a report from AAPM Task Group 119. *Med Phys* 2009;36:5359–73.
- [21] Boggula R, Lorenz F, Mueller L, Birkner M, Wertz H, Stieler F, Steil V, Lohr F, Wenz F. Experimental validation of a commercial 3D dose verification system for intensity-modulated arc therapies. *Phys Med Biol* 2010;55:5619–33.
- [22] Chang J, Heaton RK, Mahon R, Norrlinger BD, Jaffray D a., Cho Y-B, Islam MK. A method for online verification of adapted fields using an independent dose monitor. *Med Phys* 2013;40:72104.

- [23] Agnew A, Agnew C, Grattan M, Hounsell A, McGarry C. Monitoring daily MLC positional errors using trajectory log files and EPID measurements for IMRT and VMAT deliveries. *Phys Med Biol* 2014;59:N49-63.
- [24] Lee L, Le Q-T, Xing L. Retrospective IMRT dose reconstruction based on cone-beam CT and MLC log-file. *Int J Radiat Oncol Biol Phys* 2008;70:634-44.
- [25] Poppe B, Thieke C, Beyer D, Kollhoff R, Djouguela A, Ruhmann A, Willborn K, Harder D. DAVID--a translucent multi-wire transmission ionization chamber for in vivo verification of IMRT and conformal irradiation techniques. *Phys Med Biol* 2006;51:1237-48.
- [26] Fuangrod T, Woodruff HC, Rowshanfarzad P, O'Connor DJ, Middleton RH, Greer PB. An independent system for real-time dynamic multileaf collimation trajectory verification using EPID. *Phys Med Biol* 2014;59:61-81.
- [27] Rowshanfarzad P, Sabet M, Barnes MP, O'Connor DJ, Greer PB. EPID-based verification of the MLC performance for dynamic IMRT and VMAT. *Med Phys* 2012;39:6192.
- [28] Heath E, Seuntjens J. Development and validation of a BEAMnrc component module for accurate Monte Carlo modelling of the Varian dynamic Millennium multileaf collimator. *Phys Med Biol* 2003;48:4045-63.

Chapter 4

Reconstruction of high resolution MLC leaf positions using a low resolution detector for accurate 3D dose reconstruction in IMRT

Visser. R
Godart. J
Wauben. DJL
Langendijk. JA
van't Veld. AA
Korevaar. EW

Phys. Med. Biol. 61(2016) N642-N649

Abstract

In pre-treatment dose verification, low resolution detector systems are unable to identify shifts of individual leafs of high resolution multi leaf collimator (MLC) systems from detected changes in the dose deposition. The goal of this study was to introduce an alternative approach (the shutter technique) combined with a previous described iterative reconstruction method to accurately reconstruct high resolution MLC leaf positions based on low resolution measurements. For the shutter technique, two additional radiotherapy treatment plans (RT-plans) were generated in addition to the original RT-plan; one with even MLC leafs closed for reconstructing uneven leaf positions and one with uneven MLC leafs closed for reconstructing even leaf positions. Reconstructed leaf positions were then implemented in the original RT-plan for 3D dose reconstruction. The shutter technique was evaluated for a 6 MV Elekta SLi linac with 5 mm MLC leafs (Agility™) in combination with the MatriXX Evolution detector with detector spacing of 7.62 mm. Dose reconstruction was performed with the COMPASS system (v2.0). The measurement setup allowed one row of ionization chambers to be affected by two adjacent leaf pairs. Measurements were obtained for various field sizes with MLC leaf position errors ranging from 1.0 mm to 10.0 mm. Furthermore, one clinical head and neck IMRT treatment beam with MLC introduced leaf position errors of 5.0 mm was evaluated to illustrate the impact of the shutter technique on 3D dose reconstruction. Without the shutter technique, MLC leaf position reconstruction showed reconstruction errors up to 6.0 mm. Introduction of the shutter technique allowed MLC leaf position reconstruction for the majority of leafs with sub-millimeter accuracy resulting in a reduction of dose reconstruction errors. The shutter technique in combination with the iterative reconstruction method allows high resolution MLC leaf position reconstruction using low resolution measurements with sub-millimeter accuracy.

Introduction

Several techniques and systems have been described for pre-treatment dose verification of advanced radiotherapy treatment techniques such as intensity modulated radiotherapy (IMRT) [1–4]. The COMPASS system (IBA Dosimetry) is a pre-treatment dose verification system which can reconstruct a 3D dose deposition in patient CT data using 2D measurements obtained by an array of ionisation chambers (MatriXX, IBA Dosimetry). However, when measured using this method, limited spatial resolution is obtained. In relation to current high resolution multi leaf collimators (MLC) these low resolution detector arrays do not meet the Nyquist sampling theorem which could result in incorrect dose reconstruction [5]. This limitation is compensated for by the COMPASS system by using a correction kernel method, which corrects the calculated detector response used for dose calculations according to the measured detector response [6]. Even though the correction kernel reduces dose reconstruction artefacts allowing adequate pre-treatment dose verification, local dose inaccuracies still occur [7].

In a previous study we introduced an iterative reconstruction method to compensate for the limitation of low resolution detector arrays for high resolution dose reconstruction [8]. Based on 2D measurements and a simplified fluence model, detector model and optimizer, actual MLC leaf positions were reconstructed with millimetre accuracy and were well within tolerance levels (95% of the error counts <3.5 mm for step and shoot IMRT) as described in the AAPM-TG 142 report [9]. Reconstructed MLC leaf positions were adjusted in the original RT-plan for a better representation of the actual given treatment plan. The iterative reconstruction method was tested for an MLC consisting of one centimetre leafs. The measurement setup allowed one row of ionisation chambers to be affected by one leaf pair during measurements. Technological developments have led to new improved MLC's with leafs of less than one centimetre. For the MatriXX detector, one row of ionisation chambers can then be affected by multiple leaf pairs which could lead to a similar detector response for different MLC leaf positions. This effect has not been accounted for by the iterative reconstruction method and can result in incorrect reconstruction of actual MLC leaf positions. Therefore, the main objective of this study was to demonstrate the impact of incorrect MLC leaf position reconstruction on 3D dose reconstruction using the COMPASS system and to introduce an alternative approach to accurately reconstruct leaf positions of a high resolution MLC based on low resolution detector measurements.

Materials and Methods

Radiotherapy treatment plans (RT-plan) were generated in Pinnacle (v9.0) and 2D measurements were obtained with an ionization chamber array (MatriXX Evolution, IBA Dosimetry). The detector was mounted on a 6MV Elekta SLi linac with a high resolution MLC consisting of 5.0 mm leafs (Agility™). One row of ionization chambers could be affected by two adjacent leaf pairs due to a detector spacing of 7.62 mm and a source to detector distance of 762 mm.

To reduce 3D dose reconstruction errors caused by the combination of incorrect MLC leaf positioning, high resolution of the MLC, and the characteristics of the correction kernel method implemented in the COMPASS system [7], an alternative approach was introduced. The original treatment plan was adjusted in such a way that the detector response of a single ionization chamber row was affected by one MLC leaf pair instead of two. This was realized by closing even or uneven leafs during MLC leaf position reconstruction, assuming that individual MLC leaf positions errors were systematic and unaffected by neighbouring leafs during the process. Therefore, for each original RT-plan, two new RT-plans were created using Matlab (version R2014a); one with even leafs closed and one with uneven leafs closed; *i.e.* the shutter technique. Uneven MLC leaf positions were reconstructed using the RT-plan with even leafs closed and even MLC leaf positions were reconstructed using the RT-plan with uneven leafs closed. Finally, reconstructed MLC leaf positions were implemented in the original RT-plan which was used for 3D dose verification using the COMPASS system (v2.0). When no shutter technique was applied, differences between expected and measured detector response were corrected using the correction kernel method implemented in the COMPASS system [6].

Iterative reconstruction method

MLC leaf positions were reconstructed using an in house developed (Matlab R2014a) iterative reconstruction method as described in our previous study [8]. It consists of a simplified fluence model, a detector model and an optimizer (figure 1). Based on a radiotherapy treatment plan (RT-plan) a fluence is calculated. The calculated fluence is then used in combination with the detector model to predict the expected detector response. Subsequently, the optimizer minimized the differences between the expected and measured detector response by adjusting MLC leaf positions.

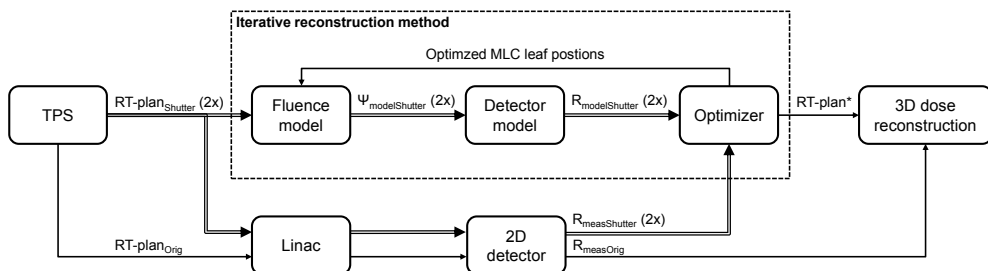


Figure 1:

Flow chart of 3D dose verification using high resolution MLC's and low resolution 2D detector measurements in combination with the iterative reconstruction method. Based on the original treatment plan ($RT\text{-}plan_{orig}$), two new treatment plans were generated using Matlab with even and uneven MLC leafs closed ($RT\text{-}plan_{Shutter}(2x)$); i.e. the shutter technique. Based on the expected fluence of the two newly created RT-plans ($\psi_{ModelShutter}(2x)$), expected detector responses were calculated ($R_{ModelShutter}(2x)$). Differences between expected and measured detector responses ($R_{MeasShutter}(2x)$) were then minimized by optimizing MLC leaf positions. Reconstructed MLC leaf positions were finally implemented in the original treatment plan ($RT\text{-}plan^*$) and used for 3D dose verification in combination with the measurement of the original treatment field ($R_{MeasOrig}$).

3D dose reconstruction error

For a 3D dose reconstruction performed with the COMPASS system, the correction kernel method only corrects for differences between expected and measured detector response. And because a low resolution detector can give a single detector response for various MLC leaf positions, completely different 3D dose reconstructions can be calculated for a single measurement. To illustrate this limitation, two rectangular fields of $15 \times 20 \text{ cm}^2$, one with even leafs closed and one with uneven leafs closed were used. For both treatment fields, the detector response was obtained using the MatrixX detector and the dose was reconstructed in a $30 \times 30 \times 10 \text{ cm}^3$ solid water phantom on a $2 \times 2 \times 2 \text{ mm}^3$ dose grid using the COMPASS system.

Film measurements

Film measurements of a clinical head and neck IMRT treatment field were used to demonstrate the impact of MLC leaf position reconstruction on the dose deposition. Radiochromic films (Gafchromic EBT2, ISP Corp.) were placed in the middle of a 30x30x10 cm³ solid water phantom and scanned on a commercial flatbed scanner (V700, Epson) the day after irradiation. Conversion of optical density to dose was corrected for non-uniformity artefacts of the flatbed scanner [10,11], and a double exposure procedure technique was performed to correct for film inhomogeneities [12].

MLC leaf position reconstruction

Error size dependency

Error size dependency was tested using one rectangular treatment field of approximately 15x20 cm² with introduced leaf position errors ranging from 1.0 mm to 10.0 mm in the left and right MLC leaf bank. Leaf displacements were introduced every four leaves. One leaf was displaced and three subsequent MLC leaves were kept at their nominal position. MLC leaf positions were reconstructed with and without the shutter technique. For the shutter technique, two additional RT-plans were created and two additional 2D detector array measurements were obtained.

Clinical head and neck IMRT treatment beam

One IMRT treatment beam of a clinical head and neck cancer patient was used to illustrate the effect of MLC leaf position reconstruction on the dose deposition. The dose reconstruction performed with the correction kernel method and shutter technique were evaluated with film measurements as a reference. The beam consisted of 13 segments with an introduced 5.0 mm leaf positioning error for five MLC leaves. MLC leaf positions were reconstructed as a systematic offset for all segments.

Results

3D dose reconstruction error

Measurements obtained for two rectangular fields ($15 \times 20 \text{ cm}^2$), one with even leaves closed, and one with uneven leaves closed resulted in a similar detector response (figure 2). Due to a minimal offset of the collimator block with retracted leaves behind it the effective leaf opening at the edge of the field was larger resulting in a peak in detector response at position -10.0 cm for the measurement with even leaves closed (figure 2, top left). As expected, for each treatment field the reconstructed dose showed different dose profiles due to different MLC leaf positioning (figure 2, right). However, information on MLC positioning could not be derived from the difference in detector response (figure 2, left). These results confirmed that a similar detector response could correspond to completely different dose depositions emphasizing the need for accurate MLC leaf position reconstruction for accurate dose verification.

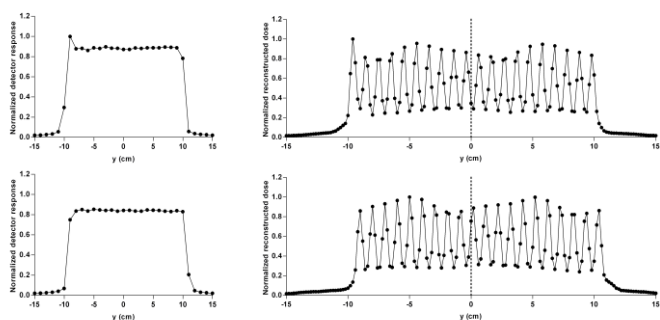


Figure 2:

A similar detector response (left) with different dose reconstruction results (right) for a rectangular treatment field ($15 \times 20 \text{ cm}^2$) with even leaves closed (top) and uneven leaves closed (bottom). The y-direction is perpendicular

to the direction of the movement of MLC leaves. Detector response and reconstructed dose was normalized to the maximum value of the treatment field with even leaves closed.

Error size dependency

The shutter technique resulted in a substantial improvement of MLC leaf position error detection (figure 3). For the shutter technique, the majority of MLC leaf positions were reconstructed with sub-millimeter accuracy. Without the shutter technique, the iterative reconstruction method was unable to discriminate between the contribution of two neighbouring MLC leaves to one detector row of ionization chambers resulting in large residual errors (up to 6.0 mm) for two neighbouring leaves.

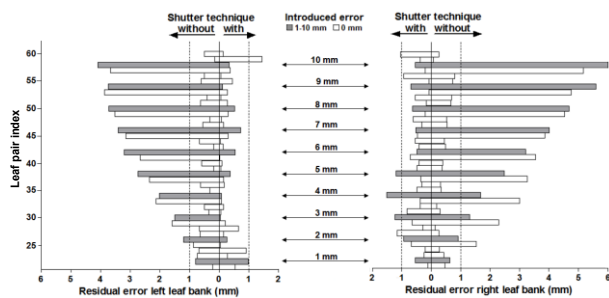


Figure 3: Residual error of reconstructed MLC leaf positions for 40 leaf pairs of the left and right leaf bank. MLC leaf positions were reconstructed with and without the shutter technique for leaves placed at their nominal position (white) and for leaves with introduced errors (grey) ranging from 1.0 mm to 10.0 mm. The vertical dashed line shows the boundary of a residual error of 1.0 mm.

Clinical head and neck IMRT treatment beam

For the shutter technique, introduced MLC leaf position errors of 5.0 mm for five MLC leaves were reconstructed with sub-millimeter accuracy. Consequently, the shutter technique showed a better dose difference agreement between the expected (figure 4B) and reconstructed (figure 4C) dose error for MLC leaves with positional errors in comparison to the correction kernel method (figure 4A). For the film measurement (figure 4B), minor over- and under dosage were seen at the edges of the treatment field indicating a film registration inaccuracy in the lateral direction. In total, 2 out of 54 MLC leaves positioned at their nominal position resulted in a residual error larger than 1.0 mm (1.2 mm and 1.3 mm). Consequently over dosage artefacts were seen in the top middle part of the treatment field caused by these specific two MLC leaves (figure 4C).

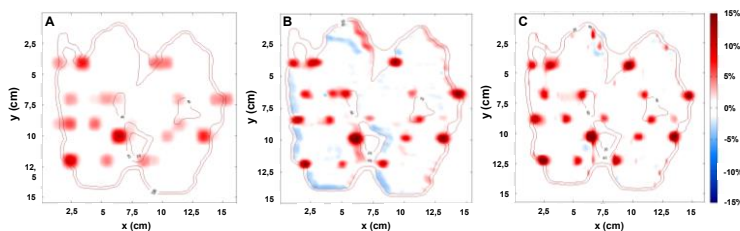


Figure 4: Reconstructed dose errors due to MLC leaf position errors determined from film measurement (B) and reconstructed dose error without (A) and with (C) the shutter technique. Blue corresponded to an underdosage, thus an MLC leave was shifted in the treatment field, blocking part of the fluence. Red corresponded to an overdosage, thus an MLC leave was shifted outside the treatment field. The 20 cGy and 40 cGy is represented. The colorbar represents the percentage dose differences relative to the prescribed dose caused by MLC leaf position errors. Comparison of difference between (A) and (B) versus difference between (C) and (B) shows that the shutter technique better identifies the introduced errors.

Discussion

Results of this study showed that the iterative reconstruction method combined with the principle of the shutter technique allows accurate leaf position reconstruction of high resolution MLC using low resolution detector array measurements and the combined method was found suitable for 3D dose verification purposes. Dose reconstruction errors of the shutter technique showed a better similarity with film measurements in comparison to dose reconstruction errors of the correction kernel method used by the COPMASS system in case of an MLC leaf position mismatch. Although the film measurements showed to have a mis-registration in the lateral direction, no increase in blurring of the reconstructed dose error is expected and therefore the similarity between error reconstruction with the shutter technique is expected superior to error reconstruction without the shutter technique. By implementing reconstructed MLC leaf positions in the RT-plan, a better representation of actual leaf positions was used for dose verification and dose reconstruction errors otherwise introduced by the correction kernel method were therefore reduced.

For the measurement setup of this study two adjacent leafs affected one row of ionization chambers. By reconstructing even and uneven MLC leaf positions independently, the contribution of even and uneven leafs to the treatment field could be determined correctly allowing accurate leaf position reconstruction. Whenever three or more MLC leafs affect one row of ionization chambers, the current approach will most likely be inadequate. As an alternative to the shutter technique, Poppe *et. al.* introduced an alternative method by shifting the detector parallel and/or perpendicular to the MLC leafs which also shows potential for high resolution dose reconstruction using low resolution detector arrays [5]. Even though this technique showed to be appropriate for dose verification purposes of IMRT, no conclusive information on individual high resolution MLC leaf positions can be derived due to the relatively low resolution of the measurement in relation to the leafs. This could be improved by adjusting the detector model of the iterative reconstruction method as it is applicable for various linear accelerators and detector systems when modelled correctly.

Error detection performance can be affected by inaccuracies in the detector model, fluence model, optimizer and/or the MLC system itself. The contribution of each source to incorrect leaf position reconstruction is difficult to determine. Nevertheless, the iterative reconstruction method has already been tested thoroughly and showed to be capable of accurately reconstructing MLC leaf positions errors independent of the position of the leaf position error in the treatment field, the size of the leaf position error, the gantry angle

and the number of monitor units [8]. For the high resolution MLC system used in this study modelling of the fluence model showed to be difficult. This is currently performed with the same detector as used for MLC leaf position reconstruction. In particular the tongue and groove effect was difficult to model due to the low detector resolution. Even so, the majority of all MLC leafs were reconstructed with sub-millimeter accuracy and were well within MLC leaf position tolerance levels for step and shoot IMRT (95% of the error counts <3.5 mm) as discussed in the AAPM TG-142 report [9].

An important limitation of the shutter technique is the reduction of time efficiency as it is a labour intensive procedure. And even though several aspects of the shutter technique such as obtaining two extra RT-plans can be automated, the described approach still demands two additional measurements which decreases efficiency substantially. Furthermore, as the number of complex radiotherapy treatments which need pre-treatment dose verification increases, departmental resources need to be used efficiently. Nevertheless, research has shown that a department with a high quality treatment machine, competent staff and an accurately modelled treatment planning system can achieve a pass rate of 99.5% for treatment plans with no relevant dose differences [13]. This underlines the possibility of performing pre-treatment dose verification by dose calculations without the need for a measurement-based dose reconstruction for each individual RT-plan consequently improving the efficiency of the quality assurance procedure [14].

Conclusion

The iterative reconstruction method combined with the described shutter technique allows high resolution MLC leaf position reconstruction using low resolution measurements. By reconstructing even and uneven MLC leaf positions independently, low resolution ionization chamber array measurements can be used for pre-treatment high resolution 3D dose verification.

References

- [1] Carrasco P, Jornet N, Latorre A, Eudaldo T, Ruiz A, Ribas M. 3D DVH-based metric analysis versus per-beam planar analysis in IMRT pretreatment verification. *Med Phys* 2012;39:5040.
- [2] van Elmpt W, Nijsten S, Mijnheer B, Dekker A, Lambin P. The next step in patient-specific QA: 3D dose verification of conformal and intensity-modulated RT based on EPID dosimetry and Monte Carlo dose calculations. *Radiother Oncol* 2008;86:86–92.
- [3] Stathakis S, Myers P, Esquivel C, Mavroidis P, Papanikolaou N. Characterization of a novel 2D array dosimeter for patient-specific quality assurance with volumetric arc therapy. *Med Phys* 2013;40:71731.
- [4] Boggula R, Jahnke L, Wertz H, Lohr F, Wenz F. Patient-specific 3D pretreatment and potential 3D online dose verification of Monte Carlo-calculated IMRT prostate treatment plans. *Int J Radiat Oncol Biol Phys* 2011;81:1168–75.
- [5] Poppe B, Djouguela A, Blechschmidt A, Willborn K, Rühmann A, Harder D. Spatial resolution of 2D ionization chamber arrays for IMRT dose verification: single-detector size and sampling step width. *Phys Med Biol* 2007;52:2921–35.
- [6] Korevaar EW, Wauben DJ, van der Hulst PC, Langendijk JA, Van't Veld AA. Clinical introduction of a linac head-mounted 2D detector array based quality assurance system in head and neck IMRT. *Radiother Oncol* 2011;100:446–52.
- [7] Godart J, Korevaar EW, Visser R, Wauben DJL, Van't Veld AA. Reconstruction of high-resolution 3D dose from matrix measurements: error detection capability of the COMPASS correction kernel method. *Phys Med Biol* 2011;56:5029–43.
- [8] Visser R, Godart J, Wauben DJL, Langendijk JA, Veld AA van't, Korevaar EW. Development of an iterative reconstruction method to overcome 2D detector low resolution limitations in MLC leaf position error detection for 3D dose verification in IMRT. *Phys Med Biol* 2016;61:N49.
- [9] Klein EE, Hanley J, Bayouth J, Yin F-F, Simon W, Dresser S, Serago C, Aguirre F, Ma L, Arjomandy B, Liu C, Sandin C, Holmes T. Task Group 142 report: Quality assurance of medical accelerators. *Med Phys* 2009;36:4197.
- [10] Menegotti L, Delana A, Martignano A. Radiochromic film dosimetry with flatbed scanners: A fast and accurate method for dose calibration and uniformity correction with single film exposure. *Med Phys* 2008;35:3078.
- [11] van Battum LJ, Hoffmans D, Piersma H, Heukelom S. Accurate dosimetry with GafChromic™ EBT film of a 6 MV photon beam in water: What level is achievable? *Med Phys* 2008;35:704.

- [12] Zhu Y, Kirov A, Mishra V, Meigooni A, Williamson J. Quantitative evaluation of radiochromic film response for two-dimensional dosimetry. *Med Phys* 1997;24:223–31.
- [13] Olson AC, Wegner RE, Scicutella C, Heron DE, Greenberger JS, Huq MS, Bednarz G, Flickinger JC. Quality assurance analysis of a large multicenter practice: does increased complexity of intensity-modulated radiotherapy lead to increased error frequency? *Int J Radiat Oncol Biol Phys* 2012;82:e77-82.
- [14] Visser R, Wauben DJL, de Groot M, Godart J, Langendijk JA, Van't Veld AA, Korevaar EW. Efficient and reliable 3D dose quality assurance for IMRT by combining independent dose calculations with measurements. *Med Phys* 2013;40:21710.

Chapter 5

**Efficient and reliable 3D dose quality assurance
for IMRT by combining independent dose
calculations with measurements**

Visser. R
Wauben. DJL
de Groot. M
Godart. J
Langendijk. JA
van't Veld. AA
Korevaar. EW

Med. Phys. 40(2013) 021710

Abstract

Purpose: Advanced radiotherapy treatments require appropriate Quality Assurance (QA) to verify 3D dose distributions. Moreover, increase in patient numbers demand efficient QA-methods. In this study, a time efficient method that combines model-based QA and measurement-based QA was developed; *i.e.* the hybrid-QA. The purpose of this study was to determine the reliability of the model-based QA and to evaluate time efficiency of the hybrid-QA method.

Material and method: Accuracy of the model-based QA was determined by comparison of COMPASS calculated dose with Monte Carlo calculations for heterogeneous media. In total, 330 intensity modulated radiation therapy (IMRT) treatment plans were evaluated based on the mean gamma index (GI) with criteria of 3%/3mm and classification of PASS ($GI \leq 0.4$), EVAL ($0.4 < GI < 0.6$) and FAIL ($GI \geq 0.6$). Agreement between model-based QA and measurement-based QA was determined for 48 treatment plans, and linac stability was verified for 15 months. Finally, time efficiency improvement of the hybrid-QA was quantified for four representative treatment plans.

Results: COMPASS calculated dose was in agreement with Monte Carlo dose, with a maximum error of 3.2% in heterogeneous media with high density (2.4 g/cm^3). Hybrid-QA results for IMRT treatment plans showed an excellent PASS rate of 98% for all cases. Model-based QA was in agreement with measurement-based QA, as shown by a minimal difference in GI of 0.03 ± 0.08 . Linac stability was high with an average GI of 0.28 ± 0.04 . The hybrid-QA method resulted in a time efficiency improvement of 15 minutes per treatment plan QA compared to measurement-based QA.

Conclusions: The hybrid-QA method is adequate for efficient and accurate 3D dose verification. It combines time efficiency of model-based QA with reliability of measurement-based QA and is suitable for implementation within any radiotherapy department.

Introduction

Radiotherapy treatment techniques like Intensity Modulated Radiation Therapy (IMRT) and Intensity Modulated Arc Therapy (IMAT) may result in complex dose distributions with numerous high dose gradient regions. These high dose gradients allow better sparing of organs at risk compared to 3D-CRT techniques [1,2] and demand appropriate quality assurance (QA) in terms of dose verification. Since conventional 2D-based QA-techniques (e.g. with film or detector arrays) are reported to be less sensitive to high dose gradients [3,4], new QA-techniques are needed.

Recently, IMRT-QA techniques have been developed to verify a dose distribution in 3D in a patient CT-data set based on either a pre-treatment dose calculation (model-based QA) [5,6], a pre-treatment dose reconstruction (measurement-based QA) [7,8] or with portal imaging during treatment allowing on-line verification [9]. As on-line verification QA methods generally involve extensive analysis procedures that require profound in-house expertise, pre-treatment measurement-based QA is still very popular and is considered in many radiotherapy centers as the standard.

Since pre-treatment measurement-based QA is time consuming, the already limited personnel and practical access to the linear accelerator (linac) threatens to impose practical limitations on QA needed for modern treatment techniques. Therefore, time efficient QA is essential to keep the required level of QA in pace with the increasing number of treatment plans that need 3D-QA.

A tempting solution to achieve a more time efficient QA is to switch from measurement-based QA to model-based QA. The consequence of this switch in QA-method is that verification of correct data transfer of the treatment plan to the linac is not included, nor the effect of incorrect linac output, leaf settings and gantry/collimator angle, *i.e.* linac behavior. However, if these verifications can be handled in other ways, the question is justified whether all or just a representative part of the treatment plans needs to be verified by a time consuming measurement-based QA. In addition, Olson *et. al.* showed that for the vast majority of treatment plans (>99.5%), no dose delivery error occurs implying the possibility of less measurement-based QA [10].

In this study, a combination of model-based QA and measurement-based QA; *i.e.* the hybrid-QA, was investigated to obtain a QA-method that combines time efficiency of dose calculations with reliability of measurements. The aim of this paper is to evaluate the hybrid-QA method for IMRT treatment plans. First, the accuracy of the model-based QA will be determined and second, the new hybrid-QA method will be evaluated in terms of reliability and time efficiency.

Material and Method

Model-based QA and measurement-based QA

In this study, the COMPASS system (version 1.2, IBA Dosimetry, Schwarzenbruck, Germany) was used for the hybrid-QA method as it can perform both model-based QA and measurement-based QA. The COMPASS system is a QA-tool that can be used to determine 3D dose deposition in a CT-data set independent from the treatment planning system (TPS). Based on water phantom measurements and linac specific parameters, multiple fluence models for various linacs can be configured and validated. The 3D dose deposition in patient CT is determined by either a dose calculation (model-based) or a dose reconstruction (measurement-based).

The model-based dose calculation is based on a commissioned fluence model and a dose engine. According to treatment plan parameters obtained from the RT-plan, fluence is calculated and combined with the CT-data set to calculate a 3D dose deposition.

The measurement-based dose reconstruction takes into account linac behavior by incorporating information of a 2D measurement obtained with an ionization chamber array (MatriXX, IBA Dosimetry). First, fluence is calculated according to treatment parameters similar to the model-based dose calculation. Second, a detector response is predicted and compared to the measured response. According to the difference between the predicted and measured response, the calculated fluence is corrected using a correction kernel [11,12]. Finally, the corrected fluence is used for dose calculation in the CT-data set.

Recent published work compared the measurement-based dose calculation performed with the COMPASS system to film measurements and concluded that the measurement-based dose calculation is adequate for dose verification of IMRT treatment plans [11–13]. However, verification of the model-based dose calculation for heterogeneous media is still the missing part for the introduction of the hybrid-QA method. Therefore, validation of the model-based dose calculation for heterogeneous media is needed to assess its accuracy and reliability for any specific indication and technique before the hybrid-QA method can be introduced.

COMPASS model-based dose calculation verification

COMPASS dose calculations were verified by comparison with Monte Carlo dose calculations and our clinical TPS (Pinnacle version 8.0h, Philips Radiation Oncology Systems, Madison, USA), all calculated on a $2 \times 2 \times 2 \text{ mm}^3$ dose grid. The Monte Carlo linac model was

created in BEAMnrc (version 2010) [14] and dose calculations were computed with DOSXYZnrc (version 2010) and validated against water phantom measurements. Six artificial CT phantoms were created with heterogeneities in a range from 0.0 to 2.4 g/cm³. Four phantoms consisted of 50x50x50 cm³ water with a 2.5 cm diameter cylinder of 0.0, 1.8, 2.0 or 2.4 g/cm³ density, respectively, at 10 cm depth. The remaining two phantoms represented patient-like geometries; one simulated a lung geometry with a tumor inside (densities of 0.25, 1.0 and 1.2 g/cm³) and the other represented a hip geometry that included tumor and bone tissue (densities of 1.0, 1.2 and 1.8 g/cm³).

Hybrid-QA

The hybrid-QA method (figure 1) combined COMPASS calculated dose (model-based QA) and COMPASS reconstructed dose (measurement-based QA). In the model-based QA, TPS calculated dose was compared with COMPASS calculated dose as independent dose verification. In the measurement-based QA, the TPS calculated dose was compared with COMPASS reconstructed dose in order to include data transfer and linac behavior in the verification. Reliability of the hybrid-QA was evaluated by comparing model-based QA with measurement-based QA results for a selection of approved treatments. In addition, stability of linac IMRT delivery was verified by a monthly evaluation of a standard head and neck IMRT treatment plan.

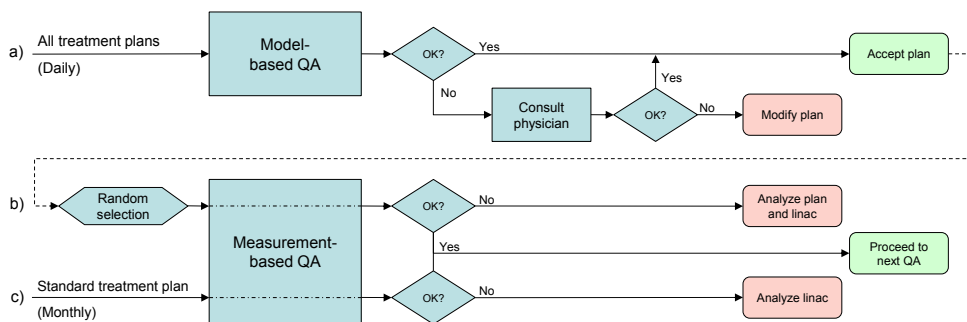


Figure 1:

Overview of the hybrid-QA method. (a) All treatment plans are verified with a model-based QA. Whenever a treatment plan fails to pass clinical acceptance criteria, the physician was consulted whether the dose differences were still clinically acceptable. (b) A random selection of approved treatment plans (approximately 15%) was evaluated with a measurement-based QA to assess the agreement between the model-based QA and measurement-based QA. (c) A standard head and neck IMRT treatment plan was evaluated monthly to verify linac stability for IMRT delivery.

Clinical evaluation

The hybrid-QA method was evaluated clinically to determine the impact on the QA-procedure in terms of reliability and time efficiency. In total, 330 IMRT treatment plans were evaluated with the hybrid-QA method over a time period of 15 months. The majority of treatment plans consisted of head and neck treatments (80%) and a subset consisted of prostate (10%) and other various indications (10%). All treatment plans were analyzed and classified with the gamma evaluation based on the work of Stock *et. al.* [15] and clinical experience of the department. For clarity reasons, only the mean gamma index (GI) was included in the manuscript. We found the mean GI to be most representative for verification of a 3D dose distribution. The mean GI was classified into PASS ($GI \leq 0.4$), EVAL ($0.4 < GI < 0.6$) or FAIL ($GI \geq 0.6$) with criteria of 3%/3mm for the hot area (50% of the prescribed dose or higher). A mean GI below 0.6 (containing both PASS and EVAL) was accepted for treatment. The EVAL criterion was introduced as an extra level of evaluation to obtain a more sensitive QA-procedure.

Reliability of the hybrid-QA method was evaluated by assessing the agreement between model-based QA and measurement-based QA for 48 treatment plans. Treatment plans in the PASS category were selected randomly (43 in total) and all treatment plans in the EVAL or FAIL category accepted for treatment were selected (five and zero respectively). In addition, stability of the linac was verified over a time period of 15 months.

Time efficiency of the hybrid-QA method was evaluated by quantification of the average work load and linac time based on four representative head and neck IMRT treatment plans for the model-based QA, the measurement-based QA and the hybrid-QA method. The work load was grouped into three phases; preparation, execution and evaluation. First, the time needed to select the treatment plan and to load the data was determined (preparation phase). Second, the time needed to obtain a 3D dose distribution, and in case of the measurement-based QA, the time needed to attach and align the detector array to the linac and delivery of the treatment plan was determined (execution phase). Third, the time needed to compare and evaluate the dose distributions of the COMPASS system and the TPS was determined (evaluation phase).

Results

COMPASS dose calculation verification

COMPASS calculated dose in heterogeneous media was in agreement with Monte Carlo dose calculations. COMPASS calculated a slightly higher dose in comparison to Monte with a maximum difference of 2.5% (for the secondary build-up region), 1.5%, 2% and 3.2% for densities of 0.0, 1.8, 2.0 and 2.4 g/cm³ respectively. Pinnacle calculated a lower compared to Monte with a maximum difference of 7% for 2.4 g/cm³ (figure 2). Furthermore, COMPASS calculated dose and Pinnacle calculated dose in patient-like phantoms consisting of materials with densities of 0.25 (lung), 1.0 (tissue), 1.2 (tumor) and 1.8 (bone) g/cm³ agreed with Monte Carlo calculated dose, as shown by dose differences well below 3% (see example in figure 3). In addition, secondary build-up effects at density transitions were accurately modeled.

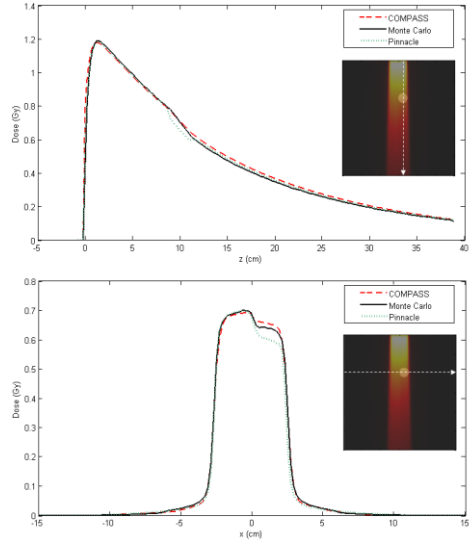


Figure 2:

Comparison of COMPASS, Pinnacle and Monte Carlo calculated depth dose curves (top) and dose profiles (bottom) in a water phantom with a 2.5 cm diameter cylinder of 2.4 g/cm³ density at 10 cm depth (inserts).

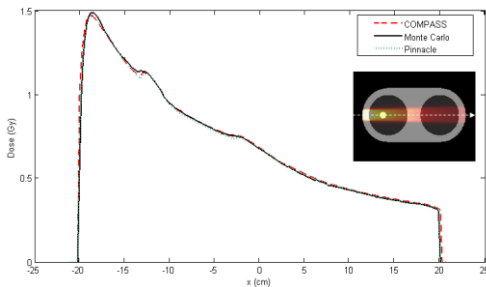


Figure 3:

Comparison of COMPASS, Pinnacle and Monte Carlo calculated depth dose curve in a lung phantom with densities of 0.25 (lung), 1.00 (tissue) and 1.20 (tumor) g/cm³ (shown in insert). Secondary build-up effects are visible at -12 cm (entrance of 'tumor') and -2 cm (entrance of 'mediastinum').

Clinical evaluation

All treatment plans verified by the model-based QA (330) were accepted for treatment, indicating correct Pinnacle dose calculation (figure 4). Only five treatment plans resulted in an EVAL classification with dose differences in high density and/or build-up regions. The treatment plan with the highest GI (0.56) was an uncommon indication

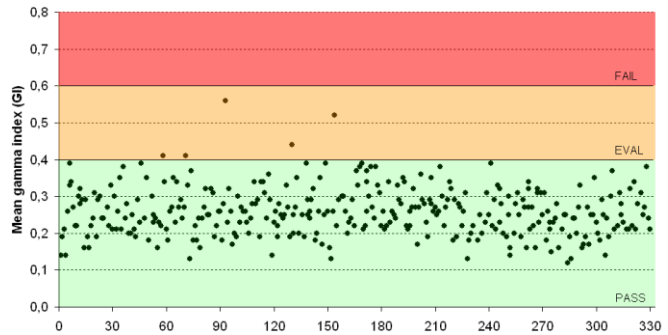


Figure 4:

Mean gamma index (GI) for 330 treatment plans with 325 PASS classifications ($GI \leq 0.4$) and five EVAL classifications ($0.4 < GI < 0.6$). No treatment plans were classified as FAIL ($GI \geq 0.6$).

(skull) with over-travelled fields, resulting in dose differences up to 4% in the planned target volume. In addition, the planned target volume was located in the build-up region and included bone tissue with densities up to 2.5 g/cm^3 .

All treatment plans that were selected for model-based QA and measurement-based QA (48) had acceptable QA results (either PASS or EVAL) for both methods, nevertheless, seven treatment plans were classified differently (figure 5). Four out of these seven treatment plans were classified PASS for the model-based QA and EVAL for the measurement-based QA and the remaining three treatment plans were classified EVAL for the model-based QA and PASS for the measurement-based QA. On average, the measurement-based QA resulted in a slightly higher GI with a mean difference of 0.03 ± 0.08 , *i.e.* well below 0.5%/0.5mm, and a maximum difference in GI of 0.19.

Monthly verification of the standard head and neck IMRT treatment plan with measurement-based QA resulted in an average GI of 0.28 ± 0.04 , indicating stable IMRT delivery by the linac over a period of 15 months.

Average work load for the hybrid-QA was derived from the work load of the model-based QA and measurement-based QA

(table 1). Preparation time was equal for all three QA-procedures. However, execution time for the hybrid-QA method was substantially lower in comparison to the measurement-based QA as only a selection of treatment plans (approximately 15%) were executed with a measurement-based QA. Vice versa, execution of a selection of treatment plans using the measurement-based QA resulted in a higher execution time for the hybrid-QA method compared to the model-based QA. Evaluation time of the hybrid-QA method was slightly higher in comparison to the model-based QA and measurement-based QA due to the re-evaluation of a selection of treatment plans. By switching from the standard measurement-based QA to the hybrid-QA, an efficiency improvement of 15 minutes per treatment plan was obtained due to decrease of linac time required for QA purposes.

Table 1:

Average work load per treatment plan in minutes based on four representative head and neck IMRT treatment plans if no problems occur and performed by an experienced user. Measurements for the four treatment plans were completed in one single measurement session.

Work load (min)	Model-based QA	Measurement-based QA	Hybrid-QA
Preparation	2	2	2
Execution	2	22	6
Evaluation	6	6	7
Average work load	10	30	15

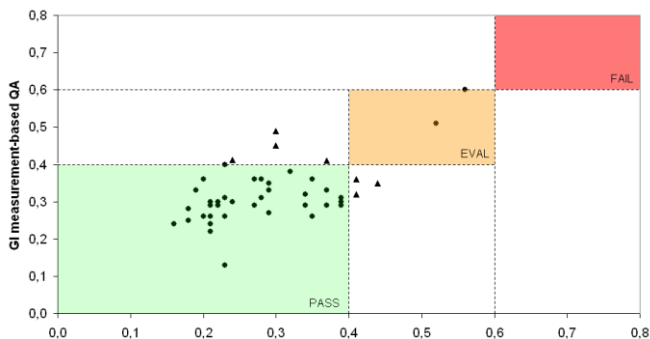


Figure 5:

Model-based QA and measurement-based QA agreed for 41 treatment plans (●) and resulted in different classification for seven treatment plans (▲). All 48 treatment plans were accepted for treatment.

Discussion

In this study, we evaluated the hybrid-QA method which combines model-based QA with measurement-based QA. Our results showed that the accuracy of the COMPASS dose calculation used in model-based QA is adequate for 3D dose verification. Only for heterogeneous media with densities above 2.0 g/cm^3 , dose differences just exceeded clinical acceptance criteria. Moreover, within the high density regions, COMPASS overestimated and Pinnacle underestimated the dose which resulted in an overestimation of the GI determined by the hybrid-QA method. Nevertheless, dose differences were clinically acceptable as the overestimation is confined to high density regions of limited size within the patient and all evaluated treatment plans were accepted for treatment.

The hybrid-QA method seems reliable as the differences observed between model-based QA and measurement-based QA had no effect on the clinical decision to accept or reject the treatment plan. All 48 treatment plans were accepted for treatment based on both evaluations. In absolute values, the average differences between the model-based QA and measurement-based QA were well below 0.5%/0.5mm, which will have little effect on the classification of the treatment plan. When outcomes of the hybrid-QA method obtained by either the model-based QA or measurement-based QA come close to the cut-off point of the PASS and EVAL classification, it will have no effect on the clinical outcome and need no extra evaluation, whereas outcomes which come close to the cut-off point of EVAL and FAIL need extra evaluation for both the model-based QA and the measurement-based QA. By determining the agreement between model-based QA and measurement-based QA for a random selection of approved treatment plans, the hybrid-QA method verifies whether results for model-based QA are still representative for measurement-based QA results. If differences between model-based QA and measurement-based QA do occur, extra analysis of the treatment plan and/or linac is necessary to determine the origin of the observed difference. In addition, monthly verification of the standard head and neck IMRT treatment plan showed stable IMRT treatment delivery by the linac strengthening the reliability of the hybrid-QA method.

We found that the introduction of the hybrid-QA method substantially decreased the required linac time, improving the time efficiency of the departments QA-procedure. And because model-based QA and measurement-based QA are in agreement for randomly selected treatment plans, all model-based QA outcomes in this study (330 treatment plans) would most likely be unaffected when performed with the measurement-based QA underlining the possibility of introducing the hybrid-QA method for pre-treatment purposes. However, there are three important issues that should be pointed out. First, it

has to be noted that the initial time effort needed to commission the QA-system has not been included in the analyses. On the other hand, this time is averaged out when performing the hybrid-QA method for a large amount of treatment plans. Second, the evaluation has been performed by an experienced user. The lack of experience with the hybrid-QA method can affect efficiency improvement, but as this learning curve is a transient effect it will eventually have little effect on the efficiency improvement. Third, the extra time needed to evaluate a treatment plan containing relevant dose differences has not been included in the analyses. Nevertheless, research has shown that no dose delivery error occurred in 99.5% of the treatment plans [10]. Therefore, a substantial time efficiency improvement is to be expected when switching from measurement-based QA to the hybrid-QA method.

A consequence of the transition from measurement-based QA to the hybrid-QA method is that correct data transfer of the treatment plan to the linac is only checked for a selection of treatment plans. And although many of these checks can be covered by safety measures, such as interrupts on faulty linac dosimetry and checks on the treatment plans stored in the database, errors can still occur. We find this has to be compensated for. Log files can be appropriate, as it allows verification of data transfer and actual linac delivery parameters like MLC positioning [16]. Whereas log files allow an indirect verification of delivered dose, alternatively, actually delivered dose information can be obtained by the introduction of measurements during patient treatment (on-line) with EPID dosimetry or a transmission detector [9,12,17,18] Implementation of these techniques is suggested to complement the current hybrid-QA method to allow dose verification for every treatment plan prior to the treatment course for independent dose verification and during the treatment course for verification of actual treatment delivery.

For this study, classification of the QA-results was determined by the mean gamma index for the hot area. The suitability of the mean gamma index for 3D dose verification of IMRT treatment plans has not been investigated thoroughly and research has shown that the gamma evaluation has its limits in terms of resolution [19] and prediction power for clinical relevance [20]. Evaluation based on dose volume histograms (DVH) may be an alternative since it allows the physicist and/or physician to accept or reject a treatment plan based on delivered dose to the organs at risk and/or tumor [7,21]. Nevertheless, we used the mean gamma index because it takes into account both dose difference and distance to agreement. In addition, the mean gamma index is widely accepted in the field of radiotherapy for QA-purposes and therefore considered suitable for the proposed method.

Our study showed that the hybrid-QA method is reliable and allows the user to verify a large number of complex treatment plans maintaining the necessary accuracy. In addition, the hybrid-QA method could be a universal method as it may be implemented for, and combined with different QA-tools. Where the model-based QA could be performed by Monte Carlo calculations, the measurement-based QA could be performed with EPID-dosimetry. Therefore, the hybrid-QA method may be implemented in many radiotherapy departments combined with different QA-tools.

Conclusion

Accuracy of the hybrid-QA method is adequate for 3D dose verification purposes. Moreover, model-based QA and measurement-based QA are in agreement underlining the possibility of performing less measurement-based QA as is done for the hybrid-QA method. Introduction of the hybrid-QA method reduced linac time substantially compared to measurement-based QA allowing the user to verify a large number of complex treatment plans improving time efficiency of the QA-procedure. In addition, the hybrid-QA method may be implemented for, and combined with different QA-tools. Therefore, we conclude that the hybrid-QA method is a reliable, time efficient and universal method for 3D dose QA suitable for implementation in any radiotherapy department.

References

- [1] Longobardi B, De Martin E, Fiorino C, Dell’oca I, Broggi S, Cattaneo GM, Calandrino R. Comparing 3DCRT and inversely optimized IMRT planning for head and neck cancer: equivalence between step-and-shoot and sliding window techniques. *Radiother Oncol* 2005;77:148–56.
- [2] Luxton G, Hancock SL, Boyer AL. Dosimetry and radiobiologic model comparison of IMRT and 3D conformal radiotherapy in treatment of carcinoma of the prostate. *Int J Radiat Oncol Biol Phys* 2004;59:267–84.
- [3] Ezzell GA, Galvin JM, Low D, Palta JR, Rosen I, Sharpe MB, Xia P, Xiao Y, Xing L, Yu CX. Guidance document on delivery, treatment planning, and clinical implementation of IMRT: report of the IMRT Subcommittee of the AAPM Radiation Therapy Committee. *Med Phys* 2003;30:2089–115.
- [4] Low DA, Moran JM, Dempsey JF, Dong L, Oldham M. Dosimetry tools and techniques for IMRT. *Med Phys* 2011;38:1313–38.
- [5] Anjum MN, Parker W, Ruo R, Aldahlawi I, Afzal M. IMRT quality assurance using a second treatment planning system. *Med Dosim* 2010;35:274–9.
- [6] Belec J, Ploquin N, La Russa DJ, Clark BG. Position-probability-sampled Monte Carlo calculation of VMAT, 3DCRT, step-shoot IMRT, and helical tomotherapy dose distributions using BEAMnrc/DOSXYZnrc. *Med Phys* 2011;38:948–60.
- [7] van Zijtveld M, Dirkx MLP, de Boer HCJ, Heijmen BJM. 3D dose reconstruction for clinical evaluation of IMRT pretreatment verification with an EPID. *Radiother Oncol* 2007;82:201–7.
- [8] van Elmpt W, Nijsten S, Mijnheer B, Dekker A, Lambin P. The next step in patient-specific QA: 3D dose verification of conformal and intensity-modulated RT based on EPID dosimetry and Monte Carlo dose calculations. *Radiother Oncol* 2008;86:86–92.
- [9] van Elmpt W, Nijsten S, Petit S, Mijnheer B, Lambin P, Dekker A. 3D in vivo dosimetry using megavoltage cone-beam CT and EPID dosimetry. *Int J Radiat Oncol Biol Phys* 2009;73:1580–7.
- [10] Olson AC, Wegner RE, Scicutella C, Heron DE, Greenberger JS, Huq MS, Bednarz G, Flickinger JC. Quality assurance analysis of a large multicenter practice: does increased complexity of intensity-modulated radiotherapy lead to increased error frequency? *Int J Radiat Oncol Biol Phys* 2012;82:e77-82.
- [11] Godart J, Korevaar EW, Visser R, Wauben DJL, Van’t Veld AA. Reconstruction of high-resolution 3D dose from matrix measurements: error detection capability of the COMPASS correction kernel method. *Phys Med Biol* 2011;56:5029–43.

- [12] Boggula R, Jahnke L, Wertz H, Lohr F, Wenz F. Patient-specific 3D pretreatment and potential 3D online dose verification of Monte Carlo-calculated IMRT prostate treatment plans. *Int J Radiat Oncol Biol Phys* 2011;81:1168–75.
- [13] Korevaar EW, Wauben DJ, van der Hulst PC, Langendijk JA, Van't Veld AA. Clinical introduction of a linac head-mounted 2D detector array based quality assurance system in head and neck IMRT. *Radiother Oncol* 2011;100:446–52.
- [14] Rogers DW, Faddegon BA, Ding GX, Ma CM, We J, Mackie TR. BEAM: a Monte Carlo code to simulate radiotherapy treatment units. *Med Phys* 1995;22:503–24.
- [15] Stock M, Kroupa B, Georg D. Interpretation and evaluation of the gamma index and the gamma index angle for the verification of IMRT hybrid plans. *Phys Med Biol* 2005;50:399–411.
- [16] Li JG, Dempsey JF, Ding L, Liu C, Palta JR. Validation of dynamic MLC-controller log files using a two-dimensional diode array. *Med Phys* 2003;30:799–805.
- [17] Nakaguchi Y, Araki F, Maruyama M, Saiga S. Dose verification of IMRT by use of a COMPASS transmission detector. *Radiol Phys Technol* 2012;5:63–70.
- [18] Poppe B, Thieke C, Beyer D, Kollhoff R, Djouguela A, Ruhmann A, Willborn K, Harder D. DAVID--a translucent multi-wire transmission ionization chamber for in vivo verification of IMRT and conformal irradiation techniques. *Phys Med Biol* 2006;51:1237–48.
- [19] Depuydt T, Van Esch A, Huyskens DP. A quantitative evaluation of IMRT dose distributions: refinement and clinical assessment of the gamma evaluation. *Radiother Oncol* 2002;62:309–19.
- [20] Nelms BE, Zhen H, Tome WA. Per-beam, planar IMRT QA passing rates do not predict clinically relevant patient dose errors. *Med Phys* 2011;38:1037–44.
- [21] Zhen H, Nelms BE, Tome WA. Moving from gamma passing rates to patient DVH-based QA metrics in pretreatment dose QA. *Med Phys* 2011;38:5477–89.

Chapter 6

Evaluation of DVH-based treatment plan verification in addition to gamma passing rates for head and neck IMRT

R. Visser
DJL. Wauben
M. de Groot
RJHM. Steenbakkers
HP. Bijl
J. Godart
AA. van't Veld
JA. Langendijk
EW. Korevaar

Radiother. Oncol. 112(2014) 389-395

Abstract

Background and purpose: Treatment plan verification of Intensity Modulated Radiotherapy (IMRT) is generally performed with the gamma index (GI) evaluation method, which is difficult to extrapolate to clinical implications. Incorporating Dose Volume Histogram (DVH) information can compensate for this. The aim of this study was to evaluate DVH-based treatment plan verification in addition to the GI evaluation method for head and neck IMRT.

Material and method: Dose verifications of 700 subsequent head and neck cancer IMRT treatment plans were categorised according to gamma and DVH-based action levels. Fractionation dependent absolute dose limits were chosen. The results of the gamma- and DVH-based evaluations were compared to the decision of the medical physicist and/or radiation oncologist for plan acceptance.

Results: Nearly all treatment plans (99.7%) were accepted for treatment according to the GI evaluation combined with DVH-based verification. Two treatment plans were re-planned according to DVH-based verification, which would have been accepted using the evaluation alone. DVH-based verification increased insight in dose delivery to patient specific structures increasing confidence that the treatment plans were clinically acceptable. Moreover, DVH-based action levels clearly distinguished the role of the medical physicist and radiation oncologist within the Quality Assurance (QA) procedure.

Conclusion: DVH-based treatment plan verification complements the GI evaluation method improving head and neck IMRT-QA.

Introduction

Radiotherapy pre-treatment plan verification is an important aspect in Quality Assurance (QA) of intensity modulated radiotherapy (IMRT) [1]. In literature, various dose verification techniques suitable for patient specific QA have been described [2–5]. Commonly, patient specific QA is performed by a physicist who accepts or rejects a treatment plan based on QA results.

From a clinical point of view, QA results used for dose verification purposes should focus on detrimental dose differences as these ultimately determine whether or not a treatment plan is acceptable for treatment. Detrimental effects can be caused by under dosage and/or over dosage in patient specific structures [6–8]. The current standard method for IMRT dose verification is the gamma index (GI) evaluation method, which combines spatial information and dose differences for a 2D plane or a 3D volume [9,10]. Nevertheless, the GI evaluation lacks information on dose to patient specific structures making it difficult to extrapolate gamma passing rates to clinical implications [11]. This is underlined by research which shows that gamma passing rates correlate weakly with dose differences in target volumes and Organs At Risk (OARs) [12–14]. Furthermore, the GI evaluation has limited accuracy in areas with high dose gradients [15]. To overcome these limitations, Dose Volume Histogram (DVH) information can be incorporated within the QA procedure, in addition to gamma passing rates. This should result in a more complete QA methodology as it consists of a global dose verification using gamma passing rates, and allows verification of detrimental dose differences for patient specific structures.

In current practice, the physicist is responsible for the entire QA procedure, and the radiation oncologist is responsible for the treatment plans used for treatment. By incorporating DVH-information in the QA procedure, involvement of the radiation oncologist is required to determine the relevance of observed dose differences between the planned dose and the QA-dose from a clinical point of view. This shift in responsibility for accepting or rejecting a treatment plan needs to be taken into account within the QA procedure, and be reflected in applicable criteria, without ambiguity in responsibility. The use of gamma passing rates can be found in literature [16] but a consensus on DVH-based action levels is still lacking.

The aim of this study was to evaluate DVH-based treatment plan verification in addition to gamma passing rates for head and neck IMRT, and to assess the consequences within the QA procedure.

Material and Method

Study population

To evaluate DVH-based dose verification, a population analysis was performed for 700 subsequent head and neck IMRT treatment plans made for clinical treatment from December 2009 to November 2012 on four Elekta SLi-15 machines and one Elekta Synergy machine. Treatment plans were created with Pinnacle (version 8.0 and 9.0, Philips Radiation Oncology Systems, Madison USA), on a 4x4x2mm³ dose grid. QA was performed with the COMPASS system (version 2.1, IBA Dosimetry, Schwarzenbruck, Germany).

QA-procedure

QA was performed following our previously described hybrid-QA procedure consisting of a combination of calculation-based QA for all treatment plans and measurement-based QA for a selection of treatment plans [17]. For the calculation-based QA, dose calculations performed by the treatment planning system (TPS) were compared to dose calculations performed by the QA-system (QA-dose). For the measurement-based QA, TPS-dose was compared to QA-dose obtained by a dose reconstruction from measurements. To verify the calculation-based QA result, measurement-based QA results were obtained for a random selection of treatment plans and for treatment plans failing the calculation-based QA. In a recent study, measurement-based QA results were found to be comparable to film dosimetry results [18]. Treatment plans were categorised according to standard pre-defined action levels used in the clinic for the GI evaluation method. For this study, an additional categorisation was developed according to DVH-based criteria.

Gamma-based action levels

Gamma passing rates for the composite dose were obtained by a global 3D gamma analysis (3%/3mm) categorised according to the GI for the hot area (volume receiving 50% or more of the prescribed dose) in the patient CT based on Stock *et al.* [16] combined with clinical experience of the department. The GI was categorised into 'PASS' (accept for treatment), 'EVAL' (evaluate by the medical physicist) or 'FAIL' (reject for treatment). Criteria for the mean gamma were classified into PASS ($GI \leq 0.4$), EVAL ($0.4 < GI < 0.6$), and FAIL ($GI \geq 0.6$), and the percentage of voxels with a GI above one was classified into PASS ($\leq 3.0\%$), EVAL ($> 3.0\%$ and $< 7.5\%$), and FAIL ($\geq 7.5\%$). A QA result was considered unjustified when a treatment plan was categorised as FAIL but accepted for treatment by the medical physicist.

DVH-based action levels

DVH-information was gathered for the Planning Target Volume (PTV) and seven types of OAR; brain, eyes, lenses, cochlea, parotid glands, submandibular glands, and spinal cord. The PTV was a therapeutic or a prophylactic volume; i.e., PTV-therapeutic or PTV-prophylactic. The mean dose (D_{mean}) was determined for all structures, and the maximum dose (D_1) for 1.0% of the volume was determined for the PTV, eyes, spinal cord, and brain (0.1% in case of the brain volume, $D_{0.1}$). The minimum dose (D_{99}) for 99% of the volume was determined for the PTV's.

Table 1:

DVH-based action levels for nine structure types with classification 'PASS' (accept for treatment), 'EVAL_{MP}' (evaluate by medical physicist), 'EVAL_{RO}' (evaluate by radiation oncologist), and 'EVAL_{MP+RO}' (evaluate by medical physicist and radiation oncologist) based on dose differences (D_{diff}), and absolute dose thresholds (D). Absolute dose levels were set for a fractionation scheme consisting of 35 fractions and adapted in case of a different fractionation.

Structure	Dose parameter	PASS	EVAL _{MP}	EVAL _{RO}	EVAL _{MP+RO}
PTV-therapeutic / PTV-prophylactic	D_{mean}	$D_{\text{diff}} \leq 2.0\%$	$2.0\% < D_{\text{diff}} < 2.5\%$	-	$D_{\text{diff}} \geq 2.5\%$
	D_{99}	$D_{\text{diff}} \leq 3.0\%$	$3.0\% < D_{\text{diff}} < 5.0\%$	-	$D_{\text{diff}} \geq 5.0\%$
	D_1	$D_{\text{diff}} \leq 3.0\%$	$3.0\% < D_{\text{diff}} < 5.0\%$	-	$D_{\text{diff}} \geq 5.0\%$
Lens	D_{mean}	$D_{\text{diff}} \leq 2.0\%$	$2.0\% < D_{\text{diff}} < 2.5\%$	-	$D_{\text{diff}} \geq 2.5\%$
Eye	D_{mean}	$D_{\text{diff}} \leq 2.0\%$	$2.0\% < D_{\text{diff}} < 2.5\%$	-	$D_{\text{diff}} \geq 2.5\%$
	D_1	$D_{\text{diff}} \leq 3.0\%$	$3.0\% < D_{\text{diff}} < 5.0\%$	-	$D_{\text{diff}} \geq 5.0\%$
Parotid gland	D_{mean}	$D_{\text{diff}} \leq 2.0\%$	$2.0\% < D_{\text{diff}} < 2.5\%$	-	$D_{\text{diff}} \geq 2.5\%$
Submandibular gland	D_{mean}	$D_{\text{diff}} \leq 2.0\%$	$2.0\% < D_{\text{diff}} < 2.5\%$	-	$D_{\text{diff}} \geq 2.5\%$
Cochlea	D_{mean}	$D_{\text{diff}} \leq 4.0\%$	$D_{\text{diff}} > 4.0\%$	$D > 53 \text{ Gy}$	$D_{\text{diff}} > 4.0\% \ \& \ D > 53 \text{ Gy}$
Spinal cord	D_1	$D_{\text{diff}} \leq 3.0\%$	$D_{\text{diff}} > 3.0\%$	$D > 56 \text{ Gy}$	$D_{\text{diff}} > 3.0\% \ \& \ D > 56 \text{ Gy}$
Brain	$D_{0.1}$	$D_{\text{diff}} \leq 3.0\%$	$D_{\text{diff}} > 3.0\%$	$D > 63 \text{ Gy}$	$D_{\text{diff}} > 3.0\% \ \& \ D > 63 \text{ Gy}$

Differences between TPS-dose and QA-dose were evaluated by the medical physicist and/or radiation oncologist according to pre-defined action levels (Table 1). To distinguish the role of the medical physicist and radiation oncologist, DVH-based QA results were categorised into; 'PASS' (accept for treatment), 'EVAL_{MP}' (evaluate by the medical physicist), 'EVAL_{RO}' (evaluate by the radiation oncologist), and 'EVAL_{MP+RO}' (evaluate by the medical physicist and radiation oncologist). Cutoff values for a 35 fractionation scheme were based on a consensus of our head and neck radiation oncologist group based on their expert opinion combined with QUANTEC data [7]. Absolute dose levels were adapted in case of a fractionation scheme different from 35 fractions.

In contrast to the gamma evaluation, no 'FAIL' was defined because all observed dose differences failing the PASS criteria had to be evaluated by the medical physicist and/or radiation oncologist. If for instance the dose in an OAR exceeded the PASS criteria but could not be reduced without compromising target coverage, the radiation oncologist could decide to accept the treatment plan for treatment. Therefore, EVAL classifications were found to be more suitable.

For individual patient QA, treatment plans categorised as EVAL_{MP} were found acceptable for treatment. The EVAL_{MP} category was used in addition to evaluate the dose accuracy of the TPS by performing a population analysis. A QA result was considered unjustified when a treatment plan was categorised as EVAL_{RO}, or EVAL_{MP+RO} but accepted for treatment.

Results

QA results

Based on the population analysis, only two out of 700 (0.3%) treatment plans were rejected for treatment. Both treatment plans, which were missed by the GI evaluation, were detected by DVH-based action levels. Both treatment plans were rejected based on an over dosage in the PTV-therapeutic. For the first treatment plan, the tumour was situated close to the patient outline. For correct dose delivery, additional build-up material was used. Due to standard planning margins used for the PTV, part of the PTV was situated inside the additional build-up material, thus outside the patient outline. In contrast to the QA-system, the TPS calculated no dose in the area outside the patient outline. To fulfil the planning-objectives for D_{mean} of the PTV, the TPS optimiser increased the dose resulting an over dosage. By lowering the air-threshold for dose calculations from 0.6 g/cm^3 to 0.1 g/cm^3 for the TPS during re-planning, the TPS also calculated dose in the build-up material resulting in avoidance of erroneous optimisation, and a better agreement with the QA-system. The adapted treatment plan with an adjusted air threshold for dose calculations was accepted for treatment. For the second treatment plan, the iso-center was positioned outside the PTV-therapeutic, approximately 6 cm cranially, resulting in over-travelled fields with less accurate dose calculations by the TPS. This effect was corrected for by re-positioning of the iso-center during re-planning.

Gamma-based action levels

For the GI evaluation, three (0.4%) treatment plans failed the mean GI, and nine (1.3%) treatment plans failed the GI>1 criteria. All treatment plans failing the GI criteria showed at least one or more EVAL classifications for the DVH-based action levels, but were found not to be clinically relevant as the observed dose differences were not expected to affect treatment outcome. Therefore, none of the treatment plans were rejected for treatment, and considered to be unjustified QA results for the gamma evaluation.

DVH-based action levels

The population analysis showed that the PTV-therapeutic, cochlea, and brain resulted in the lowest PASS rates (Figure 1). For the PTV-therapeutic, and cochlea this corresponded to a relatively large spread in the dose differences as shown in the dose statistics (Table 2). In general, calculation-based QA performed with the QA-system resulted in a slightly higher dose in comparison to TPS dose calculations with an average difference mostly less than 1 Gy. Calculation-based QA results were considered comparable to measurement-based QA result as observed average dose differences for all

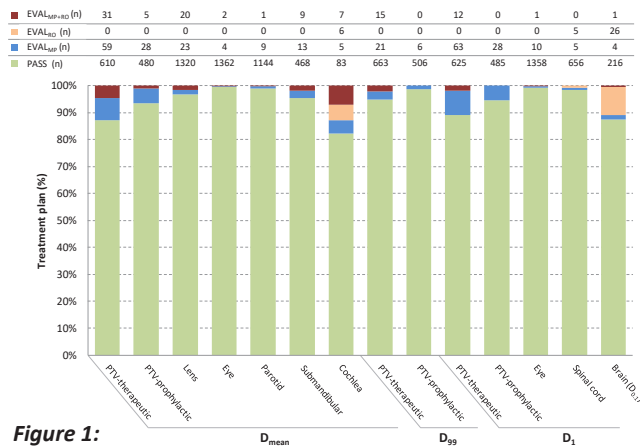


Figure 1:

QA results of 700 treatment plans for the DVH-based action levels of nine delineated structure types categorised into 'PASS' (accept for treatment), 'EVAL_{MP}' (evaluate by the medical physicist), 'EVAL_{RO}' (evaluate by radiation oncologist), and 'EVAL_{MP+RO}' (evaluate by medical physicist and radiation oncologist) for the mean dose (D_{mean}), minimum dose (D_{99}), and maximum dose (D_1 , with $D_{0.1}$ for the brain).

delineated structures, except for $D_{0.1}$ for the brain which is based on a very small fractional volume, were within 0.6 Gy and 0.8%. A representative selection of delineated structures is presented in Table 3. Furthermore, DVH-based action levels could clearly distinguish the role of the medical physicist and radiation oncologist within the QA procedure in evaluating a treatment plan.

Table 2:

QA results for nine delineated structure types with frequency (n), dose statistics and dose difference (QA-dose – TPS-dose). Indicated values are the \pm one standard deviation over all the treatment plans.

Structure	Dose parameter	n	TPS-dose (Gy)	QA-dose (Gy)	Difference (Gy)	Difference (%)
PTV-therapeutic	D_{mean}	700	63.7 \pm 9.5	64.1 \pm 9.6	0.7 \pm 0.7	1.1 \pm 1.2
	D_{99}	699	59.0 \pm 10.3	59.8 \pm 9.7	0.8 \pm 3.9	1.2 \pm 6.4
	D_1	700	66.8 \pm 10.0	67.8 \pm 10.1	1.0 \pm 0.9	1.5 \pm 1.4
PTV-prophylactic	D_{mean}	513	59.7 \pm 4.9	60.3 \pm 4.9	0.6 \pm 0.6	0.9 \pm 1.0
	D_{99}	512	50.6 \pm 3.3	50.9 \pm 3.4	0.3 \pm 0.7	0.4 \pm 1.1
	D_1	513	69.5 \pm 5.7	70.4 \pm 5.8	0.9 \pm 0.7	1.3 \pm 1.1
Lens	D_{mean}	1363	3.0 \pm 7.0	3.1 \pm 7.2	0.0 \pm 0.5	0.1 \pm 0.8
Eye	D_{mean}	1368	3.6 \pm 7.6	3.3 \pm 7.7	-0.2 \pm 0.4	-0.3 \pm 0.6
	D_1	1369	5.8 \pm 10.9	5.6 \pm 10.9	-0.2 \pm 0.6	-0.4 \pm 1.0
Parotid gland	D_{mean}	1154	26.9 \pm 16.8	27.0 \pm 17.1	0.1 \pm 0.5	0.1 \pm 0.8
Submandibular gland	D_{mean}	490	39.5 \pm 24.8	39.7 \pm 25.1	0.2 \pm 0.7	0.3 \pm 1.0
Cochlea	D_{mean}	101	26.8 \pm 17.4	27.8 \pm 18.2	1.0 \pm 1.3	1.5 \pm 1.9
Spinal cord	D_1	666	38.9 \pm 12.8	39.2 \pm 13.0	0.3 \pm 0.7	0.5 \pm 1.0
Brain	$D_{0.1}$	247	34.5 \pm 21.3	34.7 \pm 21.9	0.2 \pm 0.9	0.3 \pm 1.5

PTV-therapeutic

The population analysis of the PTV showed that for the PTV-therapeutic, 31 (4.4%) treatment plans were categorised as EVAL_{MP+RO} and needed to be evaluated by the medical physicist and radiation oncologist together. Furthermore, D_{99} of the PTV-therapeutic showed a relatively large dose spread (3.9 Gy and 6.4%). Re-evaluation of ten worst cases showed that dose differences were situated in the build-up area, and in regions with high density bone such as the skull and lower jaw ($>2.0 \text{ g/cm}^3$). Lowering the air threshold in our TPS from 0.6 g/cm^3 to 0.1 g/cm^3 resulted in a better agreement between the TPS and the QA-system. Dose increase for the QA-system calculations for high density bone was confirmed by Monte Carlo calculations. The dose calculation differences between the TPS and QA-system for high density bone were found acceptable. Two out of 31 EVAL_{MP+RO} classifications resulted into a re-planning of the treatment plan and were considered to be justified QA results.

Table 3:

Dose differences for measurement-based QA and calculation-based QA for a selection of four delineated structure types with frequency (n), and dose difference (measurement-based QA – calculated-based QA). Indicated values are the average \pm one standard deviation over all the treatment plans.

Structure	Dose parameter	n	Difference (Gy)	Difference (%)
PTV-therapeutic	D_{mean}	88	-0.2 ± 0.6	-0.3 ± 0.9
Cochlea	D_{mean}	15	-0.3 ± 0.9	-0.5 ± 1.4
Spinal cord	D_1	88	-0.4 ± 0.9	-0.6 ± 1.4
Brain	$D_{0.1}$	18	-0.9 ± 1.0	-1.2 ± 1.6

Cochlea

In total, six treatment plans were categorised as EVAL_{RO}, and seven as EVAL_{MP+RO}. All 13 treatment plans were accepted for treatment, thus QA results were considered unjustified. The dose statistics of the cochlea showed a relatively large systematic offset D_{mean} ($1.5\% \pm 1.9\%$) which contributed to the relatively low PASS rate (<85%). Analysis showed that for the worst cases, the cochlea was situated in a high dose gradient up to 4Gy/mm. The combination of the relatively small volume (approximately 0.05cm³) of the cochlea combined with high dose gradients increased the dose differences between the TPS and the QA-system ($1.0 \text{ Gy} \pm 1.3 \text{ Gy}$). Figure 2 shows a typical case of a cochlea situated in a high dose gradient. Due to a small shift in the dose, the differences between the TPS-dose dose and QA-dose increased.

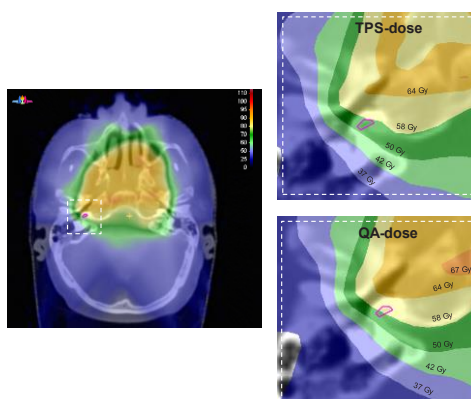


Figure 2:

A typical patient case of which the cochlea was situated in a high dose gradient. A small shift in dose deposition resulted in a difference of 5.1% for D_{mean} of the cochlea between the TPS (57.1 Gy) and QA-system (60.6 Gy) for a 4x4x2 mm³ dose grid. Adjustment of the dose grid to 2x2x2mm³ had little effect on the TPS-dose (57.5 Gy) and QA-dose (60.1 Gy). The treatment plan was categorised EVAL_{MP+RO} as the absolute dose threshold of 53 Gy was exceeded as well.

Spinal cord

Five treatment plans categorised as $EVAL_{RO}$ were considered unjustified QA results as these treatment plans were found acceptable for treatment by the radiation oncologist after evaluation. Moreover, at 50 Gy a clear cut off point was seen which was due to planning objectives used in the clinic (Figure 3). The dose differences between the TPS-dose and QA-dose ($0.5\% \pm 1.0\%$) had no negative effect on the QA results as the margin between the planning objectives and the DVH-based action level was sufficient.

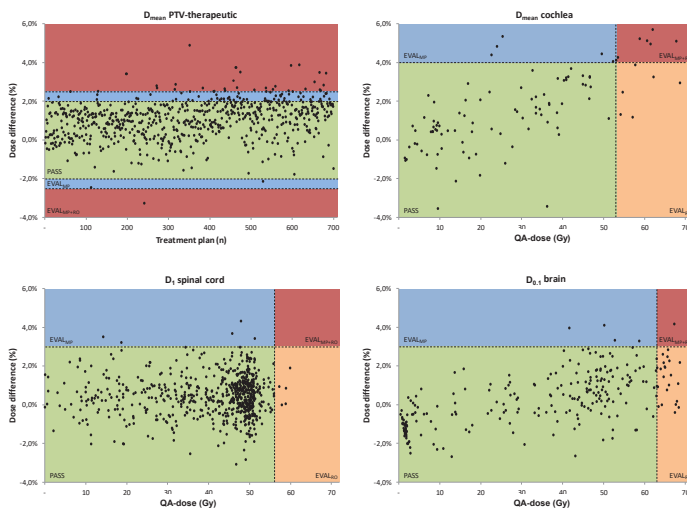


Figure 3:

DVH-based action levels for D_{mean} of the PTV-therapeutic (top left), D_{mean} of the cochlea (top right), D_1 of the spinal cord (bottom left), and $D_{0.1}$ of the brain (bottom right). Calculated dose was normalised to a fractionation schedule with 35 fractions. Action levels were categorised into 'PASS' (accept for treatment), 'EVAL_{MP}'

(evaluate by medical physicist), 'EVAL_{RO}' (evaluate by radiation oncologist), and 'EVAL_{MP+RO}' (evaluate by medical physicist and radiation oncologist).

Brain

In total, 26 treatment plans were categorised as $EVAL_{RO}$ and one treatment plan was categorised as $EVAL_{MP+RO}$. The treatment plan categorised as $EVAL_{MP+RO}$ consisted of an uncommon indication (skull) with over-travelled fields. In this situation the PTV was situated in the build-up region consisting of high density bone (2.5 g/cm^3). After evaluation, the treatment plan was accepted for treatment by the medical physicist and radiation oncologist and therefore considered to be an unjustified QA result. The 26 treatment plans categorised as $EVAL_{RO}$ were considered unjustified QA results as well because they were accepted for treatment by the radiation oncologist as the dose differences were considered not to be clinically relevant.

Discussion

This study shows that the use of DVH-information for treatment plan verification of head and neck IMRT treatment plans complements the standard gamma evaluation, as two treatment plans were identified that needed a re-planning which would have been accepted for treatment when merely the GI evaluation had been used. DVH-based dose verification increases insight in dose delivered to patient specific structures allowing a treatment plan to be accepted or rejected based on clinically relevant dose differences. Moreover, DVH-based action levels introduced in this study clearly distinguished the roles of the medical physicist and radiation oncologist within the QA-procedure. However, as Zijtveld *et. al.* pointed out, DVHs lack spatial information. This can result in large dose differences in a relatively small volume, which can possibly have a clinical impact, to go undetected [19]. Furthermore, as not all anatomical structures are delineated, clinically relevant dose differences outside delineated structures can be missed. To overcome the lack of spatial information for DVH-based dose verification our initial dose verification procedure, the GI evaluation, was incorporated in the QA-procedure for this study. It is a widely accepted method and considered to be a powerful tool for dose verification purposes [10,16]. In addition, it allows a fast and accurate visual inspection of observed dose differences. Even so, it has to be noted that the sensitivity of the GI evaluation is affected by the size of the evaluated volume. The larger the volume, the less sensitive the GI evaluation is in detecting dose differences in small volumes. Therefore, for this study, only the hot area (volume receiving 50% or more of the prescribed dose) was evaluated by GI evaluation. An interesting alternative for future research could be the introduction of cut-off values based on the absolute volume with a GI above one. For this study, the dose to OARs outside the hot area was verified by the DVH-based dose verification, underlining the fact that DVH-based dose verification is complementary to gamma passing rates.

The introduction of DVH-based treatment plan verification resulted in an increase in the number of treatment plans that needed to be re-evaluated ($\pm 10\%$), leading to some reduction in time efficiency of the QA-procedure. For this study, two important aspects contributed the most to this effect which could be compensated for. The first aspect contributing to the increase in treatment plans that needed to be re-evaluated originates from the selection of the action level verifying percentage dose differences for D_{mean} of the PTV. This was set to 2.5% and is somewhat strict resulting in multiple treatment plans to be re-evaluated even though they were found acceptable for treatment. In addition, the minor systematic dose difference between the TPS and QA-system (1.1%) increased the amount of treatment plans that needed to be re-evaluated even more. One can discuss

upon the selected criterion of 2.5% to be too sensitive as a minor adjustment would decrease the amount of unjustified QA results substantially. Nevertheless, adjustment of the criterion should be done with care to maintain correct error-detection of treatment plan verification. The second aspect contributing to the increase in treatment plans that needed to be re-evaluated originates from the patient characteristics. For multiple treatment plans, an OAR was situated close to the PTV resulting in a dose exceeding the fractionation dependent action levels ($\pm 5.0\%$). The dose exceeding the planning objectives was already accepted by the radiation oncologist prior to the QA-procedure, which in principle needed no re-evaluation unless the dose exceeded the percentage dose difference criteria. By taking this effect into account within the QA-procedure, less treatment plans will need to be re-evaluated resulting in less unjustified QA results.

The population analysis increased insight in minor systematic dose differences in dose calculations between the TPS and QA-system for patient specific structures. These minor systematic dose differences may go undetected for individual patient QA and therefore should be accounted for when determining margins between planning objectives and DVH-based action levels. Furthermore, the population analysis showed dose calculation differences between the TPS and QA-system in the build-up area and in high dose gradients. The differences in the build-up area originated from the default settings of the TPS. For multiple treatment plans, the tumour was situated close to the patient outline. For correct dose delivery, additional build-up material was used for these patients. The use of standardised planning margins for the PTV resulted in part of the PTV to be situated inside the additional build-up material, outside the patient outline. In comparison to the QA-system, the TPS calculated no dose outside the patient outline. To fulfil the planning-objectives for D_{mean} of the PTV, the TPS optimiser increased the dose resulting in large dose differences during evaluation. This effect was compensated for by reducing the air-threshold for dose calculations of the TPS. The differences in high dose gradients were attributed to less accurate modelling of the penumbra region, and found acceptable for this study. To minimise unjustified QA results, commissioning of both the TPS and QA-system is conditional in IMRT-QA. After commissioning, a powerful tool suitable to verify correct error-detection in patient specific QA can be obtained by receiver-operating-analyses [20,21]. In a previous study, we performed a similar approach and concluded the QA-system used for this study to be suitable for 3D dose verification purposes [22].

To ensure reliability of calculation-based QA results, a reference is essential. For this study, the hybrid-QA method was applied which regularly verifies calculation-based QA results with measurements. Even though our previous study, and results of this study, has shown that calculation-based QA results are comparable to measurement-based QA results [17], in our opinion, observed calculation based dose differences which can have unwanted clinical consequences should be verified by a measurement-based QA. This enhances reliability of the QA result, which increases the confidence of the medical physicist and/or radiation oncologist in deciding whether or not the treatment plan is acceptable for treatment.

DVH-based treatment plan verification is a universal methodology as it is implementable for any radiotherapy treatment technique in any treatment site. In addition, DVH-based action levels are easily adapted and therefore suitable for patient specific QA. Furthermore, to minimise unjustified QA results, DVH-based action levels should differ from planning objectives to take into account minor systematic dose differences between the TPS and QA-system. Therefore, DVH-based action levels have to be set with care. For this study, the DVH-based action levels were based on a consensus of the radiation oncologist group based on their expert opinion combined with QUANTEC data [7], and found suitable for 3D dose verification. In order to minimise unjustified QA results, a re-evaluation of QA results based on a population analysis can be performed to tailor the action levels to the QA procedure for correct error-detection.

Conclusion

DVH-based treatment plan verification improves IMRT-QA as it increases insight in the uncertainty of dose deposition to patient specific structures allowing a treatment plan to be accepted or rejected based on clinically relevant dose differences. In addition, DVH-based action levels clearly distinguish the role of the medical physicist and radiation oncologist within the QA-procedure. DVH-based treatment plan verification is a universal method suitable for patient specific QA applicable to any treatment site. Therefore we conclude that DVH-based treatment plan verification is complementary to gamma passing rates in verifying dosimetric accuracy improving head and neck IMRT-QA.

References

- [1] Ezzell GA, Galvin JM, Low D, Palta JR, Rosen I, Sharpe MB, Xia P, Xiao Y, Xing L, Yu CX. Guidance document on delivery, treatment planning, and clinical implementation of IMRT: report of the IMRT Subcommittee of the AAPM Radiation Therapy Committee. *Med Phys* 2003;30:2089–115.
- [2] van Elmpt W, Nijsten S, Petit S, Mijnheer B, Lambin P, Dekker A. 3D in vivo dosimetry using megavoltage cone-beam CT and EPID dosimetry. *Int J Radiat Oncol Biol Phys* 2009;73:1580–7.
- [3] Low DA, Moran JM, Dempsey JF, Dong L, Oldham M. Dosimetry tools and techniques for IMRT. *Med Phys* 2011;38:1313–38.
- [4] Boggula R, Jahnke L, Wertz H, Lohr F, Wenz F. Patient-specific 3D pretreatment and potential 3D online dose verification of Monte Carlo-calculated IMRT prostate treatment plans. *Int J Radiat Oncol Biol Phys* 2011;81:1168–75.
- [5] Alber M, Broggi S, De Wagter C, Eichwurz I, Engström P, Fiorino C, Georg D, Hartmann G, Knöös T, Leal A, Marijnissen H, Mijnheer B, Paiusco M, Sánchez-Doblado F, Schmidt R, Tomsej M, Welleweerd H. ESTRO booklet no. 9: Guidelines for the Verification of IMRT. Brussels: ESTRO; 2008.
- [6] Bourhis J, Overgaard J, Audry H, Ang KK, Saunders M, Bernier J, Horiot J-C, Le Maître A, Pajak TF, Poulsen MG, O’Sullivan B, Dobrowsky W, Hliniak A, Skladowski K, Hay JH, Pinto LHJ, Fallai C, Fu KK, et al. Hyperfractionated or accelerated radiotherapy in head and neck cancer: a meta-analysis. *Lancet* 2006;368:843–54.
- [7] Marks LB, Yorke ED, Jackson A, Ten Haken RK, Constone LS, Eisbruch A, Bentzen SM, Nam J, Deasy JO. Use of normal tissue complication probability models in the clinic. *Int J Radiat Oncol Biol Phys* 2010;76:S10–9.
- [8] Beetz I, Schilstra C, van der Schaaf A, van den Heuvel ER, Doornaert P, van Luijk P, Vissink A, van der Laan BF a M, Leemans CR, Bijl HP, Christianen MEMC, Steenbakkers RJHM, Langendijk J a. NTCP models for patient-rated xerostomia and sticky saliva after treatment with intensity modulated radiotherapy for head and neck cancer: the role of dosimetric and clinical factors. *Radiother Oncol* 2012;105:101–6.
- [9] Low DA, Harms WB, Mutic S, Purdy JA. A technique for the quantitative evaluation of dose distributions. *Med Phys* 1998;25:656–61.
- [10] Wendling M, Zipp LJ, McDermott LN, Smit EJ, Sonke J-J, Mijnheer BJ, van Herk M. A fast algorithm for gamma evaluation in 3D. *Med Phys* 2007;34:1647.

- [11] Chan MF, Li J, Schupak K, Burman C. Using a novel dose QA tool to quantify the impact of systematic errors otherwise undetected by conventional QA methods: clinical head and neck case studies. *Technol Cancer Res Treat* 2014;13:57–67.
- [12] Nelms BE, Zhen H, Tome WA. Per-beam, planar IMRT QA passing rates do not predict clinically relevant patient dose errors. *Med Phys* 2011;38:1037–44.
- [13] Zhen H, Nelms BE, Tome WA. Moving from gamma passing rates to patient DVH-based QA metrics in pretreatment dose QA. *Med Phys* 2011;38:5477–89.
- [14] Stasi M, Bresciani S, Miranti A, Maggio A, Sapino V, Gabriele P. Pretreatment patient-specific IMRT quality assurance : A correlation study. *Med Phys* 2012;39:7626–34.
- [15] Depuydt T, Van Esch A, Huyskens DP. A quantitative evaluation of IMRT dose distributions: refinement and clinical assessment of the gamma evaluation. *Radiother Oncol* 2002;62:309–19.
- [16] Stock M, Kroupa B, Georg D. Interpretation and evaluation of the gamma index and the gamma index angle for the verification of IMRT hybrid plans. *Phys Med Biol* 2005;50:399–411.
- [17] Visser R, Wauben DJL, de Groot M, Godart J, Langendijk JA, Van't Veld AA, Korevaar EW. Efficient and reliable 3D dose quality assurance for IMRT by combining independent dose calculations with measurements. *Med Phys* 2013;40:21710.
- [18] Korevaar EW, Wauben DJ, van der Hulst PC, Langendijk JA, Van't Veld AA. Clinical introduction of a linac head-mounted 2D detector array based quality assurance system in head and neck IMRT. *Radiother Oncol* 2011;100:446–52.
- [19] van Zijtveld M, Dirx MLP, de Boer HCJ, Heijmen BJM. 3D dose reconstruction for clinical evaluation of IMRT pretreatment verification with an EPID. *Radiother Oncol* 2007;82:201–7.
- [20] Gordon J, Siebers J. Addressing a Gap in Current IMRT Quality Assurance. *Int J Radiat Oncol Biol Phys* 2013;87:21–20.
- [21] Gordon JJ, Gardner JK, Wang S, Siebers J V. Reliable detection of fluence anomalies in EPID-based IMRT pretreatment. *Med Phys* 2012;39:4959–75.
- [22] Godart J, Korevaar EW, Visser R, Wauben DJL, Van't Veld AA. Reconstruction of high-resolution 3D dose from matrix measurements: error detection capability of the COMPASS correction kernel method. *Phys Med Biol* 2011;56:5029–43.

Chapter 7

Summarizing discussion and future perspectives

Summarizing discussion

In external beam radiotherapy the quality of the radiotherapy treatment plan (RT-plan) is verified by patient specific quality assurance (QA) techniques such as pre-treatment dose verification using dose calculations, direct dose measurements, or a combination of both. For a reliable dose verification this needs to be performed with a system independent of the treatment planning system (TPS). The dose verification system used for patient specific QA in this thesis, the COMPASS system (IBA Dosimetry), is capable of verifying in patient dose deposition based on dose calculations combined with or without measurements [1,2]. In these calculations the fluence is modelled based on the RT-plan and subsequently used for dose calculations in patient CT data. In case of a measurement based dose reconstruction, measurements are obtained with a detector array composed of ionization chambers (MatriXX Evolution, IBA Dosimetry). These measurements are used to correct, if needed, the modelled fluence used in patient dose calculations.

For measurement based dose verification, the detector resolution is an important limitation due to the relatively large detector spacing of 7.62 mm [3]. In relation to high resolution dose reconstructions (*e.g.* $2 \times 2 \times 2 \text{ mm}^3$), the low resolution detector does not meet the Nyquist sampling theorem which can result in incorrect dose reconstructions. To partly overcome the low resolution limitation of the detector array, a (low resolution) correction kernel has been introduced in the COMPASS system which corrects the modelled (high resolution) fluence in case of a difference in expected and measured detector response [1]. The limitations of the correction kernel method were evaluated in **chapter 2**. Results revealed that the use of the correction kernel allowed the system to successfully detect dose differences caused by multi leaf collimator (MLC) leaf positioning errors but that this kernel also introduced dose reconstruction artefacts resulting in overestimation and blurring of observed dose differences. In literature, alternative approaches were introduced to overcome limitations caused by the resolution of the detector by performing a detector shift [4]. For this thesis a different approach was introduced in **chapter 3** using an iterative reconstruction method for a MLC consisting of 1 cm leaves. The iterative reconstruction method used a fluence model, detector model and an optimizer to reconstruct MLC leaf positions based on measurements. Reconstructed MLC leaf positions were for reconstruction purposes implemented in the original RT plan for a better representation of the MLC leaf positions during treatment. Implementation of reconstructed MLC leaf positions minimized the need for the correction kernel, and therefore reduced dose reconstruction artefacts. Nevertheless, for a high resolution MLC

system the resolution of the detector showed to be inadequate. This was illustrated in **chapter 4** where a high resolution MLC with 5 mm leaves was used for dose reconstruction. The measurement setup allowed one row of ionization chambers to be affected by two neighbouring leaves with a dose reconstruction error as a result. The iterative reconstruction method was unable to distinguish between the contribution of a single leaf and a neighbouring leaf. To overcome the dose reconstruction error, MLC leaf position reconstruction was performed for even and uneven MLC leaves independently; *i.e.* by the use of a 'shutter technique'. In **chapter 4** promising results were obtained as MLC leaf positions were reconstructed with sub-millimetre accuracy for a high resolution MLC. However, minor MLC leaf position errors still remained. These errors resulted in a difference between modelled and measured detector response which was then corrected for by the correction kernel method introducing minor dose reconstruction artefacts. As an alternative to the iterative reconstruction method, information on MLC leaf positions could also be obtained using log file information [5,6] or other detector systems such as a flat multi-wire transmission-type ionization chamber [7] or an electronic imaging device (EPID) [8]. These could be of interest in determining high resolution MLC leaf positions needed for *in vivo* dose verification purposes. Other measurement based pre-treatment dose verification systems using detectors composed of ionization chambers have been described in literature [9–11], but are also limited by their resolution. As an alternative, EPID dosimetry has shown to be a powerful tool for accurate high resolution *in vivo* dosimetry [12,13].

Pre-treatment dose verification based on measurements is time consuming. With the increase in the number of radiotherapy treatments combined with the limited departmental resources, an efficient dose verification procedure is needed without compromising patient treatment quality. A tempting solution for efficient dose verification is to switch from measurement based to calculation based pre-treatment dose verification as research has shown that for the vast majority of treatment plans (>99.5%) no dose delivery errors occur when routine patient specific QA is performed [14]. As a consequence, verification of data transfer to the linear accelerator and treatment delivery will then be excluded. To reduce this risk, dose calculations could be combined with measurements. In **chapter 5** a methodology allowing efficient and reliable dose verification was presented; *i.e.* the hybrid-QA methodology. The hybrid-QA methodology underlined the possibility of performing efficient pre-treatment dose verification by including measurements for only a selection of treatment plans. Because the MatriXX detector was mounted on the treatment machine, the hybrid-QA methodology in combination with the MatriXX detector is not compatible with on-line dose measurements

necessary for dose verification based on actual treatment delivery (on-line dose verification). The described implementation of hybrid-QA in **chapter 5** would therefore gain substantial practical value when including detector systems suitable for on-line dose verification techniques. Research has shown newly developed detector types suitable for the COMPASS system and online dose verification [15,16]. The hybrid-QA is furthermore a universal method for 3D dose verification as it can be combined with various dose verification tools and/or treatment techniques. In particular for proton therapy the hybrid-QA can be of interest as dose verification for proton treatments using measurements is time consuming resulting in a serious bottleneck in treatment efficiency.

In current practice, dose differences are generally evaluated by physicists using various dose evaluation parameters derived from the gamma analysis which is difficult to extrapolate to clinical implications [17]. This is underlined by research which shows a weak correlation between gamma passing rates and dose volume histogram (DVH) criteria [18–20]. To overcome the limitations of the widely implemented gamma evaluation, an alternative approach was introduced in **Chapter 6** in which pre-treatment dose verification was performed using DVH-based criteria in addition to gamma passing rates. Although almost no treatment plans failed clinical acceptance criteria (0.3%), the failed treatment plans were detected by DVH-based criteria and missed by gamma passing rates. The introduction of DVH criteria furthermore allows the dose verification procedure to be tailored to individual patients as patient specific DVH-criteria can be introduced and applied. Nevertheless, it has to be noted that DVH-based dose verification is limited as well as it lacks spatial information. This can result in large dose differences within a delineated structure to go undetected [21]. In addition, as only delineated structures are evaluated in DVH-based dose verification, clinically relevant dose differences outside delineated structures can be missed. Therefore, it is advised to combine DVH criteria with gamma passing rates for a more complete pre-treatment dose verification. It furthermore has to be pointed out that DVH-criteria in itself as described in **chapter 6** may include some arbitrariness. This can be further improved when DVH-criteria are based on an overarching hospital based consensus of radiation oncologist groups expert opinion combined with QUANTEC data used for treatment planning [22].

Future perspectives

As described in the introduction, the research presented in this thesis represents only a part of the entire external beam radiotherapy treatment procedure. In terms of pre-treatment dose verification, this thesis focussed mainly on uncertainties which can occur in the TPS and the linear accelerator (linac). Accuracy of the TPS is verified by calculation based dose verifications and treatment delivery by the linac is verified using measurement based dose reconstructions. For the entire treatment procedure many uncertainties still remain however. In particular inter-fractional and intra-fractional anatomical deformations can result in discrepancies between patient geometry obtained for pre-treatment purposes and actual patient geometry during treatment [23]. Research has shown that patient geometry changes can result in unwanted target underdosage and/or OAR overdosage [24,25].

Information on actual patient geometry can be obtained by including additional imaging techniques such as cone-beam-CT (CBCT) and repeat-CT data. Inclusion of additional imaging enables quantification of inter-fractional and intra-fractional patient geometry changes during the entire external beam radiotherapy treatment. This information can then be used for day by day treatment decision purposes allowing adaptive radiotherapy (ART) [26]. The introduction of ART in daily clinical practice consequently affects the dose verification procedure. Furthermore, due to the inclusion of additional imaging, patient specific QA is shifting from offline to online dose verification.

Inter- and intra-fractional patient geometry changes

Inter- and intra- fractional patient geometry changes can partially be accounted for in the planning process by performing robust treatment planning [27,28]. Even so, in robust treatment planning, assumptions are made on expected patient geometry changes based on systematic and random setup errors [29], and motion probability distributions [27] which may deviate from the actual geometry during treatment.

Inter-fractional patient geometry changes caused by patient deformations and/or organ filling can occur throughout the entire treatment resulting in a varying patient geometry for each individual fraction. Inter-fractional patient geometry changes caused by organ filling can be accounted for during the treatment planning process by creating a set of treatment plans for various organ filling. During day to day treatment, CBCT data may then be used to quantify the organ filling of the day and to select the treatment plan which corresponds best with the current patient geometry [30,31]. In terms of dose

verification, the dataset of treatment plans for various organ filling can be verified prior to treatment delivery by calculation based dose calculations. Even though the plan of the day will in comparison to the planning CT correspond better to the actual patient geometry, there will remain discrepancies between the patient geometry used for the plan of the day and the actual patient geometry obtained with a CBCT. For a dose verification based on the actual patient geometry, dose verification using CBCT data is therefore of interest. This is challenging as obtained images suffer, in comparison to the planning CT, from an increase in radiation scatter, and therefore cannot be simply converted to electron densities needed for dose calculations [32,33]. Dose verification using CBCT data is already under development [34–37], and is expected to become part of the daily dose verification routine for external beam radiotherapy.

To guarantee treatment outcome and patient safety, unwanted target underdosage and/or OAR overdosage caused by inter-fractional patient geometry changes need to be monitored and taken into account for each fraction throughout the entire radiotherapy treatment procedure. This can be achieved by accumulating the delivered dose based on the day by day patient geometry and day by day treatment delivery throughout the treatment. By accumulating the delivered dose, decisions affecting the treatment can be performed at each time point in the treatment procedure. In literature, digital image registration (DIR) techniques have been described suitable for contour propagation and dose accumulation for planning CT data and/or CBCT data [38–41]. DIR enables alignment of image sets in a nonlinear way allowing a voxel based comparison of multiple scans. In literature, various DIR techniques have been tested and showed varying registration accuracy results for normal tissue and/or tumour tissue [42,43]. Due to the lack of a ground truth, the accuracy of a DIR system is difficult to determine. Therefore, clinical decisions based on dose accumulation using DIR has to be performed with caution. As a solution a second DIR system independent of the clinical DIR system can be introduced to enhance correct interpretation of dose accumulation results.

Unwanted intra-fractional patient geometry changes can occur by respiration and/or heartbeat induced organ motion. During treatment planning, information on intra-fractional patient geometry changes can be included by incorporating 4D-CT data [44–47]. For dose verification purposes, information on intra-fractional patient geometry changes can be obtained and integrated using 4D-CBCT data [48–50].

Online dose verification

In comparison to offline pre-treatment dose verification, online dose verification allows a direct intervention of the treatment in case of erroneous dose delivery. In particular for treatments with high dose gradients in regions with significant movement, a direct intervention of treatment delivery can be of great importance. In literature a proof of concept has already been evaluated and proven sufficient for photon therapy in combination with EPID dosimetry and the planning CT [51]. For intra-fractional dose verification such concepts are of great interest to accurately verify the actual delivered dose to the patient for each individual fraction.

A shift from offline pre-treatment dose verification to online day by day dose verifications based on actual patient geometry generates additional workload for the department. In addition, online dose verification needs to be performed on a minutes time scale while the patient is on the treatment table to minimize discomfort. This emphasizes the need for an efficient dose verification procedure even more. Efficiency can be improved by optimizing the work flow and minimizing human interaction. As stated by Olaciregui *et. al.*, an ideal *in vivo* dose verification program should (1) automatically decide which fractions need to be analysed for which treatments, (2) automatically gather treatment delivery data for these fractions, (3) automatically produce dosimetry reports, and (4) automatically raise alerts when deviations outside tolerance levels are detected [52]. Promising results were obtained as 95% of 3839 treatments were evaluated without human interventions substantially lowering the workload of pre-treatment dose verification procedure. Dose verification was performed on the planning CT and results revealed that part of the clinical non-relevant deviations originated from patient geometry changes. A more comprehensive online dose verification procedure is to be expected when including CBCT data.

Conclusion

To guarantee patient treatment quality in external beam radiotherapy, high resolution 3D dose verification of the radiotherapy treatment plan is essential. High resolution 3D dose reconstruction can be performed using available low 2D resolution measurements. By combining calculation based dose calculations with measurement based dose reconstruction techniques, efficient and effective pre-treatment dose verification for target volumes and organs at risk can be performed. In addition, inclusion of DVH-based action levels improve insight in dose delivery to target volumes and organs at risk allowing patient individualized dose verification. With the introduction of additional imaging techniques, a shift from pre-treatment to day by day online *in vivo* dose verification using actual patient geometry is foreseen emphasizing the need for an efficient dose verification procedure.

References

- [1] Korevaar EW, Wauben DJ, van der Hulst PC, Langendijk JA, Van't Veld AA. Clinical introduction of a linac head-mounted 2D detector array based quality assurance system in head and neck IMRT. *Radiother Oncol* 2011;100:446–52.
- [2] Boggula R, Lorenz F, Mueller L, Birkner M, Wertz H, Stieler F, Steil V, Lohr F, Wenz F. Experimental validation of a commercial 3D dose verification system for intensity-modulated arc therapies. *Phys Med Biol* 2010;55:5619–33.
- [3] Amerio S, Boriano A, Bourhaleb F, Cirio R, Donetti M, Fidanzio A, Garelli E, Giordanengo S, Madon E, Marchetto F, Nastasi U, Peroni C, Piermattei A, Sanz Freire CJ, Sardo A, Trevisiol E. Dosimetric characterization of a large area pixel-segmented ionization chamber. *Med Phys* 2004;31:414–20.
- [4] Poppe B, Djouguela A, Blechschmidt A, Willborn K, Rühmann A, Harder D. Spatial resolution of 2D ionization chamber arrays for IMRT dose verification: single-detector size and sampling step width. *Phys Med Biol* 2007;52:2921–35.
- [5] Agnew A, Agnew C, Grattan M, Hounsell A, McGarry C. Monitoring daily MLC positional errors using trajectory log files and EPID measurements for IMRT and VMAT deliveries. *Phys Med Biol* 2014;59:N49–63.
- [6] Lee L, Le Q-T, Xing L. Retrospective IMRT dose reconstruction based on cone-beam CT and MLC log-file. *Int J Radiat Oncol Biol Phys* 2008;70:634–44.
- [7] Poppe B, Thieke C, Beyer D, Kollhoff R, Djouguela A, Ruhmann A, Willborn K, Harder D. DAVID--a translucent multi-wire transmission ionization chamber for in vivo verification of IMRT and conformal irradiation techniques. *Phys Med Biol* 2006;51:1237–48.
- [8] Fuangrod T, Woodruff HC, Rowshanfarzad P, O'Connor DJ, Middleton RH, Greer PB. An independent system for real-time dynamic multileaf collimation trajectory verification using EPID. *Phys Med Biol* 2014;59:61–81.
- [9] Poppe B, Blechschmidt A, Djouguela A, Kollhoff R, Rubach A, Willborn KC, Harder D. Two-dimensional ionization chamber arrays for IMRT plan verification. *Med Phys* 2006;33:1005–15.
- [10] Bedford JL, Lee YK, Wai P, South CP, Warrington AP. Evaluation of the Delta4 phantom for IMRT and VMAT verification. *Phys Med Biol* 2009;54:N167–76.
- [11] Carrasco P, Jornet N, Latorre A, Eudaldo T, Ruiz A, Ribas M. 3D DVH-based metric analysis versus per-beam planar analysis in IMRT pretreatment verification. *Med Phys* 2012;39:5040.

- [12] van Elmpt W, Nijsten S, Mijnheer B, Dekker A, Lambin P. The next step in patient-specific QA: 3D dose verification of conformal and intensity-modulated RT based on EPID dosimetry and Monte Carlo dose calculations. *Radiother Oncol* 2008;86:86–92.
- [13] Mans A, Wendling M, McDermott LN, Sonke JJ, Tielenburg R, Vijlbrief R, Mijnheer B, van Herk M, Stroom JC. Catching errors with in vivo EPID dosimetry. *Med Phys* 2010;37:2638–44.
- [14] Olson AC, Wegner RE, Scicutella C, Heron DE, Greenberger JS, Huq MS, Bednarz G, Flickinger JC. Quality assurance analysis of a large multicenter practice: does increased complexity of intensity-modulated radiotherapy lead to increased error frequency? *Int J Radiat Oncol Biol Phys* 2012;82:e77-82.
- [15] Boggula R, Jahnke L, Wertz H, Lohr F, Wenz F. Patient-specific 3D pretreatment and potential 3D online dose verification of Monte Carlo-calculated IMRT prostate treatment plans. *Int J Radiat Oncol Biol Phys* 2011;81:1168–75.
- [16] Thoelking J, Fleckenstein J, Sekar Y, Boggula R, Lohr F, Wenz F, Wertz H. Patient-specific online dose verification based on transmission detector measurements. *Radiother Oncol* 2015;119:351–6.
- [17] Chan MF, Li J, Schupak K, Burman C. Using a novel dose QA tool to quantify the impact of systematic errors otherwise undetected by conventional QA methods: clinical head and neck case studies. *Technol Cancer Res Treat* 2014;13:57–67.
- [18] Nelms BE, Zhen H, Tome WA. Per-beam, planar IMRT QA passing rates do not predict clinically relevant patient dose errors. *Med Phys* 2011;38:1037–44.
- [19] Zhen H, Nelms BE, Tome WA. Moving from gamma passing rates to patient DVH-based QA metrics in pretreatment dose QA. *Med Phys* 2011;38:5477–89.
- [20] Stasi M, Bresciani S, Miranti A, Maggio A, Sapino V, Gabriele P. Pretreatment patient-specific IMRT quality assurance : A correlation study. *Med Phys* 2012;39:7626–34.
- [21] van Zijtveld M, Dirkx ML, de Boer HC, Heijmen BJ. 3D dose reconstruction for clinical evaluation of IMRT pretreatment verification with an EPID. *Radiother Oncol* 2007;82:201–7.
- [22] Marks LB, Yorke ED, Jackson A, Ten Haken RK, Constine LS, Eisbruch A, Bentzen SM, Nam J, Deasy JO. Use of normal tissue complication probability models in the clinic. *Int J Radiat Oncol Biol Phys* 2010;76:S10-9.

- [23] Brouwer CL, Steenbakkers RJHM, Langendijk JA, Sijtsema NM. Identifying patients who may benefit from adaptive radiotherapy: Does the literature on anatomic and dosimetric changes in head and neck organs at risk during radiotherapy provide information to help? *Radiother Oncol* 2015;115:285–94.
- [24] Yan D, Lockman D, Martinez A, Wong J, Brabbins D, Vicini F, Liang J, Kestin L. Computed tomography guided management of interfractional patient variation. *Semin Radiat Oncol* 2005;15:168–79.
- [25] Hansen EK, Bucci MK, Quivey JM, Weinberg V, Xia P. Repeat CT imaging and replanning during the course of IMRT for head-and-neck cancer. *Int J Radiat Oncol Biol Phys* 2006;64:355–62.
- [26] Yan D. Adaptive Radiotherapy: Merging Principle Into Clinical Practice. *Semin Radiat Oncol* 2010;20:79–83.
- [27] Chan TCY, Bortfeld T, Tsitsiklis JN. A robust approach to IMRT optimization. *Phys Med Biol* 2006;51:2567–83.
- [28] Vrančić C, Trofimov A, Chan TCY, Sharp GC, Bortfeld T. Experimental evaluation of a robust optimization method for IMRT of moving targets. *Phys Med Biol* 2009;54:2901–14.
- [29] Van Herk M. Errors and Margins in Radiotherapy. *Semin Radiat Oncol* 2004;14:52–64.
- [30] Murthy V, Master Z, Adurkar P, Mallick I, Mahantshetty U, Bakshi G, Tongaonkar H, Shrivastava S. “Plan of the day” adaptive radiotherapy for bladder cancer using helical tomotherapy. *Radiother Oncol* 2011;99:55–60.
- [31] Heijkoop ST, Langerak TR, Quint S, Bondar L, Mens JWM, Heijmen BJM, Hoogeman MS. Clinical implementation of an online adaptive plan-of-the-day protocol for nonrigid motion management in locally advanced cervical cancer IMRT. *Int J Radiat Oncol Biol Phys* 2014;90:673–9.
- [32] Siewerdsen JH, Jaffray DA. Cone-beam computed tomography with a flat-panel imager: magnitude and effects of x-ray scatter. *Med Phys* 2001;28:220–31.
- [33] Oelfke U, Tücking T, Nill S, Seeber A, Hesse B, Huber P, Thilmann C. Linac-integrated kV-cone beam CT: Technical features and first applications. *Med Dosim* 2006;31:62–70.
- [34] Yoo S, Yin FF. Dosimetric feasibility of cone-beam CT-based treatment planning compared to CT-based treatment planning. *Int J Radiat Oncol Biol Phys* 2006;66:1553–61.
- [35] van Zijtveld M, Dirx M, Heijmen B. Correction of conebeam CT values using a planning CT for derivation of the “dose of the day.” *Radiother Oncol* 2007;85:195–200.

- [36] Ding GX, Duggan DM, Coffey CW, Deeley M, Hallahan DE, Cmelak A, Malcolm A. A study on adaptive IMRT treatment planning using kV cone-beam CT. *Radiother Oncol* 2007;85:116–25.
- [37] Yang Y, Schreibmann E, Li T, Wang C, Xing L. Evaluation of on-board kV cone beam CT (CBCT)-based dose calculation. *Phys Med Biol* 2007;52:685–705.
- [38] Simon A, Nassef M, Rigaud B, Cazoulat G, Castelli J, Lafond C, Acosta O, Haigron P, De Crevoisier R. Roles of Deformable Image Registration in adaptive RT: From Contour propagation to dose monitoring. *Proc. Annu. Int. Conf. IEEE Eng. Med. Biol. Soc. EMBS*, vol. 2015–Novem, IEEE; 2015, p. 5215–8.
- [39] Moteabbed M, Sharp GC, Wang Y, Trofimov A, Efstathiou JA, Lu H-M. Validation of a deformable image registration technique for cone beam CT-based dose verification. *Med Phys* 2015;42:196–205.
- [40] Onozato Y, Kadoya N, Fujita Y, Arai K, Dobashi S, Takeda K, Kishi K, Umezawa R, Matsushita H, Jingu K. Evaluation of on-board kV cone beam computed tomography-based dose calculation with deformable image registration using hounsfield unit modifications. *Int J Radiat Oncol Biol Phys* 2014;89:416–23.
- [41] Veiga C, McClelland J, Moinuddin S, Lourenço A, Ricketts K, Annkah J, Modat M, Ourselin S, D’Souza D, Royle G. Toward adaptive radiotherapy for head and neck patients: Feasibility study on using CT-to-CBCT deformable registration for “dose of the day” calculations. *Med Phys* 2014;41:31703.
- [42] Castadot P, Lee JA, Parraga A, Geets X, Macq B, GrOgoire V, Gregoire V. Comparison of 12 deformable registration strategies in adaptive radiation therapy for the treatment of head and neck tumors. *Radiother Oncol* 2008;89:1–12.
- [43] Mencarelli A, Van Kranen SR, Hamming-Vrieze O, Van Beek S, Nico Rasch CR, Van Herk M, Sonke JJ. Deformable image registration for adaptive radiation therapy of head and neck cancer: Accuracy and precision in the presence of tumor changes. *Int J Radiat Oncol Biol Phys* 2014;90:680–7.
- [44] Yaremko BP, Guerrero TM, Noyola-Martinez J, Guerra R, Lege DG, Nguyen LT, Balter PA, Cox JD, Komaki R. Reduction of Normal Lung Irradiation in Locally Advanced Non-Small-Cell Lung Cancer Patients, Using Ventilation Images for Functional Avoidance. *Int J Radiat Oncol Biol Phys* 2007;68:562–71.
- [45] van der Geld YG, van Triest B, Verbakel WFAR, van Sörnsen de Koste JR, Senan S, Slotman BJ, Lagerwaard FJ. Evaluation of Four-Dimensional Computed Tomography-Based Intensity-Modulated and Respiratory-Gated Radiotherapy Techniques for Pancreatic Carcinoma. *Int J Radiat Oncol Biol Phys* 2008;72:1215–20.

- [46] Colgan R, McClelland J, McQuaid D, Evans PM, Hawkes D, Brock J, Landau D, Webb S. Planning lung radiotherapy using 4D CT data and a motion model. *Phys Med Biol* 2008;53:5815–30.
- [47] Yamamoto T, Kabus S, Von Berg J, Lorenz C, Keall PJ. Impact of four-dimensional computed tomography pulmonary ventilation imaging-based functional avoidance for lung cancer radiotherapy. *Int J Radiat Oncol Biol Phys* 2011;79:279–88.
- [48] Sonke J-J, Zijp L, Remeijer P, van Herk M. Respiratory correlated cone beam CT. *Med Phys* 2005;32:1176–86.
- [49] Wang M, Sharp GC, Rit S, Delmon V, Wang G. 2D/4D marker-free tumor tracking using 4D CBCT as the reference image. *Phys Med Biol* 2014;59:2219–33.
- [50] O'Brien RT, Kipritidis J, Shieh C-C, Keall PJ. Optimizing 4DCBCT projection allocation to respiratory bins. *Phys Med Biol* 2014;59:5631–49.
- [51] Spreeuw H, Rozendaal R, Olaciregui-ruiz I, Mans A, Mijnheer B, Herk M Van. Online 3D EPID-based dose verification : proof of concept. *Med Phys* 2016;43:1–13.
- [52] Olaciregui-Ruiz I, Rozendaal R, Mijnheer B, van Herk M, Mans A. Automatic in vivo portal dosimetry of all treatments. *Phys Med Biol* 2013;58:8253–64.

Appendices

MENT 3D
IFICATION
SITY
ED
RAPY

Nederlandse samenleving

MENTAL
SD
IFICATION
SITY
ED
RAPY

Nederlandse samenvatting

Bij de behandeling van kanker door middel van radiotherapie wordt de patiënt bestraald met een hoog energetische stralenbundel. Door de tumor vanuit verschillende hoeken te bestralen wordt gezond omliggend weefsel gespaard waardoor de patiënt beter en sneller kan herstellen. Aan de hand van complexe bestralingsplannen is het mogelijk om met intensiteit gemoduleerde radiotherapie (IMRT) hoge dosis gradiënten te creëren. Deze hoge dosis gradiënten maakt het mogelijk kritieke organen te sparen met behoud van de vereiste tumordekking [1–3].

Om de kwaliteit van deze complexe bestralingsplannen te waarborgen wordt de door het treatment planning system (TPS) berekende dosisafgifte geverifieerd door een onafhankelijk dosisverificatie systeem. Dit kan aan de hand van driedimensionale (3D) dosisberekeningen, directe dosismetingen of een combinatie van beide. Ondanks de hoge kwaliteit van 3D dosisberekeningen kunnen er verschillen optreden tussen de dosisafgifte die berekend is door het TPS en de daadwerkelijke dosisafgifte door bijvoorbeeld afwijkingen in de posities van de multi-leaf-collimatoren (MLC). Om deze verschillen tijdig te achterhalen is het van belang informatie over de af te geven behandeling te integreren in de dosisverificatie procedure. Dit kan gerealiseerd worden door middel van directe dosismetingen gebruik makend van speciaal ontwikkelde sensoren en/of detectoren [4,5].

Over het algemeen worden er twee type tweedimensionale (2D) detectoren gebruikt voor 3D dosisverificatie; de electronic portal imaging device (EPID) en 2D detectoren opgebouwd uit diodes of ionisatiekamers. De EPID detector werd geïntroduceerd ten behoeve van positieverificatie. Uitvoerig onderzoek heeft er vervolgens toe geleid dat de verkregen beelden van de EPID detector gebruikt kunnen worden voor het reconstrueren van de dosis [6]. Een groot voordeel van de EPID detector is de hoge resolutie en het feit dat de detector geïntegreerd is in de lineaire versneller. Dit maakt het mogelijk informatie over de dosisafgifte tijdens de behandeling te verzamelen. In tegenstelling tot een EPID detector worden 2D detectoren bestaande uit ionisatiekamers over het algemeen op de kop van de lineaire versneller of behandeltafel geplaatst zonder dat de patiënt op de behandeltafel ligt. Dit heeft als gevolg dat er geen informatie verzameld kan worden tijdens de daadwerkelijke behandeling [7–9]. Daarnaast is de resolutie van dit type detectoren beperkt. Daar tegenover staat dat onderzoek heeft aangetoond dat informatie verzameld met lage resolutie detectoren geschikt is voor het reconstrueren van hoge resolutie dosisverdelingen [10]. Door technologische ontwikkelingen van 2D detectoren opgebouwd uit ionisatiekamers wordt het ook mogelijk de dosis met dit type detector te

meten tijdens de daadwerkelijke behandeling van de patiënt op de behandelafel [11]. Desalniettemin is het gebruik van detectoren voor het reconstrueren van de dosis een tijdrovende procedure. Door een toename in complexiteit en het aantal radiotherapeutische behandelingen is een efficiënte en effectieve dosisverificatie procedure van essentieel belang.

Het dosisverificatie systeem beschreven in **dit proefschrift** maakt gebruik van een fluentie model, een detector model, een 3D dosisberekeningsmodule en een lage resolutie 2D detector bestaande uit 1020 ionisatie kamers [7]. Aan de hand van een bestralingsplan wordt de fluentie gemodelleerd. Deze fluentie kan direct als input gebruikt worden voor de 3D dosisberekeningsmodule. Indien er gebruik wordt gemaakt van een 2D meting wordt aan de hand van de berekende fluentie en het detector model een verwachte detector response berekend. Wanneer er verschillen optreden tussen de berekende en gemeten detector response wordt de berekende fluentie gecorrigeerd door middel van een correctie kernel. Afhankelijk van de grootte van de verschillen wordt de correctie kernel in meer of mindere mate toegepast. De gecorrigeerde fluentie wordt uiteindelijk gebruikt als input voor de 3D dosisberekeningsmodule voor het berekenen van de dosis op basis van de patiënt-CT.

In **hoofdstuk 2** van dit proefschrift is het effect van de correctie kernel op het reconstrueren van de dosis beschreven en geëvalueerd. Indien de kernel wordt toegepast, wordt de berekende dosis uitgesmeerd rond de positie waar het verschil tussen de berekende en gemeten detector respons optreedt. De gedetecteerde fout wordt daardoor enigszins overschat. Daarnaast verschilt het effect van de correctie kernel per positie in relatie tot de individuele ionisatie kamer. Met name op de rand van de ionisatie kamer wordt de gedetecteerde fout overschat. Desalniettemin worden verschillen tussen het TPS en het daadwerkelijke bestralingsplan als gevolg van een MLC verschuiving voldoende gedetecteerd ten behoeve van de dosisverificatie van IMRT bestralingsplannen.

In **hoofdstuk 3** is een alternatieve methode geïntroduceerd en geëvalueerd om het effect van de kernel zoals beschreven in hoofdstuk 2 te verminderen. Door middel van een iteratieve reconstructie methode zijn nog voor de daadwerkelijke dosisberekening de posities van de MLC gereconstrueerd aan de hand van een 2D meting. De meetopstelling was zodoende dat één rij ionisatiekamers van de detector afgedekt konden worden door één MLC paar. Het reconstrueren van de MLC posities heeft als gevolg dat de verwachte en gemeten detector response weinig tot geen verschillen vertonen waardoor de kernel in mindere mate toegepast wordt en de gedetecteerde fout minder wordt overschat. Posities van individuele MLC-leafs waren met hoge precisie te reconstrueren, onafhankelijk van de grootte van de fout, de positie van de fout in relatie tot de ionisatie

kamer en het aantal monitor eenheden. Dit gold echter alleen voor de beschreven meetopstelling.

De beschreven methode in hoofdstuk 3 was beperkt door de meetopstelling. Wanneer één rij ionisatiekamers van de detector werd afgedekt door meer dan één MLC paar kon de iteratieve reconstructie methode geen onderscheid maken tussen de verschillende MLC-leafs. Een aanvulling op de methode beschreven in hoofdstuk 3 is beschreven en geëvalueerd in **hoofdstuk 4**. Het bestralingsplan werd zodoende aangepast dat er twee extra metingen werden verzameld. Naast de originele meting van het reguliere bestralingsplan werd er één meting met alle even MLC-leafs gesloten en één meting met alle oneven MLC-leafs gesloten. Zodoende kon de iteratieve reconstructie methode voor de twee extra metingen wel onderscheid maken tussen de bijdrage van de even en oneven MLC-leafs. Door deze aanpassing was het mogelijk de positie van individuele MLC-leafs met hoge precisie te bepalen. De gereconstrueerde posities werden ten slotte gebruikt voor het verifiëren van de dosis voor het reguliere bestralingsplan.

Door de toename in complexiteit van de bestralingsplannen wordt de kans op het ontstaan van fouten vergroot. Om deze fouten tijdig te detecteren is het van belang het effect van de lineaire versneller te integreren in de dosisverificatie procedure. Dit kan gerealiseerd worden door het reconstrueren van de dosis gebruik makend van directe dosismetingen. Dit is echter een tijdrovende procedure en door de toename van het aantal bestralingsplannen is een efficiënte en betrouwbare dosisverificatie procedure van essentieel belang. In **hoofdstuk 5** van dit proefschrift is een methode ontwikkeld en geëvalueerd waarbij de snelheid van dosisberekeningen gecombineerd werd met de betrouwbaarheid van directe dosismetingen. Uit de resultaten bleek dat deze hybride aanpak het mogelijk maakte grote hoeveelheden complexe bestralingsplannen efficiënt en effectief te verifiëren.

Geobserveerde dosisverschillen worden over het algemeen in kaart gebracht met een methodiek die absolute dosisverschillen combineert met een verschuiving van de dosis; de gamma index. In vergelijking met een dosis volume histogram (DVH) is de gamma index moeilijk te vertalen naar klinische relevantie. In **hoofdstuk 6** van dit proefschrift is de meerwaarde van dosisverificatie criteria op basis van DVH informatie onderzocht. De combinatie van DVH criteria en de gamma index verhoogde inzicht in de geobserveerde dosisverschillen tussen het TPS en het onafhankelijk dosisverificatie systeem binnen de IMRT dosisverificatie procedure. Daarnaast werd het mogelijk in samenwerking met de radiotherapeut dosisverificatie criteria af te stemmen op de individuele patiënt.

Om de kwaliteit van complexe bestralingsplannen te waarborgen is een hoogwaardige 3D dosisverificatie procedure van essentieel belang. Het onderzoek beschreven in **dit proefschrift** heeft aangetoond dat lage resolutie 2D detectoren geschikt zijn voor het nauwkeurig reconstrueren van hoge resolutie 3D dosis. Het combineren van dosis berekeningen met directe dosismetingen maakt het mogelijk grote hoeveelheden complexe bestralingsplannen efficiënt en effectief te controleren. Daarnaast wordt het mogelijk een patiënt geïndividualiseerde dosisverificatie uit te voeren door DVH-criteria toe te voegen aan de dosisverificatie procedure wat de kwaliteit van de behandeling ten goede komt.

Referenties

- [1] Arbea L, Ramos LI, Martínez-Monge R, Moreno M, Aristu J. Intensity-modulated radiation therapy (IMRT) vs. 3D conformal radiotherapy (3DCRT) in locally advanced rectal cancer (LARC): dosimetric comparison and clinical implications. *Radiat Oncol* 2010;5:17.
- [2] Longobardi B, De Martin E, Fiorino C, Dell’oca I, Broggi S, Cattaneo GM, Calandrino R. Comparing 3DCRT and inversely optimized IMRT planning for head and neck cancer: equivalence between step-and-shoot and sliding window techniques. *Radiother Oncol* 2005;77:148–56.
- [3] Schubert LK, Gondi V, Sengbusch E, Westerly DC, Soisson ET, Paliwal BR, Mackie TR, Mehta MP, Patel RR, Tomé WA, Cannon GM. Dosimetric comparison of left-sided whole breast irradiation with 3DCRT, forward-planned IMRT, inverse-planned IMRT, helical tomotherapy, and topotherapy. *Radiother Oncol* 2011;100:241–6.
- [4] Mijnheer B, Beddar S, Izewska J, Reft C. In vivo dosimetry in external beam radiotherapy. *Med Phys* 2013;40:70903.
- [5] Low DA, Moran JM, Dempsey JF, Dong L, Oldham M. Dosimetry tools and techniques for IMRT. *Med Phys* 2011;38:1313–38.
- [6] van Elmpt W, McDermott L, Nijsten S, Wendling M, Lambin P, Mijnheer B. A literature review of electronic portal imaging for radiotherapy dosimetry. *Radiother Oncol* 2008;88:289–309.
- [7] Korevaar EW, Wauben DJ, van der Hulst PC, Langendijk JA, Van’t Veld AA. Clinical introduction of a linac head-mounted 2D detector array based quality assurance system in head and neck IMRT. *Radiother Oncol* 2011;100:446–52.
- [8] Boggula R, Jahnke L, Wertz H, Lohr F, Wenz F. Patient-specific 3D pretreatment and potential 3D online dose verification of Monte Carlo-calculated IMRT prostate treatment plans. *Int J Radiat Oncol Biol Phys* 2011;81:1168–75.
- [9] Nakaguchi Y, Araki F, Maruyama M, Saiga S. Dose verification of IMRT by use of a COMPASS transmission detector. *Radiol Phys Technol* 2012;5:63–70.
- [10] Poppe B, Blechschmidt A, Djouguela A, Kollhoff R, Rubach A, Willborn KC, Harder D. Two-dimensional ionization chamber arrays for IMRT plan verification. *Med Phys* 2006;33:1005–15.
- [11] Venkataraman S, Malkoske KE, Jensen M, Nakonechny KD, Asuni G, McCurdy BM. The influence of a novel transmission detector on 6 MV x-ray beam characteristics. *Phys Med Biol* 2009;54:3173–83.

Dankwoord

MENT 3D
FICATION
SITY
ED
RAPY

Dankwoord

Na jaren van hard werken is het eindelijk zover. Het meest gelezen deel van het proefschrift kan geschreven worden, het dankwoord ☺. Via dit dankwoord wil ik graag iedereen bedanken die op wat voor manier dan ook betrokken is geweest bij het tot stand komen van dit proefschrift.

Allereerst wil ik mijn promotoren **prof. dr. J. A. Langendijk** en **prof. dr. C. van der Schans** bedanken voor de kans en het vertrouwen dat ze mij hebben gegeven om dit promotietraject succesvol af te ronden.

Mijn beide copromotoren **dr. ir. Erik Korevaar** en **dr. ir. Aart van 't Veld** wil ik bedanken voor de inhoudelijke ondersteuning, het stellen van kritische vragen en de nodige feedback. Jullie bijdrage heeft de kwaliteit van het proefschrift zeer zeker verhoogd.

Dr. Henk Bijl en **dr. Roel Steenbakkers** wil ik bedanken voor de prettige samenwerking en jullie waardevolle klinische blik.

The reading committee, **prof. dr. S. Brandenburg**, **prof. dr. B. W. Raaymakers** and **prof. dr. B. Poppe** for reviewing my thesis.

Mijn teamleiders van de Hanzehogeschool **Ada Gorter** en **Gerdien Kikstra**. Bedankt voor het faciliteren en de mogelijkheden die jullie mij hebben gegeven om mijn onderzoek te kunnen combineren met het onderwijs.

Alle **collega's van de MBRT** wil ik bedanken voor de interesse die getoond werd in mijn onderzoek en bedankt voor de bijna altijd opbeurende gesprekken wanneer er weer een vakantie voor de deur stond waarin ik verder kon werken aan mijn onderzoek.... ☺

Alle **studenten van de MBRT** die oprechte interesse toonden in mijn werk als docent onderzoeker.

Judith van der Boom, bedankt voor de prettige samenwerking en goede gesprekken over meer dan alleen mijn promotie traject.

Voor het ontwerp van het proefschrift wil ik **Pascal Montsma** bedanken voor zijn inzet en het vorm geven van mijn proefschrift. Je hebt de belangrijke aspecten van onze gesprekken in beeld weten te brengen.

Paul Wittendorp, één van mijn lotgenoten ten tijde van het promotietraject. De gesprekken die we hebben gevoerd hielpen mij tegenslagen te relativeren.

Verder wil ik **Charlotte Brouwer**, één van mijn vele kamergenoten in het UMCG van de afgelopen jaren, bedanken voor de tips tijdens het afronden van mijn promotietraject.

Sanne van Dijk, bedankt voor de gezellige lunches en gesprekken. En niet te vergeten het etentje wat we nog steeds niet gepland hebben. Zullen we beginnen met een borrel op 17 mei? Heel veel succes met je promotie. Jouw drive en kennis zullen je daar zeker bij helpen.

Roel Kierkels wil ik bedanken voor de gesprekken, zowel inhoudelijk als niet werk gerelateerd, en de prettige samenwerking bij het schrijven van twee extra artikelen. Bedankt!

Martijn de Groot, ook jou wil ik ontzettend bedanken. In de eerste jaren als promovendus heb jij mij geholpen structuur aan te brengen in mijn gedachten en zo ook mijn promotietraject. De steun die je mij in deze periode hebt gegeven waardeer ik enorm.

Nog vóór de tijd van flexwerken, **mijn kamergenoten van A1.09 en A1.34**. Bedankt voor de gezelligheid en het spiegelen van mijn gemopper wanneer werk en privé weer eens uit balans was.

Dames 1 wil bedanken voor één van de weinige zekerheden in het leven; het structureel goed presteren op het jaarlijkse zaalvoetbaltoernooi en de ongeslagen status tegen onze rivaal **De Campingploeg**.

Alle vrienden wil bedanken voor de interesse die ze toonden in mijn onderzoek en in het bijzonder **Tjaart, Wiebe, Anna Rixt en Femke** voor de etentjes, uitjes, kroegmomentjes en gezelligheid. Ik waardeer jullie vriendschap.

Lieve familie, bedankt voor de steun tijdens het promotietraject, en **Johan** bedankt voor het beschikbaar stellen van je kantoor zodat ik een deel van de weekenden ongestoord door kon werken.

Janna en Tjisse, bedankt voor het onvoorwaardelijke vertrouwen in mij. Ik ben ontzettend blij met jullie als zus en broer. En Tjisse, de tijd van windsurfen op Molkwar, Starum en Skier kan weer op de agenda gezet worden!

Ook **Jeremy** en **Dave** wil ik bedanken. Tijdens mijn promotietraject hebben we nauw samengewerkt en mooie dingen gecreëerd. Ik heb veel steun aan jullie gehad als collega's en het weekendje Parijs was zeer geslaagd. Ontzettend bedankt!

Erik, ik wil voor de tweede keer mijn dank naar jou toe uitspreken. Naast dat je altijd klaar stond om mij te helpen heb ik jouw rust en kwaliteit om kritische vragen te stellen enorm gewaardeerd. Ik heb het getroffen met jou als begeleider.

Wouter, mijn paranimf en enige lotgenoot die tegen dezelfde problemen aanliep bij het combineren van ons werk als docent en promovendus. De talloze gesprekken hebben mij geholpen het vertrouwen in een goede afloop te behouden. Alleen een beetje jammer dat je na al die jaren als collega de Friese taal niet een beetje beter onder de knie hebt weten te krijgen. Jout neat, hear.

Heit en mem, sûnder jim hie ik hjir net stean kint. Jim hawwe my altyd steunt yn alles en dogge dat nog hieltyd. Tanke foar alles, ik hâld van jim.

Jente en Hidde, ek jim wol ik bedanke. Jim plezier en blydskip hagge mien libben extra kleur jûn en ik genietsje in hiel soad fan jim. En dan kreie jim ek nog een **broerke**. Ik kin net wachtsje om mei us fieven leuke dingen te gean dwaan.

As lêste wol ik de wichtichste bedanke. **Froukje**, sûnder dy hie ik dit nooit berikke kint. Do stiest altyd foar my klear en stiest my by wer mogelijk. Foar dy wie it net altyd makkelik as ik wer ris in wiekein of jûn oan it wurk moast. As it oan my lei moast der een titel wêze foar degene die't it tichst by de promovendus stiet. Do wist my noch altyd te prikelfjen en skerp te hâlden. Ik hâld van dy en sil dat altyd dwaan bliuwe.

Curriculum Vitae

MENT 3D
IFICATION
SITY
ED
RAPY

Curriculum Vitae

Ruurd Visser werd op 27 februari 1983 geboren te Drachten. In 2001 behaalde hij het HAVO diploma aan het Drachtster Lyceum en ging hij studeren in Groningen. Na het afronden van de opleiding elektrotechniek in 2005 aan de Hanzehogeschool Groningen werd de keuze gemaakt om verder te studeren. De opleiding Biomedische Technologie aan de Rijksuniversiteit Groningen werd in 2008 voltooid waarna Ruurd ging werken als docent aan de Hanzehogeschool Groningen bij de opleiding Medisch Beeldvormende en Radiotherapeutische Technieken (MBRT). Vanaf 2009 combineerde Ruurd zijn werkzaamheden als docent aan de Hanzehogeschool met zijn promotieonderzoek in het Universitair Medisch Centrum Groningen (UMCG). Het onderzoek heeft uiteindelijk geresulteerd in dit proefschrift. Momenteel is Ruurd weer volledig werkzaam als docent onderzoeker bij de MBRT. Naast zijn werkzaamheden als docent wil hij studenten en docenten ondersteunen in het verder ontwikkelen van onderzoeksvaardigheden en binnen de opleiding een bredere basis leggen voor toegepast wetenschappelijk onderzoek.



nl.linkedin.com/in/ruurdvisser

Publications

MENT 3D
IFICATION
SITY
ED
RAPY

Publications

Godart J, Korevaar EW, **Visser R**, Wauben DJL, Van't Veld AA. Reconstruction of high-resolution 3D dose from matrix measurements: error detection capability of the COMPASS correction kernel method. *Phys Med Biol* 2011;56:5029–43.

Visser R, Wauben DJL, de Groot M, Godart J, Langendijk JA, Van't Veld AA, Korevaar EW. Efficient and reliable 3D dose quality assurance for IMRT by combining independent dose calculations with measurements. *Med Phys* 2013;40:21710.

Visser R, Wauben DJL, de Groot M, Steenbakkens RJHM, Bijl HP, Godart J, Van't Veld A a, Langendijk J a, Korevaar EW. Evaluation of DVH-based treatment plan verification in addition to gamma passing rates for head and neck IMRT. *Radiother Oncol* 2014;112:389–95.

Kierkels RG, **Visser R**, Bijl HP, Langendijk J a, van 't Veld A a, Steenbakkens RJ, Korevaar EW. Multicriteria optimization enables less experienced planners to efficiently produce high quality treatment plans in head and neck cancer radiotherapy. *Radiat Oncol* 2015;10.

Visser R, Godart J, Wauben DJL, Langendijk JA, Veld AA van't, Korevaar EW. Development of an iterative reconstruction method to overcome 2D detector low resolution limitations in MLC leaf position error detection for 3D dose verification in IMRT. *Phys Med Biol* 2016;61:N49.

Visser R, Godart J, Wauben DJL, Langendijk JA, Van 't Veld AA, Korevaar EW. Reconstruction of high resolution MLC leaf positions using a low resolution detector for accurate 3D dose reconstruction in IMRT. *Phys Med Biol* 2016;61.

Kierkels RGJ, Wopken K, **Visser R**, Korevaar EW, van der Schaaf A, Bijl HP, Langendijk JA. Multivariable normal tissue complication probability model-based treatment plan optimization for grade 2-4 dysphagia and tube feeding dependence in head and neck radiotherapy. *Radiother Oncol* 2016;121:374–80.